# THE SYNTHESIS OF TRIPHOSPHINE LIGANDS AND THEIR MACROCYCLES

**A thesis submitted for the degree of Philosophiae Magister**

**By**

**Tom Hollamby**

**School of Chemistry**
**Cardiff University**
**Wales**

**2013**

## DECLARATION

This work has not been submitted in substance for any other degree or award at this or any other university or place of learning, nor is being submitted concurrently in candidature for any degree or other award.


Signed……………………………………… (candidate)   Date ………………...



## STATEMENT 1

This thesis is being submitted in partial fulfillment of the requirements for the degree of …………………………(insert MCh, MD, MPhil, PhD etc, as appropriate)

Signed………………………………… (candidate) Date ………………………



## STATEMENT 2

This thesis is the result of my own independent work/investigation, except where otherwise stated.
Other sources are acknowledged by explicit references.  The views expressed are my own.

Signed………………………………… (candidate) Date ………………………



## STATEMENT 3

I hereby give consent for my thesis, if accepted, to be available for photocopying and for inter-library loan, and for the title and summary to be made available to outside organisations.

Signed ………………………………… (candidate) Date ………………………

**Abstract**

A new synthesis is described for the production of a single monodentate aromatic phosphine ligand for coordination to a metal centre. 2-fluorophenyl phosphine was synthesised in good yield and has been coordinated to a variety of metal centres. There seems to be no inhibiting factors preventing the phosphine coordinating to any metal centres in a facial manner. Further investigation will be required to see if the 2-fluorophenyl phosphine can be cyclised with a suitable base before the macrocycle can be liberated from the metal centre.

Linear triphosphine ligands have previously been reported to coordinate to metal centres as tridentate chelating ligands. Cyclisation to produce the macrocycle has been achieved through cyclocondensation reactions utilising high dilution, high temperature techniques. Reported here is a new synthetic route to a linear triphosphine by coupling benzyl phosphine with two equivalents of vinyl phosphonate before it's reduction using lithium aluminium hydride. An attempted cyclisation of the triphosphine utilising calcium iodide as the metal centre in a template synthesis is described.

**Table of Contents**

# Chapter 1

## Introduction

# 1.1 Overview - Phosphine Ligands

The discipline of coordination chemistry utilizing phosphine ligands has grown into a substantial field since its early beginnings seventy years ago. This area now consists of numerous examples of mono-, bi-dentate and polydentate chelating phosphine ligands[1] containing a wide variety of different substituents. This substantial expanse of possible phosphine ligands has resulted in the large library of published reactions today but still leaves a plethora of different areas to explore.

Of these, tertiary phosphines, $PR_3$, are particularly important because of their steric and electronic interactions. They can be altered in a specific and systematic way to gain desired modifications with relative ease. Furthermore, they have the ability to stabilize a wide variety of ligands when they are in a complex with a metal centre that has other ligands present, $(R_3P)_nM - L$.

There are numerous instances of applications of phosphine ligands, a prime example of which is that of Wilkinson's catalyst **1**, which is highly suited for catalysing the hydrogenation of alkenes, a representative mechanism is shown below in **Scheme 1.1**[2].
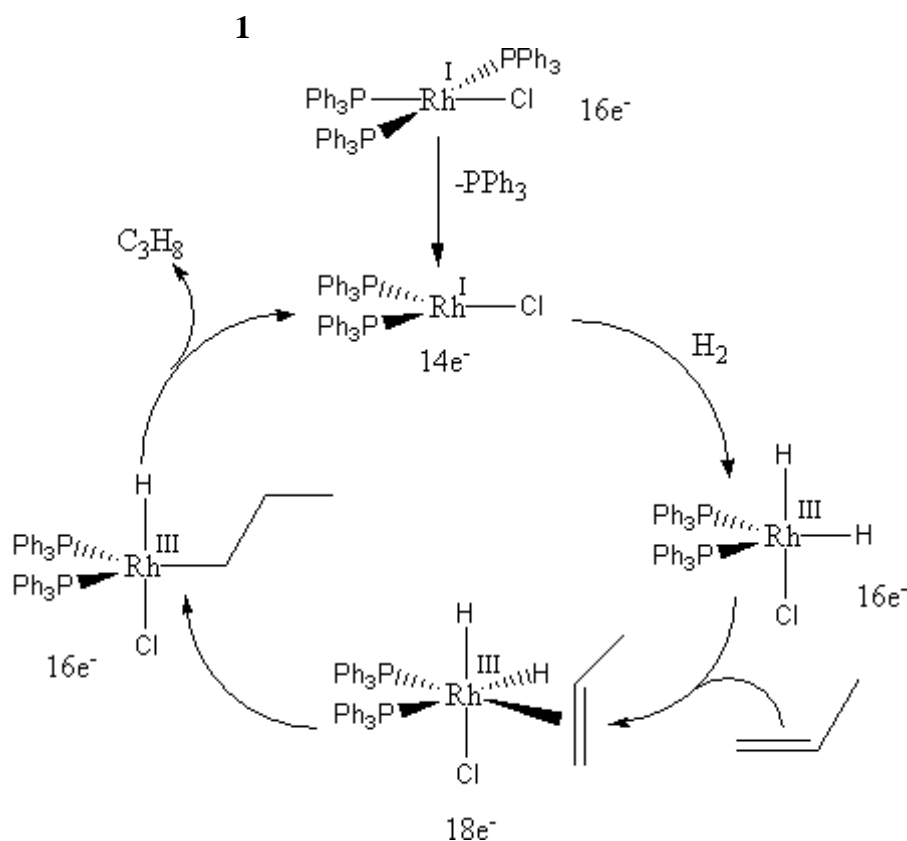


**Scheme 1.1** – Wilkinson's Catalyst 1 and the mechanism of alkene hydrogenation

A further example is the phosphine containing technetium-99m labelled drug Myoview[TM] **2**, **Figure 1.1**, used in medicine as a cardiac imaging agent in the diagnosis of heart disease[3]. A Myoview scan can be used to aid the diagnosis of coronary artery disease or myocardial infarction, as the radioactive technetium tracer allows the imaging of perfusion of blood into the heart tissue.
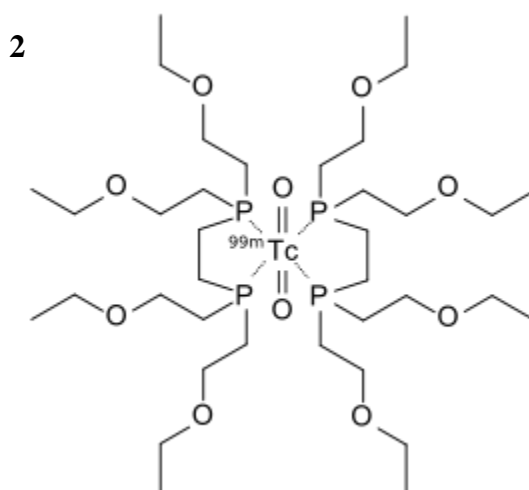


Figure 1.1 – Technetium-99m labelled drug Myoview **2**

## 1.2 Properties of Phosphine Ligands

### 1.2.1 Electronic[4-6]

Tertiary phosphines, similar to $NH_3$, have a lone pair of electrons on the central phosphorus and form a pyramidal structure. The lone pair of electrons enables phosphines to coordinate to metal centres through a σ-bond. However, unlike $NH_3$, they can also accept electron density within their π-orbitals, thereby acting as a π–acid. The extent of their π–acidity is limited by their R groups, of which the Alkyl phosphines are the weakest. The more electronegative the R group becomes the stronger a π–acid it is, as illustrated in **Figure 1.2** below:

$$PMe_3 < PAr_3 < P(OMe)_3 < P(OAr)_3 < PCl_3 < PF_3 \approx CO$$

Figure 1.2 – Relative π-acidity of differing phosphine ligands

The degree of π-acid character can be determined quantitatively from the position of the CO stretch in the IR spectrum of selected metal complexes. If the π-acceptor ability of the phosphine ligand is increased, the carbonyl stretch shifts to higher wavenumbers because the phosphine ligand competes more effectively with the carbonyl groups for the electron density.

| Phosphine | $\nu$ (cm$^{-1}$) | $\theta$ /$^o$ |
|---|---|---|
| P($t$-Bu)$_3$ | 2056.1 | 182 |
| PMe$_3$ | 2064.1 | 118 |
| PPh$_3$ | 2068.9 | 145 |
| P(OMe)$_3$ | 2079.5 | 107 |
| P(OPh)$_3$ | 2085.3 | 128 |
| PCl$_3$ | 2097.0 | 124 |
| PF$_3$ | 2110.8 | 104 |

**Table 1.1**: Position of carbonyl stretches with varying phosphine ligands of the type Ni(CO)$_3$L[8]

Today, it is commonly accepted that the combination of a 3d orbital of the phosphorus and the σ* (antibonding) orbitals of the P-R bonds[7] act together as the M-P bonding acceptor orbital.

When the R group becomes more electronegative, the orbital used by the R group to bond to phosphorus lowers in energy, thereby making the σ* orbital more stable. At the same time the contribution from phosphorus to the σ* orbital also increases. This lengthens the gap between the two different atomic orbitals of P and R, increasing the contribution from the most and least stable atomic orbitals to the σ and σ* orbitals respectively. This makes the σ* orbital more accessible for back donation.

Given that the occupation of the P-R σ* orbital is due to back bonding, it would seem reasonable to hypothesise that the length of the P-R bond should increase. However, no lengthening is observed because at the same time electron density is donated by the

P lone pair to the metal, which shortens the P-R bond. This is due to lone pair (P) - bonding pair (R) electron repulsions.

Phosphines are also able to exhibit $\pi$-acceptor character as evidenced by the diamagnetism of the octahedral $d^2$ complex, trans-$TiMe_2(dmpe)_2$. To be diamagnetic, the three $\pi$ orbitals need to split as shown in **Figure 1.3**. To enable this, the equatorial ligands must be $\pi$-acceptors or the axial ligands must be $\pi$-donors. Methyl was shown not to be a considerable $\pi$ donor, so the dmpe ligand must be an acceptor.
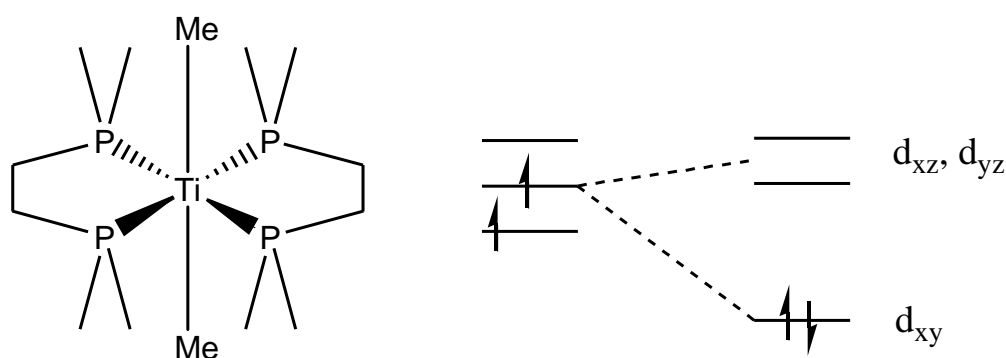


Figure 1.3 - Evidence of diamagnetism in trans-$TiMe_2(dmpe)_2$ complex

## 1.2.2 Steric

In the case of phosphines, the steric effects of R groups must be considered equally to their electronic properties, when fine tuning the specific requirements for a ligand. Chadwick Tolman developed what is now known as the Tolman Cone Angle[8] to quantify the steric properties of phosphines and other ligands. This is defined as the angle, $\theta$, from the apex at the metal, centred 2.28 Å from the centre of the P atom, which just touches the van de Waals radii of the outermost atoms of the R group, as shown below in **Figure 1.4**. This information allows us to determine that $PH_3$ is one of the smallest known phosphines and P(t-butyl)$_3$ conversely is one of the biggest. Through Tolman's work it has become far easier to fine tune a metal complex. As an example larger phosphine ligands can be used to accelerate a reaction where dissociation of the phosphine is desired.
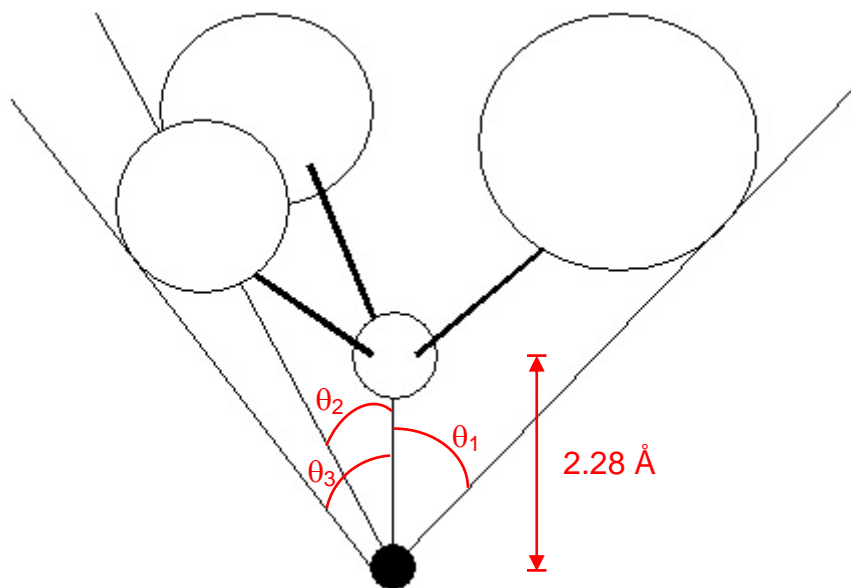
**Figure 1.4** - Tolman Cone Angle, θ. The angle measured from the centre of the metal to the edge of the van de waals radii of the outermost atom of the R group [8]

Phosphine ligands unlike amines are resistant to pyramidal inversion due to large energetic barriers, typically in the range $\Delta G^{\ddagger}$ = 124-149 kJmol$^{-1}$[9]. Therefore the phosphines retain any chirality within them and in asymmetric catalysis the complexes formed show selectivity towards one particular enantiomer.

N. Fey et al[10,11] have recently developed knowledge bases for phosphorus(III) donor ligands and the metal phosphorus bond using DFT-calculated descriptors. This data allows for the estimation of ligand space so that models can be obtained for complexes of the type MPR$_3$.

## 1.3 The Chelate and Macrocyclic Effect

It is generally observed that when polydentate ligands bind to a metal centre the complex becomes more kinetically inert and thermodynamically stable than when monodentate ligands bind to the same metal centre. This is termed the chelate effect. In 1952 Schwarzenbach[12] explained the higher stability of metal chelate compounds over compounds containing fewer chelate rings. He produced a model following a number of assumptions that could also be used to explain the lower stabilisation energy of chelate compounds with larger rings. Essentially he explained that it is

entropically favourable for polydentate ligands to replace monodentate. If one imagines that a bidentate ligand has one end attached to the metal centre then the other end is restricted in the distance it can move away from the metal. This increases the effective concentration and the shorter the chain the more the restricted the movement is of the second donor group, leading to higher stabilisation energies. This is illustrated in **Table 1.2** below[13].

| | $\Delta G^0$ | $\Delta H^0$ | $\Delta S^0$ |
|---|---|---|---|
| *Unidentate Complex* | | | |
| $[Ni(NH_3)_2(H_2O)_4]^{2+}$ | -6.93 | -7.8 | -3 |
| $[Ni(NH_3)_4(H_2O)_2]^{2+}$ | -11.07 | -15.6 | -15 |
| $[Ni(NH_3)_6]^{2+}$ | -12.39 | -24.0 | -39 |
| $[Cu(NH_3)_2(H_2O)_4]^{2+}$ | -10.68 | -11.1 | -1 |
| $[Cu(NH_3)_4(H_2O)_2]^{2+}$ | -17.74 | -22.0 | -14 |
| *Chelate Analog* | | | |
| $[Ni(En)(H_2O)_4]^{2+}$ | -10.31 | -9.0 | 4 |
| $[Ni(En)_2(H_2O)_2]^{2+}$ | -19.09 | -18.3 | 3 |
| $[Ni(En)_3]^{2+}$ | -25.09 | -28.0 | -10 |
| $[Cu(En)(H_2O)_4]^{2+}$ | -14.64 | -13.1 | 5 |
| $[Cu(En)_2(H_2O)_2]^{2+}$ | -27.54 | -25.5 | 7 |

**Table 1.2:** Thermodynamic contributions to the chelate effect in complexes of Cu(II) and Ni(II)

The chelate effect can also be extended to include cyclic rings. These cyclic polydentate rings show more kinetic and thermal stabilisation than their acyclic counterparts with an equivalent number of atoms. This is down mainly to entropic factors. The preorganisation of the macrocycle overcomes all the repulsive forces between the polar donor groups, unlike the acyclic counterpart where the repulsive forces must be overcome so that the donor groups can be forced closer together towards the metal centre to form the complex. This is illustrated in **Table 1.3** below for a series of Ni complexes with differing tetramines[14], **Figure 1.5**.

| 2,3,2-tet N, N'-bis(2-aminoethyl)-1,3-propanediamine | [14]aneN$_4$(cyclam) 1,4,8,11-tetraazacyclo-tetradecane | C(5,12)-*ms*-Me$_2$ [14]aneN$_4$ (Me2cyclam) *meso*-5,12-dimethyl-1,4,8,11-tetraazacyclotetradecane |
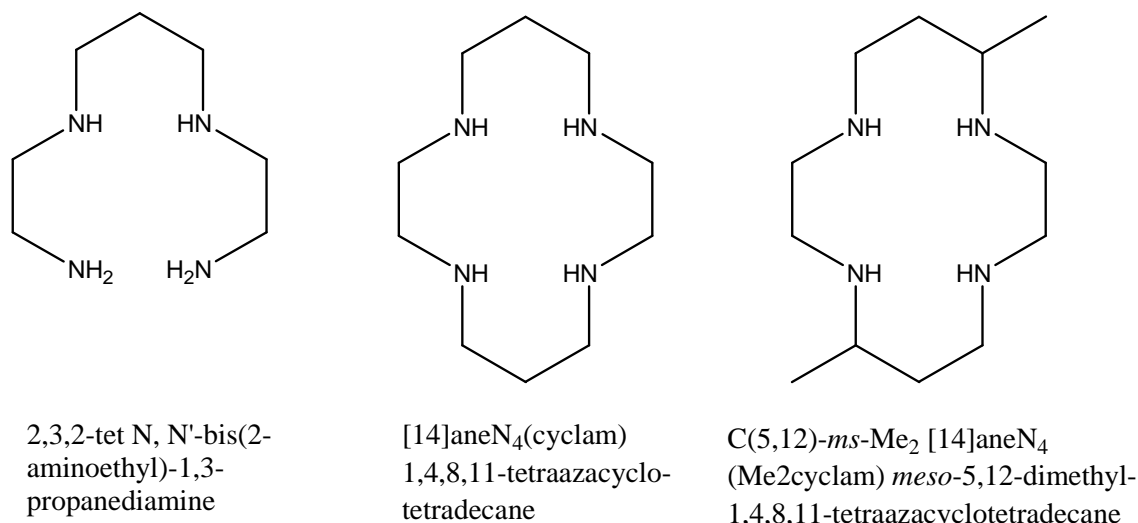
**Figure 1.5**: Tetramines used to demonstrate the differences observed in stability constants, enthalpy and entropy of formation

| Complex | logK$_{NiL}$ | $\Delta H^0$ (kcal/mol) | $\Delta S^0$ cal / (deg mol) |
|---|---|---|---|
| Ni(trien)$^{2+}$ | 13.8 | -14.0 | 16.0 |
| Ni(trien)$^{2+}$(sp) | 11.9 | -10.6 | 18.7 |
| Ni(2,3,2-tet)$^{2+}$ | 15.8 | -19.4 | 7.2 |
| Ni(2,3,2-tet)$^{2+}$(sp) | 15.3 | -16.8 | 13.8 |
| Ni(C(5,12)-ms-Me$_2$[14]aneN$_4$)$^{2+}$ | 21.9 | -28.0 | 8.0 |
| Ni([14]aneN$_4$)$^{2+}$ | 22.2 | -31.0 | -2.0 |

**Table 1.3**: Stability constants, enthalpy and entropy of formation of Ni complexes tetramines (sp - $\Delta H^0$ and $\Delta S^0$ are corrected to complete formation of the square-planar coordination geometry of the complex using log K).

As can be seen from the table, the entropic effect is clearly not the only factor contributing to the increased macrocyclic stability. Changes in enthalpy, conformation and ring size can all affect the observed stability. The sum of these contributions has been defined as the macrocyclic coordination effect. The ring size of macrocycles can strongly influence the stability of the complex formed due to the mismatch between the metal ion and ring size. This is illustrated in the following **Figure 1.6** and **Table 1.4**[15].
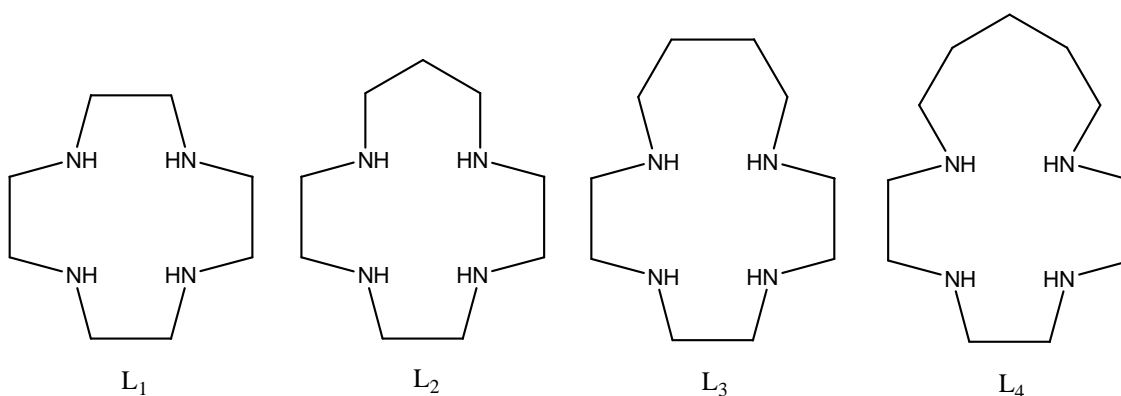
**Figure 1.6**: Tetramines of varying ring size

| Metal Ion | Formation Constants ($\log K_1$) | | | |
| --- | --- | --- | --- | --- |
| | $L_1$ | $L_2$ | $L_3$ | $L_4$ |
| $Cu^{2+}$ | 23.29 | 24.36 | 22.36 | 19.25 |
| $Ni^{2+}$ | 16.4 | 17.98 | 15.47 | 11.74 |
| $Zn^{2+}$ | 16.2 | 15.6 | 12.90 | 10.70 |
| $Cd^{2+}$ | 14.3 | 12.71 | 11.30 | 10.18 |
| $Pb^{2+}$ | 15.9 | 13.48 | 11.59 | 9.5 |

**Table 1.4**: Formation constants for a number of metal centres with a series of tetra-aza

## 1.4 General methods for the synthesis of phosphorus Macrocycles

The synthesis of phosphorus macrocycles is not without its obstacles. The precursors, primary and secondary phosphines, are known to be toxic, air sensitive and volatile, thereby providing a significant challenge in trying to find a route of synthesis. There are essentially two methods that can be utilised in macrocycle synthesis: high dilution reactions and template synthesis[16].

## 1.4.1 High Dilution Reactions

High-dilution reactions are performed by adding two substituents in low concentration solvent solutions dropwise to separate dilution chambers continuously charged with hot solvent by distillation. The mixing of these solutions results in the formation of a macrocycle. It was Kyba and co-workers in the period of 1977–1985 that first synthesised a wide variety of tridentate 11-membered rings[17-19] and tetradentate 14-membered rings[20] utilising high dilution techniques. These reactions involved lithium salts of diphosphines and bis electrophiles, with and without phosphino groups, in very low concentrations. Some of the macrocycles synthesised are illustrated in **Figure 1.7** below:



11[ane]X$_2$Y

X = P, S, As

Y = N, O, S, P, As

14[ane]PXYZ

X = P, S

Y = N, O, S, P, As

Z = N, O, S, P, As
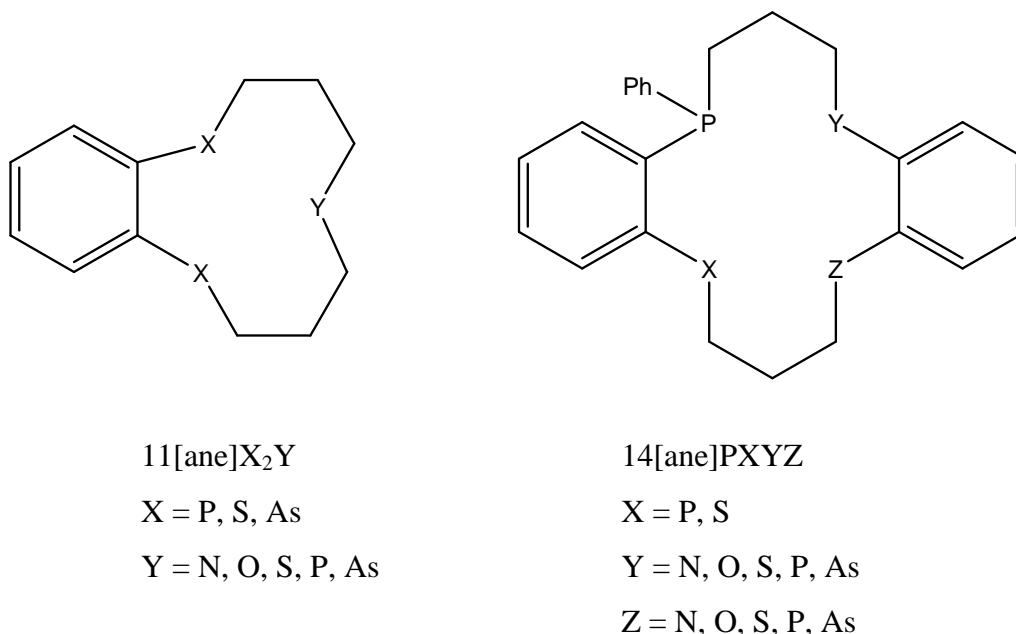
**Figure 1.7**: Examples of phosphorus macrocycles synthesised via high dilution reactions

There are a number of issues associated with the high dilution method of synthesising macrocycles. Firstly the yield on the macrocycle is typically quite poor. The reaction is conducted in very low concentrations so as to discourage polymerisation. There is also a lack of stereoselectivity in reactions leading to a number of different stereoisomers reducing the yield further of the desired macrocycle. Kyba's 11[ane]X$_2$Y macrocycle is indicative of the possible stereoselectivity problems encountered. It is able to form 3 different stereoisomers, two meso forms and one *dl* pair as shown in **Figure 1.8** below. Furthermore larger rings with an increased

number of phosphorus atoms would lead to even more complex macrocycles with an even larger number of possible stereoisomers.
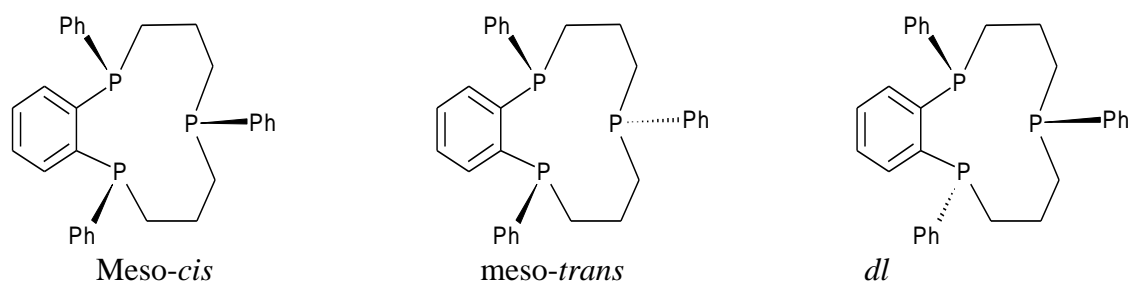


**Figure 1.8**: Different stereoisomers of 11[ane]$X_2Y$ formed through high dilution reactions

The one advantage of this methodology is that no additional demetallation step is required to obtain the macrocycle from the metal centre it was formed on.

## 1.4.2 Template Synthesis

Polymerisation competes with macrocycle formation. One way to combat this using a metal template assisted reaction. Pre-coordinating the macrocycle substituents to a metal centre brings the reactive centres close together, aiding ring closure. Therefore, the problems associated with high dilution reactions are eliminated here. Polymerisation is inhibited by the proximity of the pre-organised substituents and the problem of stereoselectivity is overcome due to the conformation of the substituents held to the metal centre.
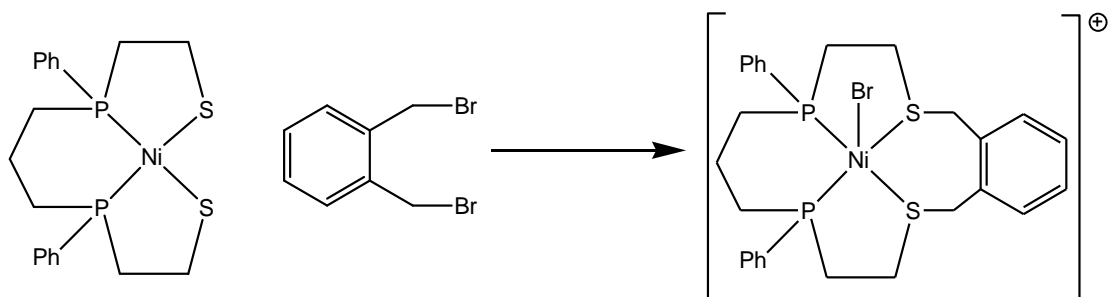


**Scheme 1.2**: Template Synthesis

The reaction scheme in **Scheme 1.2** above[21] shows an example of the first phosphorus containing macrocycle synthesised in 1970 by utilising the template synthesis method.

Metal directed reactions have a number of advantages; good yield, mild reaction conditions, greater control of the stereoselectivity and conformation. However there are a number of disadvantages associated with this method; not all metals can act as a template for the desired reaction, a template reaction doesn't always produce the desired result and most significantly, it may be difficult to obtain the free macrocycle due to its strong coordination to the metal centre.

Liberation of the metal from a macrocyclic centre (demetallation) is required if the macrocycles reactivity is to be investigated. There are two general methods that can be used to liberate the metal centre:

i) Addition of a strongly competing ligand to a solution of the macrocycle complex to induce demetallation.

ii) Addition of a reagent to a solution of the macrocycle which chemically modifies the donor atoms making the macrocycle labile.

## 1.5 Macrocyclic Phosphines as Ligands

These compounds can behave as six electron donors (tridentate) upon coordination to a metal centre as a neutral analogue of the anionic $\eta^5$-Cp ligand. Since the ligand is neutral, access to lower oxidation state complexes are achievable. Furthermore, since these tridentate macrocycles coordinate to a metal in a facial fashion, the remaining reaction sites are forced to be mutually *cis* to each other. The extra stability associated with the macrocyclic coordination effect can be expected to inhibit decomposition of the catalyst during the catalytic cycle, resulting in a more stable catalyst that will produce higher product yields per mole of catalyst. Most metal-promoted catalysis favours the mutually *cis* coordination sites and therefore tridentate phosphine macrocycles are preferred over tetradentate phosphine macrocycles, which usually coordinate in a square planar configuration[22,23].

## 1.5.1 Tridentate Phosphines

A number of triphosphorus macrocycles have been synthesised using a variety of techniques and conditions. One synthesis by Norman et al[24] sees three equivalents of allyl phosphine coordinated to a molybdenum metal centre with three carbonyl groups also attached, shown in **Scheme 1.3**. Cyclisation within these groups through a radical intramolecular hydrophosphination reaction using AIBN [2,2'-azobis(isobutyronitrile)] with heating to give the tridentate phosphorus macrocycle. This synthesis proved to work particularly well as the addition of P-H to C=C is regio and stereoselective producing one stereoisomer in a good yield.
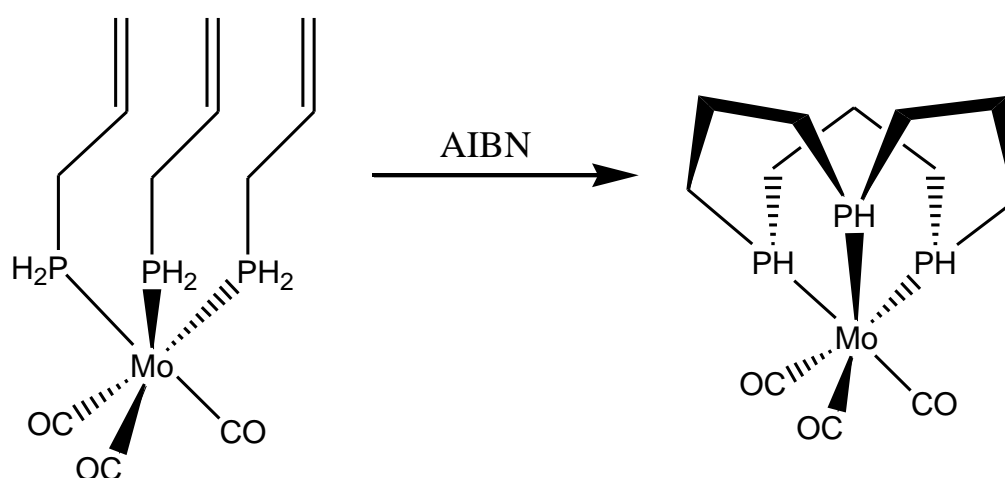


**Scheme 1.3**: Synthesis of a purely aliphatic triphosphorus macrocyle on a Molybdenum tricarbonyl template

This led to further work investigating the use of butenyl phosphine ligands as an alternative method to cyclise the ligands into a tridentate 15 membered macrocycle following this preparation on a molybdenum template[25]. Norman et al were then able to replace the PH hydrogens with various alkyl and aryl group[26] before achieving liberation of the $R_3$-[12]ane$P_3$ ligand by oxidation of the molybdenum metal centre prior to digestion with sodium hydroxide[27].

The advantages of using metal template supported cyclisation reactions are clear: high stereoselectivity control, mild reaction conditions and no need for a high dilution medium. However there are also disadvantages associated with this method: not all metals are suitable to act as centres, expected cyclisations are not always observed

and liberation of the macrocycle from the metal centre can be particularly difficult due to the strong coordinating forces.

The Edwards group[26] conducted a number of successful reactions on the $\eta^5$-CpFe template. Included in this, is the synthesis of a benzannulated triphosphorus macrocycle with an *o*-phenylene bridge using trivinylphosphines and 1,2-diphosphinobenzenes as illustrated in **Scheme 1.4** below.
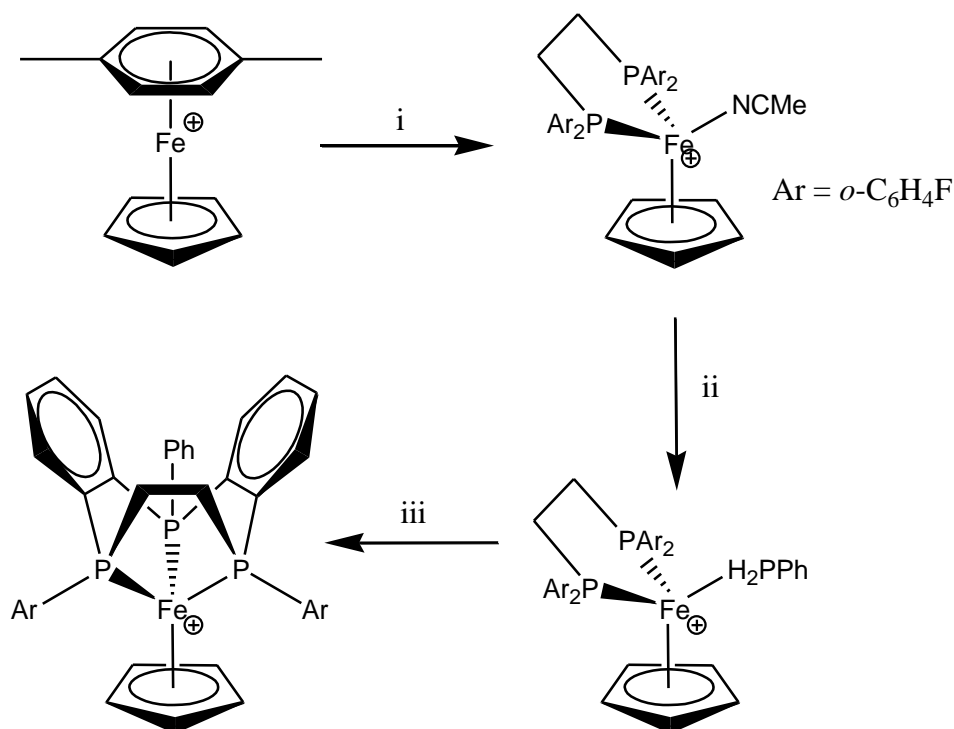


**Scheme 1.4**: Synthesis of a benzannulated triphosphine macrocyle on a CpFe template. *Reagents and Conditions*: (i) *hv*, $Ar_2PC_2H_4PAr_2$, MeCN (ii) $H_2PPh$, 1,2-dichloroethane, $60^O$C (iii) 2eq. $KOBu^t$, THF

## 1.5.2 Tetradentate Phosphines

The number of tetradentate phosphorus macrocycles successfully synthesised in literature is very low, the majority of which used nickel or palladium templates. The reasoning for this could be due to the extra thermal and kinetic stability offered by a fourth phosphorus - metal bond. This stability increases the difficulty in liberating the macrocycle from the metal centre after cyclisation. However Lambert[27] has managed to find a synthetic route for the tetraphosphorus macrocycle and liberate it from its

copper metal centre using hydrogen sulphide, as shown in **Scheme 1.5**. The reaction sequence consists of coordination of phenyl[2-(phenylphosphino)ethyl]phosphine to the Cu(I) triflate complex under an inert atmosphere. Two possible macrocycles can then be made from this one precursor, one aliphatic and the other benzannulated. The aliphatic macrocycle is synthesised simply by adding 1,3-dibromopropane to the precursor and stirring for 4 days under an inert atmosphere. A similar approach is used for the benzannulated macrocycle but *o*-dichloroxylene is used instead.
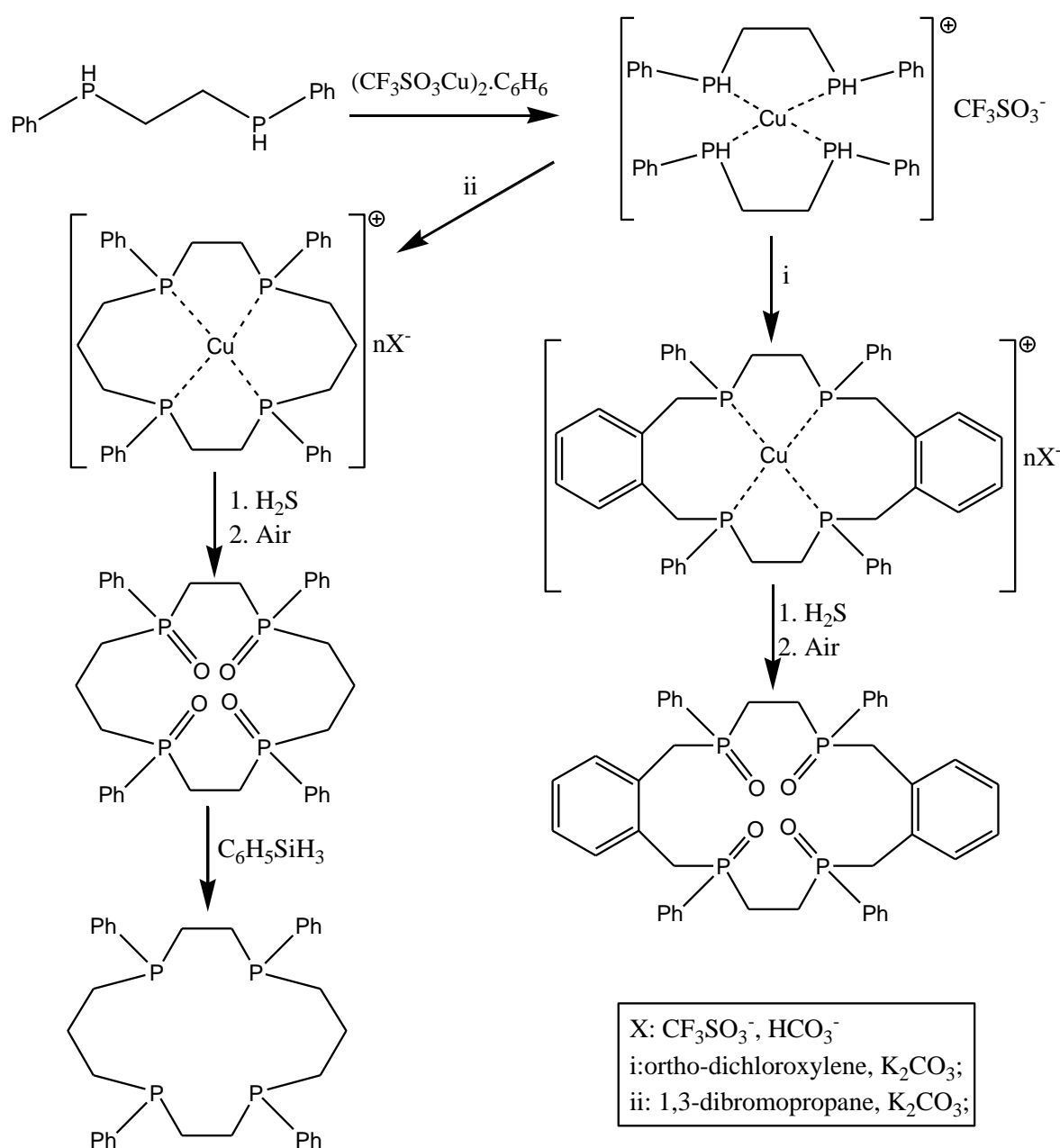


**Scheme 1.5**: Reaction scheme for the synthesis of polyphosphine by square planar template cyclisation and demetallation

15

Both of these macrocycles can then undergo the demetallation using hydrogen sulphide. The phosphonates then formed are easily reduced using lithium aluminium hydride to produce the free macrocycle.

## 1.6 Aim of this Thesis

Phosphorus macrocyclic ligands are a potentially lucrative area of investigation and have many different applications ranging from catalysis to medical imaging. Of particular interest are 9 membered triphosphine benzannulated macrocycles synthesised from a singular ligand species. This thesis will focus on devising a pathway to the formation of aromatic triphosphine macrocycles. It is hoped that the rigidity of the aromatic backbone will aid the resistance of decomposition as a free macrocyclic ligand. Furthermore, it would be of great benefit to use a single ligand species for the formation of a macrocyclic ligand, principally time and cost. This will be accomplished by the coordination of a triphosphine tridentate ligand to a metal centre before completion of the macrocyclic ring via a synthetic route. This will rely on template synthesis techniques to help us achieve our goal.

# Chapter 2

## Towards [9]aneP$_3$ Benzannulated Macrocycles

## 2.1 Introduction

Over the past 10 years the Edwards group have been investigating the synthesis of 9-12 membered tridentate phosphorus macrocycles. Although routes to aliphatic saturated forms have been investigated by other groups the Edwards group focused mainly on the formation of benzannulated macrocycles identifying two main routes of synthesis. The first route involves coordinating a bidentate aromatic phosphine ligand (typically 4-membered) followed by a monodentate aromatic phosphine before cyclising with an appropriate base, as shown in **Scheme 2.1**.
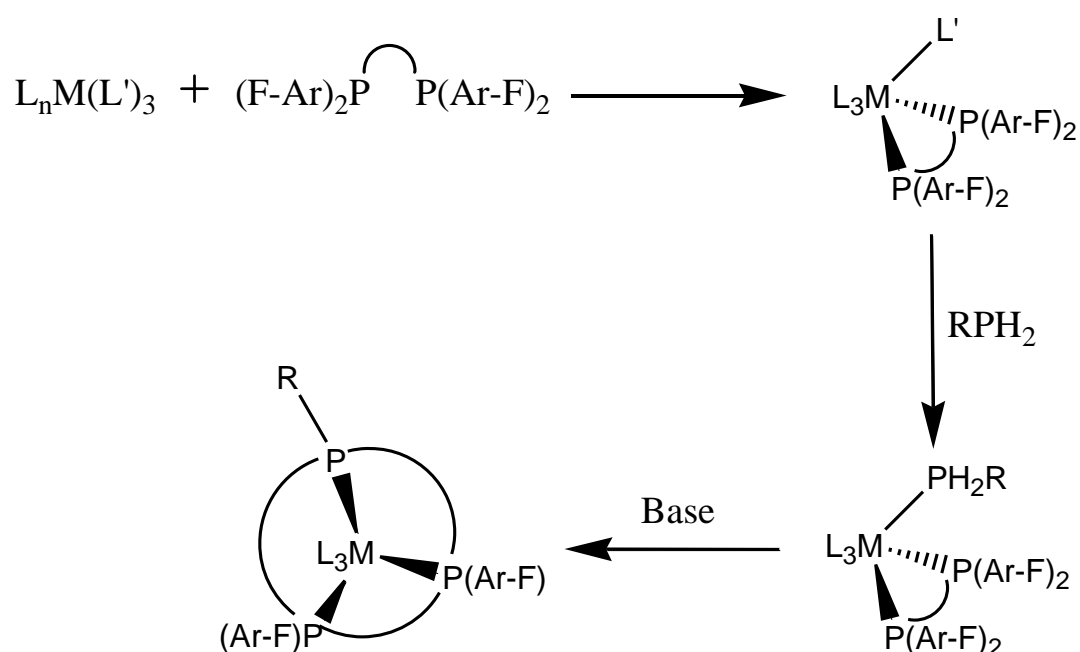


**Scheme 2.1**: Synthetic route showing the formation of a phosphorus macrocycle using a monodentate aromatic phosphine as previously investigated by the Edwards group.

It has recently been noted that intramolecular nucleophilic displacement of fluoride can occur when situated in the *ortho* position to an electron withdrawing group[30]. This is illustrated in the mechanism below, in **Scheme 2.2**, where a phosphine group, located in the *ortho* position, activates the fluoride bearing carbons allowing for substitution.
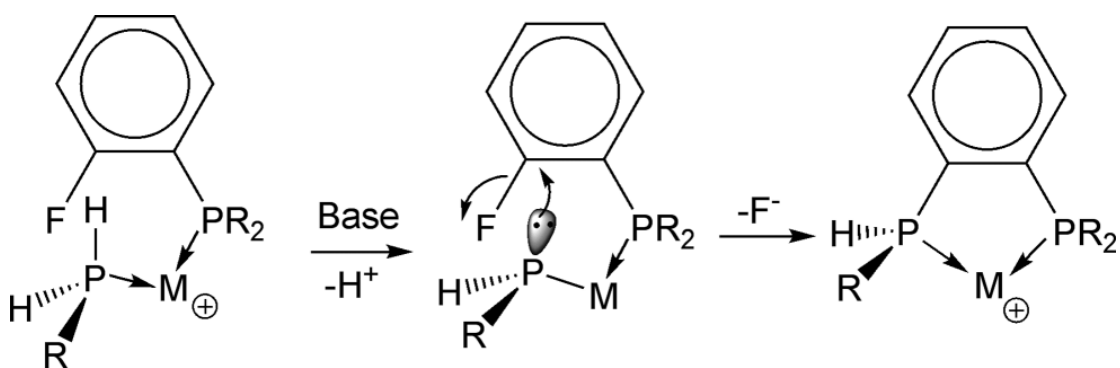
**Scheme 2.2**: Mechanism for the base promoted substitution of fluoride initiated by a phosphine group.

Initial deprotonation of the primary phosphine is required, which can be fulfilled by a suitable base. It is important for the phosphide to retain its nucleophilic character after deprotonation so that the 18 electron complex is unaffected. This work was initially carried out using Cp-iron templates[31] but has recently seen triphosphamacrocyclic ligands successfully prepared on manganese and cobalt metal templates [32-33].

The second route sees an aliphatic bidentate phosphine ligand coordinated to the metal centre before an aromatic monodentate ligand is added as seen in **Scheme 2.3**. These substituents are then cyclised using a base to form the triphosphine macrocycle, before converting the two remaining PH hydrogens with alkyl groups using two equivalents of alkyl lithium and base.

$$L_nM(L')_3 \ + \ H_2P \frown PH_2 \longrightarrow$$
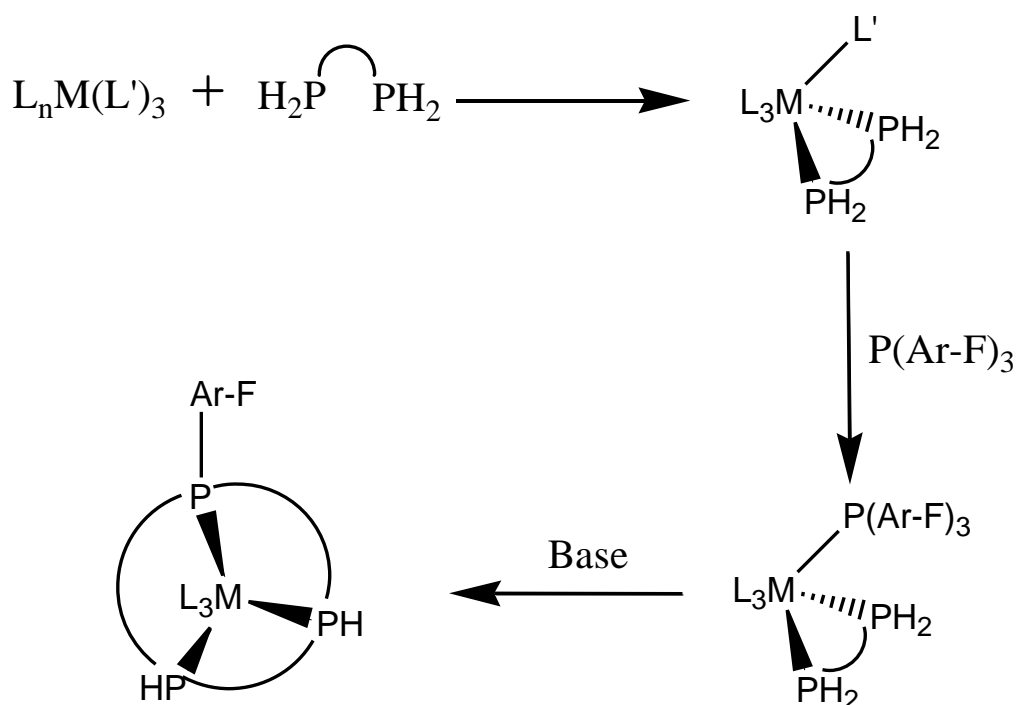
$$\text{Scheme 2.3: Synthetic route showing the formation of a phosphorus macrocycle using a monodentate aliphatic phosphine as previously investigated by the Edwards group.}$$

The advantages of these synthetic routes are that the selective substitution works for manganese and to a lesser extent chromium and molybdenum. Furthermore, tri-tertiary and mono-tertiary coordinated phosphines can be achieved independently through two different routes. Finally the macrocyclisation step for these complexes are typically very efficient (almost spontaneous) and produce a high yield. However there are a few problems with this proposed synthesis, firstly it not being possible to obtain a trialkyl phosphine. Secondly in both syntheses a 2-fluoraryl substituent remains which could interfere with the reactivity of the complex. Therefore the ability to modify functional groups to tune electronic, solubility and steric properties is restricted.

However because of its subsequent reactivity the manganese template remains attractive.

$$(mac)Mn(CO)_3^+ \rightarrow (mac)Mn(CO)_{3-n}L_n$$
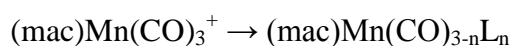
The carbonyls attached to the manganese are susceptible to substitution by other ligands. Furthermore the metal should be susceptible to oxidation disrupting the kinetically inert Mn (I) d$^6$ state thus labilising the ligands to liberate the metal. This provides a good starting point to test the synthetic strategy for the synthesis of a new macrocycle. Furthermore if the manganese is too difficult to liberate from the macrocycle then alternative more labile metals to bypass this problem can be investigated as described below in **Scheme 2.4**.



**Scheme 2.4**: Synthesis of 2-fluorophenyl phosphine metal complexes
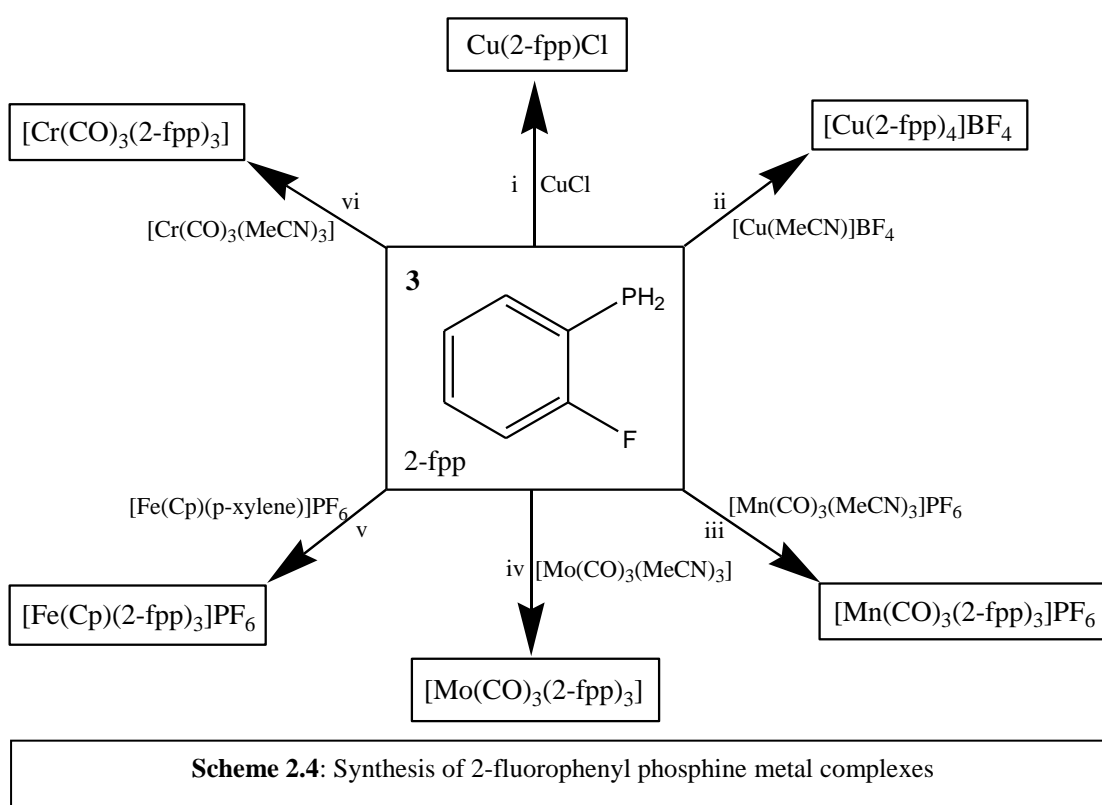
It would be a great advantage to simplify the phosphorus precursor chemistry and synthesise macrocycles bearing secondary phosphine units without reactive 2-fluorophenyl groups. The ability to introduce a number of different functional groups onto the secondary phosphine would also be greatly advantageous. It will then be of interest to investigate the chemistry of the new macrocycles and the various influences ($\sigma$-basicity, $\pi$-acidity and steric bulk that could be fine tuned) of different functional groups upon structure and reactivity. The reactivity is of particular interest in relation to catalysis especially with regard to the ability of macrocyclic ligands to stabilise reaction intermediates.

## 2.2 Synthesis of Symmetrical Tridentate Phosphorus Macrocycles

To address the issues outlined above our initial synthetic strategy for producing symmetrical tridentate phosphorus macrocycles involves forming the previously unreported single phosphorus precursor, in our case via the aromatic secondary phosphonate using a procedure adapted from that reported by Tavs[34]. 1-fluoro-2-bromobenzene (1) is reacted with triethylphosphite in the presence of a NiBr$_2$ catalyst, forming the aromatic phosphonate (2) in place of the bromide. Then a hydridic reduction adapted from Kyba's protocol[35] could be used to synthesise the desired precursor ligand, 2-fluorophenylphosphine (2-fpp), (3) as illustrated in **Scheme 2.5** below.
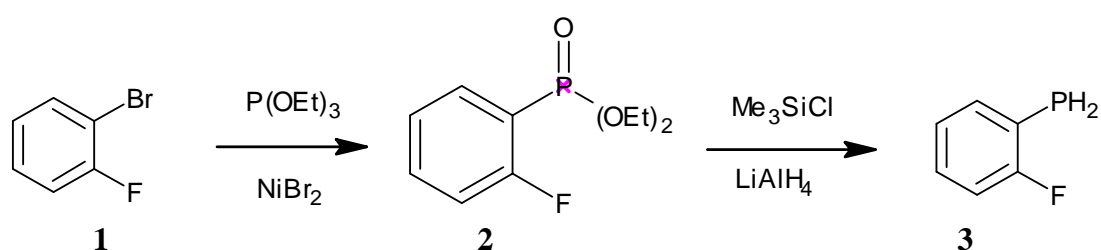


**Scheme 2.5**: Synthesis of 2-fluorophenyl phosphine

Once the precursor phosphine ligand has been synthesised it will then be coordinated to a metal centre (4) in a tridentate facial manner. Once this has been achieved a base will be added (for example potassium t-butoxide) to promote an intramolecular nucleophilic substitution of fluoride forming the desired tri-secondary, symmetrical 9-membered macrocycle (5). The fluoride from one ligand will be removed along with a hydrogen ion from the phosphorus on the adjacent ligands. The ultimate goal will be the removal of the metal centre as illustrated in **Scheme 2.6** below:
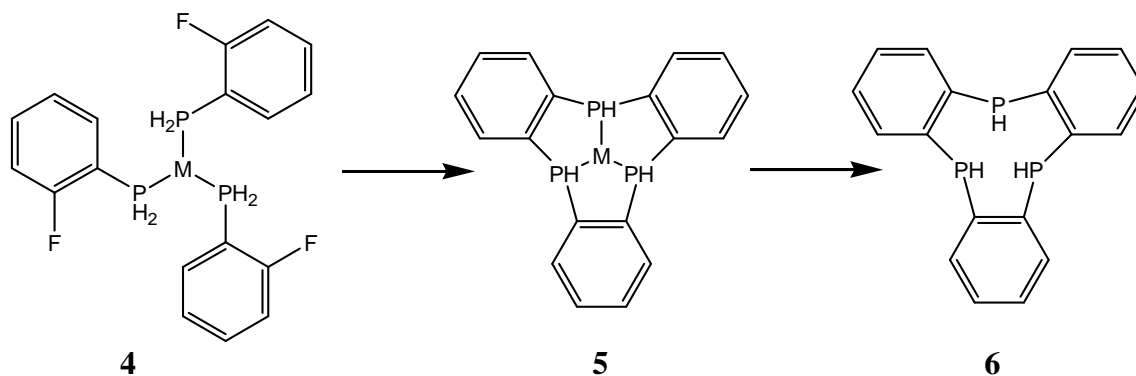


**Scheme 2.6** Synthesis of the free tridentate phosphine macrocycle

As already mentioned, if manganese is reluctant to release the macrocycle then a number of other metals that may be more amenable can be investigated. A number of properties will need to be considered when choosing the metal centre:

- Conformation – both octahedral and tetrahedral geometries would be suitable in a *fac*-L$_3$ML'$_3$ or L$_3$ML' ligand set (L = macrocycle precursor phosphine). Clearly, stereochemical properties may effect the viability of the macrocyclisation, particularly those that influence the non-bonded P-P distance in the precursor. It has been established that octahedral complexes and 'piano stool' structures where idealised ligand-ligand angles would be 90$^O$, readily support the criteria required for successful cyclisation. It may be however that increasing the inter ligand bond angle, as expected in a tetrahedral structure, may increase the non-bonded P-P distance to an extent that will disfavour cyclisation. This can be tested by studying Cu(I) templates.

- Lability – if a metal centre holds onto ligands too tightly then it will make the demetallation step particularly difficult, too loosely held and ligand substitution can occur, preventing macrocycle formation. This relates to in particular the 18 electron rule and whether the metal holds a charge.

Liberating the macrocycle from the metal centre will be a crucial step in obtaining our macrocycle. For the initial template of manganese it will be important to disrupt the inert d$^6$ configuration by oxidation. By studying the replacement of CO ligands it should be possible to facilitate the demetallation step as CO ligands strongly stabilise the manganese 1+ oxidation state d$^6$ configuration and increase the magnitude of $\Delta^o$. Alternative octahedral templates could be based upon group 6 metal tricarbonyl units in a similar manner to the strategy employed by Norman[24]. In these syntheses oxidation of the metal and liberation of 12-membered triphosphorus macrocycles has been achieved utilising AIBN in a radical reaction. It will be of interest to see firstly if the nucleophilic P-C bond forming, ring closing reaction can work on these neutral templates and if so, whether the established liberation method can work. For tetrahedral templates, i.e. copper, it will be necessary to oxidise Cu(I) to Cu(II). d$^9$ Cu(II) is chemically a very labile configuration due to its Jahn Teller Distortion which

could pose some problems. Either a scavenging ligand for the oxidised metal will need to be added or the complex destroyed by digestion by base (to produce metal oxides/hydroxides and liberate the macrocycle).

If successful, it may also be possible to try synthesising metal phosphine complexes for metals that are not typically receptive to phosphine coordination such as the lanthanides, actinides and alkali metals. This will be particularly difficult due to the highly labile and reactive nature of these metals but would be of great interest to see what would be possible.

The specific aims for this synthesis are to investigate the use of a single pre-cursor phosphine in a template synthesis of a tridentate benzannulated 9-membered macrocycle. Initially the template of choice will be $[Mn(CO)_3(MeCN)_3]PF_6$ since its already known to readily form facial complexes with phosphines that support the ring closing methods being applied. Subsequently it will be necessary to expand the chemistry to study alternative more labile octahedral and tetrahedral complexes, for example Cu(I). Macrocyclic templates formed will be studied for liberation of the free ligand as well as the chemical and physical properties of the macrocyclic complexes themselves.

## 2.3 Results and Discussion

### 2.3.1 Synthesis of 2-fluorophenylphosphine, 3

The preparation of 2-fluorophenylphosphine, **2-fpp**, **3**, was initially attempted according to an adapted literature method from Tavs et al[34] using bromobenzene. In our approach, an Arbusov style coupling of 2-fluoro-bromobenzene with triethylphosphite was catalysed by nickel chloride. To a mixture of nickel chloride and 2-fluoro-bromobenzene, heated to 160 $^O$C under nitrogen, was added triethylphosphite. A dark-violet, mobile mixture was observed for a short period of time as the triethylphosphite was added dropwise. This appearance of colour was attributed, in the literature, to the catalytic nickel intermediate. The colour changed rapidly to a brown solution upon addition of triethylphosphite as ethyl bromide started

being eliminated from the reaction mixture. The liquid product was then isolated by distillation under vacuum, however on repeated attempts only small quantities ($< 5\%$) of the desired product (identified by $^{31}$P{$^1$H} NMR spectroscopy by comparison with literature values) were obtained compared to that reported in the literature (90%). As this method appeared to consistently fail, innovations to the method were considered. Substituting the nickel chloride in the literature procedure for nickel bromide followed by heating and addition of reagents as before, was much more successful. In this case using nickel bromide, formation of the initial violet reaction mixture was more pronounced and lasted longer. A work-up of the reaction mixture, as before, gives rise to reasonable yields (approximately 60%) reproducibly. 2-fluorophenyl-diethylphosphonate, **2**, was characterised by its $^{19}$F{$^1$H}, $^{31}$P{$^1$H}, $^1$H and $^{13}$C{$^1$H} NMR spectra. In the $^{31}$P{$^1$H} NMR spectrum a singlet is observed at 14.3 ppm as is the case in the $^{19}$F{$^1$H} NMR spectrum where a singlet is seen at -101.3 ppm. In the $^1$H spectrum, four complex individual resonances are seen in the aromatic region for phenyl hydrogens as well as a multiplet for the hydrogen environment closest to the esteric oxygen. A triplet relating to the terminal hydrogens are also observed. In the $^{13}$C{$^1$H} NMR spectrum resonances due to the presence of fluoride carbons are observed at $\delta$ 163.7 (d, $^2J_{\text{C-F}}$ = 252 Hz), two doublets are witnessed at $\delta$ 62.8 (d, $^2J_{\text{C-P}}$ = 5.5 Hz) and $\delta$ 16.5 (d, $^3J_{\text{C-P}}$ = 6.5 Hz) confirming the presence of esteric carbons.

Reduction of the phosphonate, **2**, by lithium aluminium hydride was adapted from the literature method of Kyba[35] for the synthesis of 1,2-diphosphinobenzene. In our case and in order to minimise the risk of cleavage of fluorine from the phosphonate precursor (**2-fpdp**) the reducing mixture was added to the phosphonate (rather than the other way round in Kyba's procedure) to keep the relative concentration of hydridic reducing agent to a minimum. Conventional work-up followed by distillation allowed isolation of the new phosphine, **3**, product in reasonable yield (approximately 60%) reproducibly. The product, **3**, appears to be stable upon storage neat at -25 $^\text{O}$C for periods of up to 2 months when no signs of decomposition (e.g. HF eliminations or phosphine quaternisation) by NMR spectroscopy were apparent. The phosphine, **3**, is very air-sensitive, as is expected, and must be handled with appropriate provision for the exclusion of oxygen. Reaction of solutions of **3**, with air, rapidly result in oxidation to the phosphonic acid, **4**, which has been characterised by X-ray

crystallography (confirming the identity of the parent primary phosphine) as seen by **Figure 2.1**.
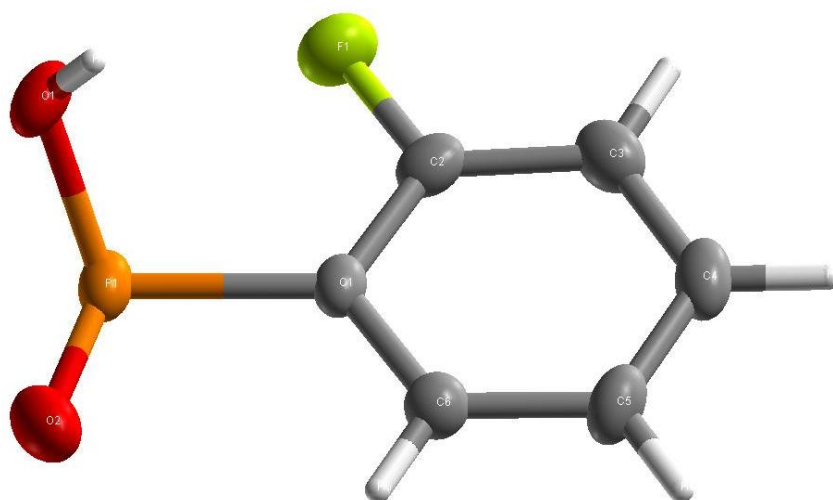


Figure 2.1: Crystal structure of the phosphonic acid, **4**, of **2-fpp** after being exposed to air

It is likely that the phosphonic acid is formed by initial oxidation to the intermediate tautomeric phosphinic acid, followed by a second oxidation **Scheme 2.7**.
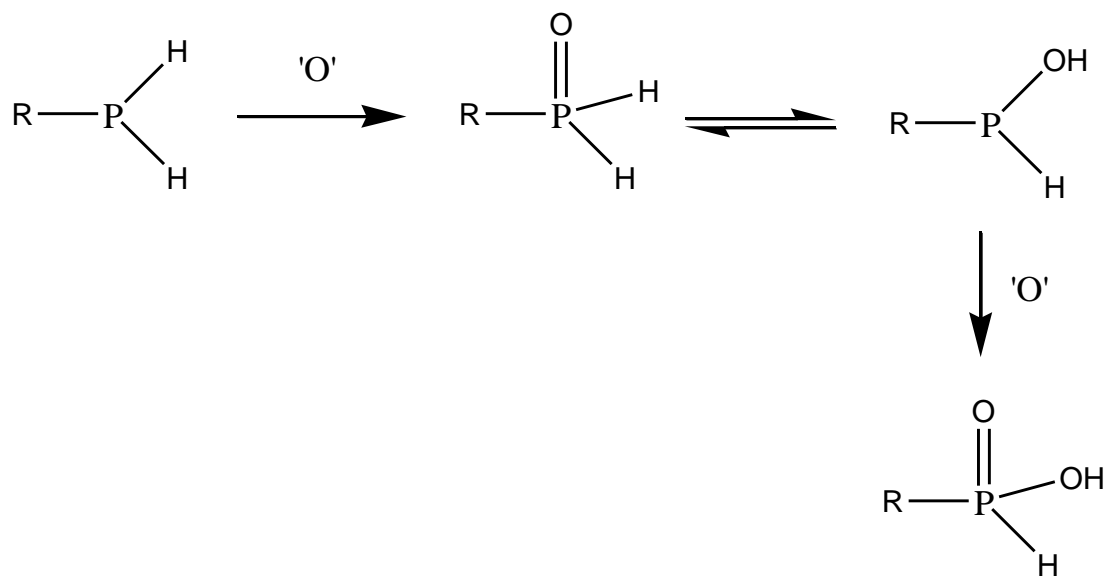


Scheme 2.7: Reaction scheme to show the likely route of decomposition of **2-fpp**

**2-fpp** is characterised by its $^{19}$F{$^1$H}, $^{31}$P{$^1$H}, $^1$H and $^{13}$C{$^1$H} NMR spectra. In the $^{31}$P{$^1$H} NMR spectrum a singlet is observed at -150 ppm as is the case in the $^{19}$F{$^1$H}

NMR spectrum where any three bond coupling ($^3J_{P-F}$) is small with respect to the spectrum resolution. In the $^1H$ NMR spectrum there are resonances due to the phosphine PH protons ($\delta$ 3.81, $^1J_{P-H}$ = 205.2 Hz) as well as a complex pattern in the aromatic region showing four separate hydrogen environments. In the $^{13}C\{^1H\}$ spectrum resonances due to the presence of fluoride carbons are witnessed ($\delta$ 162.0, $^1J_{C-F}$ = 251 Hz).

## 2.3.2 Metal Complexes

### 2.3.2.1 [Cu(2-fpp)₃Cl], 7

The copper complex of **2-fpp** was made by stirring copper (I) chloride with the phosphine, **2-fpp**, in dichloromethane for 10 minutes. The reaction was designated as complete once all the insoluble copper chloride had dissolved (complexation with **2-fpp** being soluble in the dichloromethane) to afford a clear colourless solution. The reaction was worked up by filtering, evaporating to dryness, triturating with petrol and finally recrystallising from dichloromethane. [Cu(**2-fpp**)₃Cl] is characterised by its $^{31}P\{^1H\}$, $^1H$ and $^{13}C\{^1H\}$ NMR spectra. The $^1H$ and $^{13}C\{^1H\}$ NMR spectra show the same environments (although slightly shifted) as those seen in the spectra for **2-fpp**. This proves that the ligand is intact and has not altered in anyway. The $^{31}P\{^1H\}$ NMR spectrum shows again a singlet but has shifted to -128.8 ppm from -151 ppm. The $^{19}F\{^1H\}$ NMR spectrum shows a singlet with the same shift as that of the free ligand - 101.9 ppm.

### 2.3.2.2 [Cu(2-fpp)₄]BF₄, 8

The tetra phosphine copper complex was made by stirring [Cu(MeCN)₄]BF₄ with four equivalents of the phosphine, **2-fpp**, in dichloromethane for 10 minutes. Once all the insoluble copper chloride had dissolved the reaction was designated as complete affording a clear colourless solution. The reaction was worked up by filtering, evaporating to dryness and triturating with petrol, which produced a white gelatinous solid. It was not possible to refine this solid any further and recrystallisation did not

produce any crystals. The complex produced a singlet resonance in the $^{19}F\{^1H\}$ NMR spectrum at δ -102.8 ppm which is close to that of the free phosphine ligand as would be expected. There is also a peak at δ -151.9 ppm relating to the $BF_4$ counter ion. The $^{31}P\{^1H\}$ NMR spectrum shows a singlet resonance at δ -122.0 ppm which confirms the coordination of the phosphine to the copper metal. Interestingly, a difference of 7.0 ppm is observed between the $[Cu(2\text{-}fpp)_4]BF_4$ and $[Cu(2\text{-}fpp)_3Cl]$ , which could be attributed to the differing counter ions and stoichiometry. The complex could not be characterised further as both the $^1H$ and $^{13}C\{^1H\}$ NMR spectra were too broad to resolve any individual resonances.

### 2.3.2.3 $[Mn(CO)_3(2\text{-}fpp)_3]PF_6$, 9

The manganese complex of **2-fpp** was made by stirring $[Mn(CO)_3(MeCN)_3]PF_6$ with the phosphine, **2-fpp**, in dichloromethane for 3 hours. The insoluble manganese tricarbonyl trisacetonitrile dissolved to afford a bright clear yellow solution. The product was isolated by filtering, evaporating to dryness, triturating with petroleum ether, which produced a yellow gelatinous solid. It was not possible to refine this solid any further and recrystallisation did not produce any crystals. The $^{31}P\{^1H\}$ NMR spectrum shows a singlet resonance at δ -40.4 ppm which confirms the coordination of the phosphine to the manganese metal, there is also a singlet at -143.1 ppm which relates to the hexafluorophosphate counter ion. This is further confirmed in the $^{19}F\{^1H\}$ NMR spectrum, which shows a doublet at -70.7 ($^1J_{P\text{-}F}$ = 757.89Hz) for the hexafluorophosphate counter ion along with a singlet at δ -101.5 ppm confirming that the phenyl fluorine is unaltered. The complex could not be characterised further as both the $^1H$ and $^{13}C\{^1H\}$ NMR spectra were too broad to resolve any individual resonances due to the manganese quadrupole.

### 2.3.2.4 $[Mo(CO)_3(2\text{-}fpp)_3]$, 10

The molybdenum complex of **2-fpp** was made by stirring molybdenum tricarbonyl trisacetonitrile with the phosphine, **2-fpp**, in dichloromethane for 30 minutes. The insoluble yellow/brown molybdenum tricarbonyl trisacetonitrile dissolved to produce

a clear pale brown solution. The reaction was worked up by filtering, evaporating to dryness, triturating with petrol and finally recrystallising from dichloromethane via vapour diffusion using petroleum ether. [Mo(**2-fpp**)$_3$(CO)$_3$] is characterised by its $^{31}$P{$^1$H}, $^1$H, $^{13}$C{$^1$H} and $^{19}$F{$^1$H} NMR and mass spectra. The $^1$H, $^{13}$C{$^1$H} and $^{19}$F{$^1$H} NMR spectra showed similar environments as those seen in the spectra for **2-fpp**. This proves that the ligand has not been affected by the coordination. The $^{31}$P{$^1$H} NMR spectrum shows again a singlet resonance, which has shifted to $\delta$ − 75.8 ppm which is consistent with a facial coordination geometry (meridional geometry would be expected to give rise to a A$_2$B pattern). This compares favourably with the phenyl phosphine analogue, [Mo(CO)$_3$(PhPH$_2$)$_3$], which shows a singlet resonance in the $^{31}$P{$^1$H} NMR spectrum at $\delta$ − 53.5 ppm [36]. The mass spectrum confirms the formulation of the compound as a tris-phosphine complex where the molecular ion plus acetonitrile is observed at 604.9103. The solid state structure was determined by X-Ray crystallography on crystals obtained by vapour diffusion. A diagram of the structure is shown in **Figure 2.2**, including elements of disorder. In this case positional disorder is observed where one atom occupies more than one site within the unit cell.


The crystal was of high enough quality to confirm the structure of the complex and the coordination of three equivalents of **2-fpp**. Mo-P bond lengths for the facially capping [Mo(CO)$_3$(PhPH$_2$)$_3$] complex are taken as an average of 2.498 Å [36] and is negligible when compared to 2.4870(6), 2.4878(6) and 2.4902(6) Å for this complex (the numbers in brackets are the standard deviation for that particular bond length). There is also a slight variation in the P-C bond length, typical bond lengths are in the region of 1.84 Å[37], whereas this complex has an average bond length of 1.822(2) Å. This difference of approximately 0.02 Å suggests that the benzene ring is accepting electron density from the phosphorus, strengthening the P-C bond and conversely weakening the Mo-P bond. The angles between the phosphine ligand, **2-fpp**, and the Mo metal centre deviate only slightly (88.12(6)$^O$, 86.64(7)$^O$ and 89.70(6)$^O$) from the optimum octahedral angle of 90$^O$. The non-bonded P-F distances between the phosphorus atom of one ligand and the aryl fluorine of another ligand were measured as an average of 5.313 Å over a range of 4.145 - 6.238 Å. This gives an impression only (distances can vary in solution as opposed to those seen in crystallography due to rotation of bonds) of the distances that need to be overcome in the base promoted substitution of fluoride resulting in the formation of the macrocycle.

In the infrared spectrum a sharp absorption was observed at 1940 cm$^{-1}$ with a much broader absorption at 1836 cm$^{-1}$, which can be assigned to the carbonyl groups. This is somewhat lower than for other carbonyl stretches associated with phosphines on molybdenum metals like PPh$_2$OEt, 1973 cm$^{-1}$ [38]. This would suggest that **2-fpp** is a less effective π–acid as its carbonyl stretches appear at lower wavenumbers. Another broad peak at 2309 cm$^{-1}$ can be attributed to the P-H stretch.
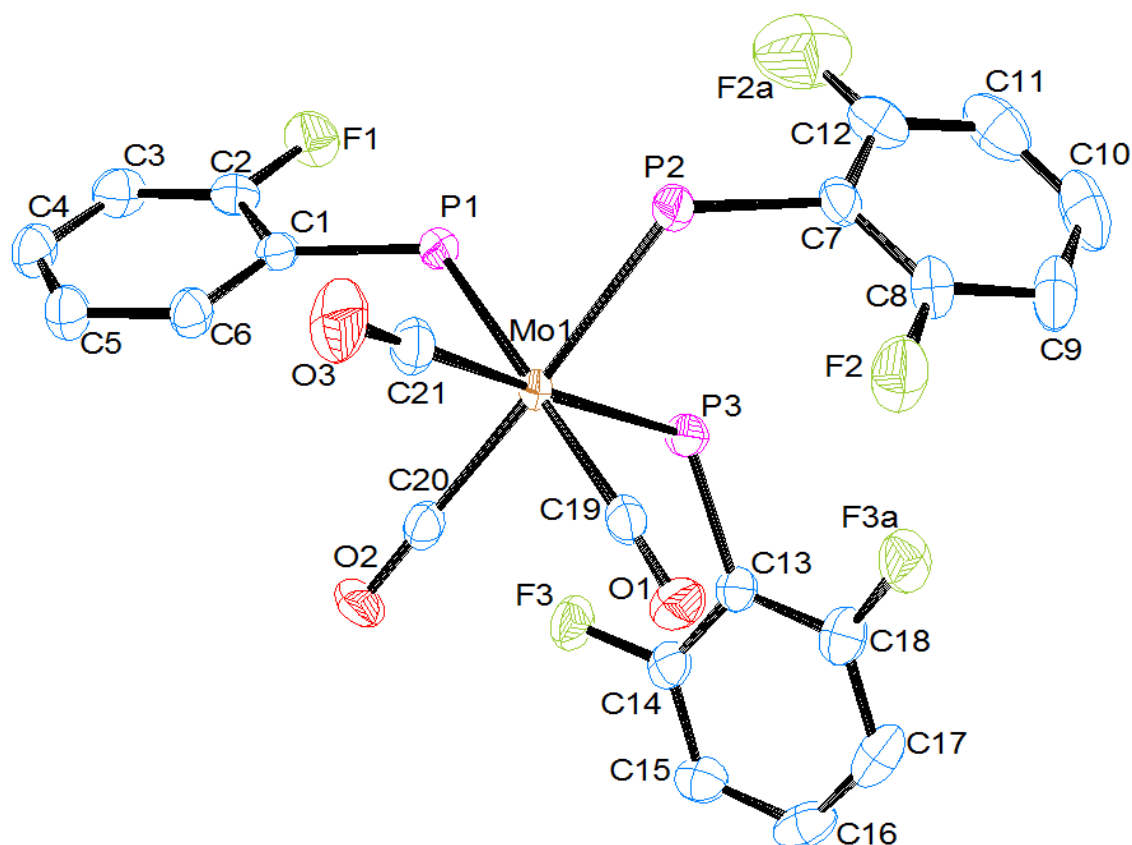


**Figure 2.2**: The crystal structure of **[Mo(CO)$_3$(2-fpp)$_3$]** including disorder at F2(F2a) and F3(F3a). Selected bond lengths (Å) and angles ($^O$): C19-Mo1, 1.988(2); C20-Mo1, 1.980(2); C21-Mo1, 1.984(2); Mo1-P3, 2.4870(6); Mo1-P2, 2.4878(6); Mo1-P1, 2.4902(6); C7-P2, 1.822(2); C13-P3, 1.818(2); C1-P1, 1.827(2); C20-Mo1-P3, 92.19(7); C19-Mo1-P3, 88.12(6); C21-Mo1-P2, 86.64(7); C19-Mo1-P2, 92.39(6); C20-Mo1-P1, 89.70(6); C21-Mo1-P1, 94.68(7).

### 2.3.2.5 [Fe(Cp)(2-fpp)$_3$]PF$_6$, 11

The iron complex of **2-fpp** was made by stirring the [Fe(Cp)(p-xylene)]PF$_6$ with the phosphine, **2-fpp**, in dichloromethane for 12 hours. A clear dark red solution appeared once the reaction was complete as all the yellow insoluble iron precursor complex had

dissolved. The reaction was worked up by filtering, evaporating to dryness, triturating with petrol and finally recrystallising from dichloromethane by vapour diffusion with petroleum ether. [Fe(Cp)(2-fpp)$_3$]PF$_6$ is characterised by its $^{31}$P{$^1$H}, $^1$H, $^{13}$C{$^1$H} and $^{19}$F{$^1$H} NMR spectra. The $^1$H and $^{13}$C{$^1$H} NMR spectra shows the same environments (although slightly shifted) as those seen in the spectra for **2-fpp** confirming that the ligand is intact and has not altered upon coordination. The $^{31}$P{$^1$H} NMR spectrum shows again a singlet but has shifted to -24 ppm. A septet coupling is also observed at -146 ppm relating to the PF$_6$ counter ion. The complex produced a singlet resonance in the $^{19}$F{$^1$H} NMR spectrum at δ -103.75 ppm which is sufficiently close to that of the free phosphine ligand that it can be inferred that the phenyl fluorine bond is unaltered. There is also a peak at δ -71.70 (d, $^1$J$_{P-F}$ = 757.89 Hz) ppm relating to the PF$_6$ counter ion. The mass spectrum confirms the formulation of the compound as a tris-phosphine complex, the molecular ion is observed at 505.0302. The solid state structure was determined by X-Ray crystallography, a diagram of which is shown below **Figure 2.3,** including positional disorder of the fluorine.
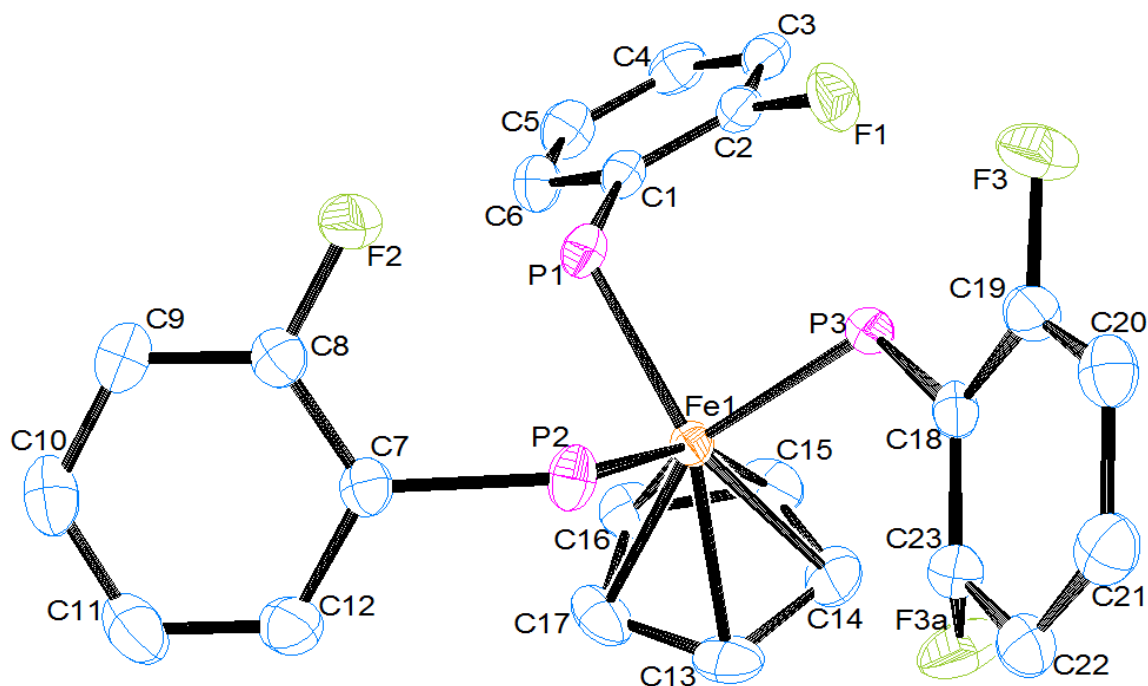


**Figure 2.3**: The crystal structure of **[Fe(Cp)(2-fpp)$_3$]PF$_6$** including disorder at F3(F3a). Selected bond lengths (Å) and angles ($^O$): P1-Fe1, 2.1667(7); P2-Fe1, 2.1750(6); P3-Fe1, 2.1715(6); C7-P2, 1.820(2); C1-P1, 1.822(2); C18-P3, 1.863(7); C15-Fe1, 2.075(2); C16-Fe1, 2.081(2); C17-Fe1, 2.087(2); C14-Fe1, 2.087(2); C13-Fe1, 2.092(2); C1-P1-Fe1, 119.29(7); C7-P2-Fe1, 119.94(7); C18-P3-Fe1, 118.0(3);

It shows the coordination of three phosphine ligands, **2-fpp**, to the iron metal centre, which is also coordinated to a cyclopentadiene ligand, the hexafluorophosphate counter ion is also present, but not shown in **Figure 2.3**. The Fe-P bond lengths were 2.1667(7) Å, 2.1715(6) Å and 2.1750(6) Å which average at 2.171 Å and are almost identical to that of an *o*-phenylene phosphorus atom (Fe-P = 2.177Å)[39]. The P-C bond lengths are 1.863(7) Å, 1.822(2) Å and 1.820(2) Å which are significantly longer than the typical 1.810 Å[40]. These P-C bond lengths are very close to those seen in the [Mo(CO)$_3$(**2-fpp**)$_3$]PF$_6$ complex despite the difference in charge on the metal centre and the difference in bond lengths between Mo-P and Fe-P of 0.2773 Å. The non-bonded Fe-P distances are taken as an average of 4.544 Å ranging from 3.196 - 5.521 Å which are considerably shorter than those for the molybdenum complex suggesting that the Cp ligand is forcing the phosphine ligands closer together.

### 2.3.2.6 [Cr(CO)$_3$(2-fpp)$_3$], 12

The chromium complex of **2-fpp** was made by stirring chromium tricarbonyl trisacetonitrile with the phosphine, **2-fpp**, in dichloromethane for 30 minutes. The yellow insoluble chromium precursor complex dissolved (complexation with **2-fpp** being soluble in dichloromethane) to afford a lime green solution. The reaction was worked up by filtering, evaporating to dryness, triturating with petroleum ether and finally recrystalisation in dichloromethane from vapour diffusion with petroleum ether. [Cr(CO)$_3$(**2-fpp**)$_3$] is characterised by it's $^{31}$P{$^1$H}, $^1$H and $^{13}$C{$^1$H} NMR spectra. The same environments as those seen in the spectra for **2-fpp**, were also apparent in the $^1$H, $^{13}$C{$^1$H} and $^{19}$F{$^1$H} NMR spectra for this complex. Showing that the ligand has not been affected by the complexation. The $^{31}$P{$^1$H} NMR spectrum shows again a singlet but has shifted to −38 ppm. The mass spectrum confirms the formulation of the compound as a tris-phosphine complex, the molecular ion +K$^+$ is observed at 558.9476. The solid state structure was determined by X-Ray crystallography of crystals obtained from vapour diffusion. A diagram of the structure obtained is shown below in **Figure 2.4**, including the positional disorder of two different fluorine atoms.
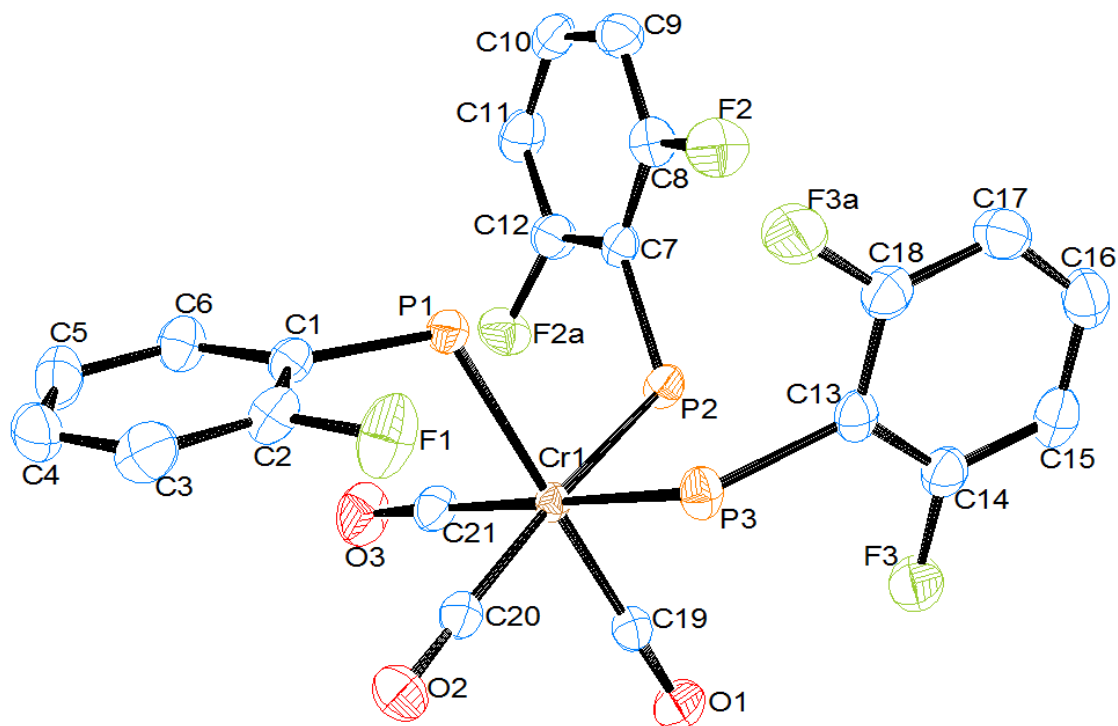
**Figure 2.4**: The crystal structure of **[Cr(CO)₃(2-fpp)₃]** including disorder at F2(F2a) and F3(F3a). Selected bond lengths (Å) and angles (°): C1-P1, 1.8218(17); C7-P2, 1.8208(16); C13-P3, 1.8232(17); Cr1-P2, 2.3248(5); Cr1-P3, 2.3296(5); Cr1-P1, 2.3344(5); C19-Cr1, 1.8438(17); C20-Cr1, 1.8499(17); C21-Cr1, 1.8445(18); C19-Cr1-P2, 85.25(5); C21-Cr1-P2, 90.23(6); C19-Cr1-P3, 91.42(6); C20-Cr1-P3, 87.74(5); P2-Cr1-P3, 93.819(17); C21-Cr1-P1, 87.40(5); C20-Cr1-P1, 91.68(5);

The crystal confirms the structure of the complex with the coordination of three equivalents of **2-fpp** in a facial manner to the chromium metal centre. Typical values for Cr-P bond lengths are approximately 2.379 Å[41] compared to the smaller bond lengths of 2.3248(5) Å, 2.3296(5) Å and 2.3344(5) Å for this complex, a difference of approximately 0.049 Å. There is also a slight variation in the P-C bond length, typical bond lengths are in the region of 1.810 Å[36], whereas this complex has an average bond length 1.822(17) Å. This difference of 0.012Å is that same as those seen in the molybdenum and iron complexes. The angles between the phosphine ligand, **2-fpp**, and the chromium metal centre deviate only slightly (90.23(6)°, 91.42(6)° and 91.68(5)°) from the optimum octahedral angle of 90°. The non-bonded P-F distances were taken as an average of 4.647 Å with a range of 3.716 - 6.059 Å which are shorter than those seen for the molybdenum complex. This could be attributed to the relative

sizes of two metal centres and the difference between Cr-P and Mo-P average bond lengths of 0.1587 Å. In the infrared spectrum a sharp absorption was observed at 1932 cm$^{-1}$ with a much broader absorption at 1827 cm$^{-1}$, which can be assigned to the carbonyl groups. This is similar to that of the molybdenum complex, although with a value 8 cm$^{-1}$ lower and this would suggest weaker π-acidity than the molybdenum complex. Another broad peak at 2305 cm$^{-1}$ can be attributed to the P-H stretch. In comparison, the facial complex of [Cr(CO)$_3$(PMe$_2$Ph)$_3$] also has similar absorptions for carbonyl stretches at 1923 and 1820 cm$^{-1}$ [42].

### 2.3.3 Metal Complexes Comparison

Since the degree of π-acid character can be determined quantitatively from the position of the CO stretch in the IR spectrum it is pertinent to compare the complexes synthesised here with those in the literature, as in **Table 2.1**.

| Complex | $v_{CO}$ (cm$^{-1}$) | $^{31}$P NMR (ppm) | Ref. |
|---|---|---|---|
| [Mn(CO)$_3$(PH$_2$Ph)$_3$]CF$_3$SO$_3$ | 2041, 1963 | -23.0 | [43] |
| [Fe(Cp)(CO)$_2$(PH$_2$Ph)]I | 2038, 1965 | | [44] |
| [Cr(CO)$_4$(PH$_2$Ph)$_2$] | 2023, 1939 | | [44] |
| [Mo(CO)$_3$(PH$_2$Ph)$_3$] | 1957, 1866 | | [45] |
| [W(CO)$_3$(PH$_2$Ph)$_3$] | 1951, 1858 | -72.0 | [45] |
| [Mn(CO)$_3$(PHPh$_2$)$_3$]ClO$_4$ | 2038, 1965 | | [43] |
| [Mo(CO)$_3$(PHPh$_2$)$_3$] | 1947, 1855 | 22.0 | [45] |
| [W(CO)$_3$(PHPh$_2$)$_3$] | 1942, 1851 | 4.3 | [45] |
| [Cr(CO)$_3$(PPh$_3$)$_3$] | 1940, 1840 | | [46] |
| [W(CO)$_3$(PPh$_3$)$_3$] | 1935, 1840 | | [46] |
| [Mo(CO)$_3$(PPh$_3$)$_3$] | 1935, 1835 | | [46] |
| | | | |
| [Fe(Cp)(**2-fpp**)$_3$]PF$_6$, (**11**) | - | -24.7 | - |
| [Mo(CO)$_3$(**2-fpp**)$_3$], (**10**) | 1940, 1836 | -75.8 | - |
| [Cr(CO)$_3$(**2-fpp**)$_3$], (**12**) | 1932, 1827 | -38.6 | - |

**Table 2.1** Comparison of a selection of phosphine complexes with a variety of metal centres with the synthesised 2-fluorphenyl phosphine complexes

Comparing the various molybdenum complexes, it can be seen that with 2-fluorphenyl phosphine as a ligand, the π-acid character is mid-way between that of triphenyl phosphine (1935cm$^{-1}$) and diphenyl phosphine (1947cm$^{-1}$). Phenyl phosphine is the best π-acid of these ligands with a $v_{CO}$ stretch at 1957cm$^{-1}$. Conversely, the chromium complexes see a slight variation in these values. The 2-fluorophenyl phosphine complex produces a $v_{CO}$ stretch at 1932cm$^{-1}$, 8cm$^{-1}$ lower than that of the triphenylphospine complex. This indicates that, for chromium at least, the 2-fluorophenyl phosphine complex is a worse π-acid compared with triphenylphosphine. It would appear from the literature values, that a manganese complex with phenyl phosphine is still the best template for creating a strong π-acid.

## 2.4 Experimental

### 2.4.1 General Procedures

All synthetic procedures were carried out under an atmosphere of dry nitrogen using standard Schlenk line techniques. All solvents were freshly distilled under nitrogen from sodium (diethyl ether, petroleum ether and tetrahydrofuran) or calcium hydride (acetonitrile, dichloromethane and chloroform) before use. $^1$H NMR spectra were obtained using Bruker 250, 400 and 500 MHz spectrometers referenced to tetramethylsilane ($\delta$= 0 ppm). $^{31}$P{$^1$H} (and $^{31}$P), $^{19}$F{$^1$H} and $^{13}$C{$^1$H} NMR spectra were recorded on a Jeol Eclipse 300 MHz spectrometer operating at 121.17 MHz, 282.8 MHz and 75.6 MHz respectively. $^{31}$P{$^1$H} and $^{19}$F{$^1$H} chemical shifts are referenced to external $H_3PO_4$ ($\delta$= 0 ppm) and external $CFCl_3$ respectively. All NMR spectra were recorded at 293 K unless otherwise stated. Infrared spectra were recorded from the pure solid on a Shimadzu IRAffinity-1 FTIR spectrometer. Mass spectra were obtained using a Waters LCT Premier XE mass spectrometer.

### 2.4.2 2-fluorophenyl-diethylphosphonate, 2

Triethylphosphite (85.7 ml, 0.05 mol) was added dropwise to a suspension of nickel bromide (5.44 g, 0.025 mol) in 1-fluoro-2-bromobenzene (54.7 ml, 0.05 mol) at 160 $^O$C in a standard distillation apparatus in a nitrogen atmosphere. After no more ethyl bromide distilled over the residue was distilled in vacuo to give the title compound as a clear liquid. Yield 56.4 g (49%) $^1$H-NMR (CDCl$_3$): $\delta$ 7.83 (m, 1H, H$_{AR}$), 7.51 (m, 1H, H$_{AR}$), 7.21 (m, 1H, H$_{AR}$), 7.11 (m, 1H, H$_{AR}$), 4.13 (m, 4H, **OCH$_2$**CH$_3$), 1.31 (t, $^3J_{H-H}$ = 7.1 Hz, 6H, OCH$_2$**CH$_3$**) $^{13}$C{$^1$H}-NMR (CDCl$_3$): $\delta$ 163.7 (d, $^2J_{C-F}$ = 252 Hz) 135.2 (s) 135.1 (s) 124.5 (dd, $^4J_{C-P}$ = 3.3 Hz, $^3J_{C-F}$ = 13.8 Hz) 117.5 (dd, $^3J_{C-P}$ = 7.9 Hz. $^4J_{C-F}$ = 22.5 Hz) 116.7 (dd, $^1J_{C-P}$ = 187 Hz, $^2J_{C-F}$ = 18.4 Hz) 62.8 (d, $^2J_{C-P}$ = 5.5 Hz) 16.5 (d, $^3J_{C-P}$ = 6.5 Hz) $^{19}$F{$^1$H}-NMR (CDCl$_3$): $\delta$ -101.34. $^{31}$P{$^1$H}-NMR (CDCl$_3$): $\delta$ 14.3

### 2.4.3 2-fluorophenyl phosphine, 3

Trimethylsilylchloride (31.7 ml, 0.25 mol) was added dropwise at -78 $^O$C to a stirred solution of lithium aluminum hydride (9.49 g, 0.25 mol) in THF (50 ml) under $N_2$. The mixture was allowed to warm to room temperature and stir for 2 hours. Then a solution of 2-fluorophenyl-diethylphosphonate (27.86 g, 0.12 mol) and THF (50 ml) was added dropwise at -30 $^O$C, then allowed to warm to room temperature and stir for 22 hours. Water (5 ml) was then added, followed by 15% NaOH (5 ml) and water (15 ml) again separating the two layers. The aqueous layer was extracted with diethyl ether (2 x 40 ml), the organic layers combined, dried over magnesium sulfate and concentrated to form the title compound as a clear liquid, 11.79 g (77%). $^1$H-NMR (CDCl$_3$): δ 7.38 (m, 1H, H$_{AR}$), 7.21 (m, 1H, H$_{AR}$), 6.97 (m, 2H, H$_{AR}$), 3.81 (dd, $^1$J$_{P-H}$ = 205.2 Hz, $^4$J$_{F-H}$ =4.1 Hz, 2H, **PH$_2$**) $^{13}$C{$^1$H}-NMR (CDCl$_3$): δ 162.0 (d, $^1$J$_{C-F}$ = 251 Hz) 134.5 (dd, J = 5 Hz, J = 17 Hz) 128.7 (d, J = 8 Hz) 128.0 (d, J = 8 Hz) 122.3 (dd, J = 4 Hz, J = 5 Hz) 114.1 (d, J = 13 Hz) $^{19}$F{$^1$H}-NMR (CDCl$_3$): δ -101.98. $^{31}$P{$^1$H}-NMR (CDCl$_3$): δ -149.13

### 2.4.4 [Cu(2-fpp)$_3$Cl], 7

To a stirred solution of CuCl (0.020 g, 2.2x10$^{-4}$ mol) in dichloromethane (dried and degassed) under $N_2$ was added 2-fluorophenylphosphine (0.10 g, 7.7x10$^{-4}$ mol) and stirred for 10 minutes until completion of the reaction. The solution was filtered, reduced in vacuo, washed with petroleum ether and then recrystallised from dichloromethane utilising vapour diffusion to produce the title compound as a white solid. Yield 0.08 g (75%) $^1$H-NMR (CDCl$_3$): δ 7.81 (m, 1H, H$_{AR}$), 7.33 (m, 1H, H$_{AR}$), 7.05 (m, 2H, H$_{AR}$), 4.35 (d, $^1$J$_{P-H}$ = 300.48 Hz, **PH$_2$**) $^{13}$C{$^1$H}-NMR (CDCl$_3$): δ 163.60 (d, $^1$J$_{C-F}$ = 900 Hz) 137.10 (d, J = 77 Hz) 132.59 (s) 124.71 (d, J = 59 Hz) 115.34 (d, J = 91 Hz) $^{19}$F{$^1$H}-NMR(CDCl$_3$): δ -101.9 $^{31}$P{$^1$H}-NMR (CDCl$_3$): δ -128.8

### 2.4.5 [Cu(2-fpp)$_4$]BF$_4$, 8

To a stirred solution of [Cu(MeCN)$_4$]BF$_4$ (0.35 g, 1.11 x 10$^{-3}$ mol) in dichloromethane (dried and degassed) under N$_2$ was added 2-fluorophenylphosphine (0.50 g, 3.89 x 10$^{-3}$ mol) and stirred for 10 minutes until completion of the reaction. The solution was filtered, reduced under vacuo, washed with petroleum ether to produce the title compound as a white gel. Yield 0.41 g (64%) $^{19}$F{$^1$H}-NMR(CDCl$_3$): δ -102.8 $^{31}$P{$^1$H}-NMR (CDCl$_3$): δ -121.99

### 2.4.6 [Mn(CO)$_3$(2-fpp)$_3$]PF$_6$, 9

To a stirred solution of [Mn(CO)$_3$(MeCN)$_3$]PF$_6$ (0.10 g, 2.5x10$^{-4}$ mol) in dichloromethane (dried and degassed) under N$_2$ add 2-fluorophenylphosphine (0.11 g, 8.75x10$^{-4}$ mol) and stir until completion of the reaction. The solution was then filtered, evaporated to dryness and triturated in petroleum ether. Yield 0.10 g, (60%) $^1$H-NMR (CDCl$_3$): δ 7.14 (m, 4H, H$_{AR}$), 5.22 (m, 2H, **PH$_2$**) $^{19}$F{$^1$H}-NMR(CDCl$_3$): δ -101.47 (s, **C-F**) -70.74 (d, $^1$J$_{P-F}$ = 757.89 Hz, **PF$_6$**) $^{31}$P{$^1$H}-NMR (CDCl$_3$): δ -40.40 (s, **Mn-P**) -143.14 (p, $^1$J$_{P-F}$ = 1754.73 Hz, **PF$_6$**)

### 2.4.7 [Mo(CO)$_3$(2-fpp)$_3$], 10

To a stirred solution of [Mo(CO)$_3$(mesitylene)] (0.15 g, 5.0x10$^{-4}$ mol) in dichloromethane (dried and degassed) under N$_2$ add 2-fluorophenylphosphine (0.22 g, 1.75x10$^{-3}$ mol) and stir until completion of the reaction. The solution was then filtered, evaporated to dryness and triturated in petroleum ether. Crystals of the title compound were obtained by recrystallisation through vapour diffusion. Yield 0.24 g (85%) $^1$H-NMR (CDCl$_3$): δ 7.33 (m, 1H, H$_{AR}$), 7.24 (m, 1H, H$_{AR}$), 7.03 (m, 1H, H$_{AR}$), 6.95 (m, 1H, H$_{AR}$), 5.07 (d, , $^1$J$_{P-H}$ = 331.485 Hz, **PH$_2$**) $^{13}$C{$^1$H}-NMR (CDCl$_3$): δ 162.56 (d, $^1$J$_{C-F}$ = 975 Hz) 134.32 (s), 131.83 (d, J = 27.6 Hz) 124.55 (s) 115.20 (d, J = 91 Hz) $^{19}$F{$^1$H}-NMR(CDCl$_3$): δ -103.6 $^{31}$P{$^1$H}-NMR (CDCl$_3$): δ -75.76 IR: 2308 (s, PH) 1940 (s, CO) 1836 (s, CO) HRMS (ES): expected 564.2262, obtained 604.9103 (+MeCN 41.0527)

## 2.4.8 [Fe(Cp)(2-fpp)$_3$]PF$_6$, 11

To a stirred solution of [Fe(Cp)(p-Xylene)]PF$_6$ (0.20 g, 5.5x10$^{-4}$ mol) in dichloromethane (dried and degassed) under N$_2$ add 2-fluorophenylphosphine (0.25 g, 1.925x10$^{-3}$ mol) and stir for twelve hours. The solution was then filtered, evaporated to dryness and triturated in petroleum ether. Crystals of the title compound were obtained by recrystallisation through vapour diffusion. Yield 0.34 g (95%) $^1$H-NMR (CDCl$_3$): δ 7.41 (m, 1H, H$_{AR}$), 7.19 (m, 1H, H$_{AR}$), 7.05 (m, 2H, H$_{AR}$), 4.66 (d, $^1$J$_{P-H}$ = 156.375 Hz, **PH$_2$**) $^{19}$F{$^1$H}-NMR(CDCl$_3$): δ -103.75 (s, **C-F**) -71.70 (d, $^1$J$_{P-F}$ = 757.89 Hz, **PF$_6$**) $^{31}$P{$^1$H}-NMR (CDCl$_3$): δ -24.72 (s, **Fe-P**) -143.50 (p, $^1$J$_{P-F}$ = 1762 Hz, **PF$_6$**) IR 1940 (s, CO) 1836 (s, CO) HRMS (ES): expected 505.1867, obtained 505.0302

## 2.4.9 [Cr(CO)$_3$(2-fpp)$_3$], 12

To a stirred solution of [Cr(CO)$_3$(MeCN)$_3$] (0.181 g, 7.0 x 10$^{-4}$ mol) in dichloromethane (dried and degassed) under N$_2$ was added 2-fluorophenylphosphine (0.31g, 2.45 x 10$^{-3}$ mol) and stir until completion of the reaction. The solution was then filtered, evaporated to dryness and triturated in petroleum ether. Crystals of the title compound were obtained by recrystallisation through vapour diffusion. Yield 0.331 g (91%) $^1$H-NMR (CDCl$_3$): δ 7.31 (m, 1H, H$_{AR}$), 7.19 (m, 1H, H$_{AR}$), 7.09 (m, 1H, H$_{AR}$), 7.01 (m, 1H, H$_{AR}$) 5.16 (d, $^1$J$_{P-H}$ = 329.83 Hz, **PH$_2$**) $^{13}$C{$^1$H}-NMR (CDCl$_3$): δ 162.80 (d, $^1$J$_{C-F}$ = 957 Hz) 133.86 (m) 132.02 (m) 124.84 (m) 115.71 (m) $^{19}$F{$^1$H}-NMR(CDCl$_3$): δ -104.17 $^{31}$P{$^1$H}-NMR (CDCl$_3$): δ -38.61 IR: 2304 (s, PH) 1932 (s, CO) 1827 (s, CO) HRMS (ES): expected 520.2822, obtained 558.9476 (+K 39.098)

## 2.5 Conclusion

In conclusion, our novel approach to producing a single monodentate ligand for coordination to a metal centre has been successful. 2-fluorophenyl phosphine, **3**, was synthesised in good yield from its phosphonate precursor, **2**, using a standard lithium aluminium hydride reduction. It has been coordinated to a variety of metal centres, **7-12**, both neutral and cationic, with no preference for differing counter ions or the first and second row transition metals. There seems to be no inhibiting factors preventing the phosphine coordinating to any of the metal centres in a facial manner as all reactions were completed in under 30 minutes (apart from iron, which must be stirred overnight). The copper metal, **7-8**, seemed to be the most accepting of the phosphine ligand as the reaction was completed almost instantaneously. However it was particularly difficult to work up, often decomposing during the process and this is likely due to the highly labile nature of the copper centre. Further investigation will be required to see if the 2-fluorophenyl phosphine, **3**, can be cyclised with a suitable base and then the macrocycle liberated from the metal centre.

# Chapter 3

Towards [9]aneP$_3$R$_1$

Macrocyles

## 3.1 Introduction

Lowry and Helm[47] have produced a direct synthesis of a triphosphacyclononane macrocycle without the use of a transition metal complex. The synthesis was accomplished through the reaction of lithium bis(2-phenylphosphidoethyl)phenyl phosphine with 1,2-dichloroethane, shown in **Scheme 3.1**, using low concentration and high temperature conditions.
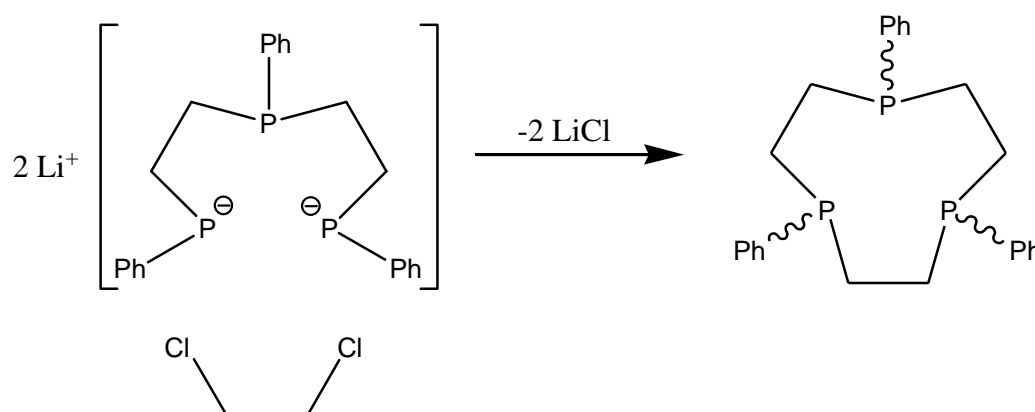


**Scheme 3.1**: Synthesis of [9]aneP$_3$Ph$_3$ by high dilution reaction of lithium bis(2-phenylphosphidoethyl)phenyl phosphine with 1,2-dichloroethane

Syntheses such as these are not without their problems, the Helm group produced a mixture of syn-syn and syn-anti isomers at a ratio of 3:7, along with 15% of the yield being lost to polymerisation. Furthermore high dilution techniques require significant quantity of solvents which can add significant costs to the synthesis.

Making an aliphatic triphosphine such as Helm's but using a different synthesis for the ring formation, could be very advantageous. Work by R. B. King[48] has shown suitable syntheses of aliphatic triphosphines through the reaction of primary phosphines with two equivalents of vinyl phosphonates. To complete the macrocyclic ring, template synthesis will need to be utilised, coordinating the triphosphine before closing the ring. Calcium would make a suitable template metal due to its empty d orbitals which will readily accept the π-back bonding from the phosphorus atoms.

## 3.2 Synthesis of [9]aneP$_3$Bz

The synthesis of the triphosphine is achieved through the coupling of two equivalents of vinyl phosphonate with a primary phosphine using potassium *tert*-butoxide as a base. This is then reduced using a standard lithium aluminium hydride mixture to produce the linear triphosphine, as shown in **Scheme 3.2**.
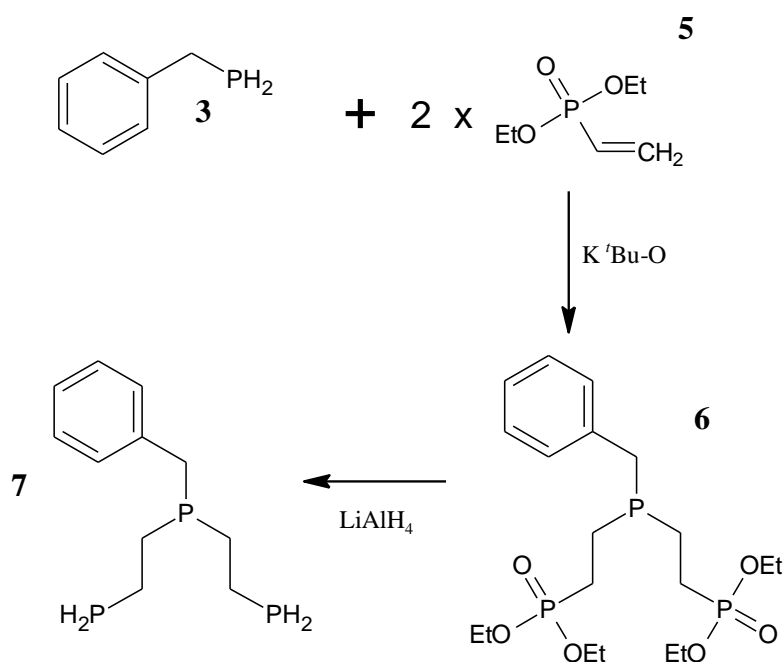


**Scheme 3.2**: Proposed synthesis of BzP(EtPH$_2$)$_2$, **7**

The triphosphine produced can then be deprotonated at the terminal phosphines by using a suitable reagent, such as sodium dimsyl[49]. This dinucleophile can then be used to attack an electrophilic metal source such as calcium chloride to give the metal phosphide. The hope is that this template will allow a ring-closing metathesis with ethylene sulfate[50] to produce the desired triphosphine macrocycle, as shown in **Scheme 3.3**.
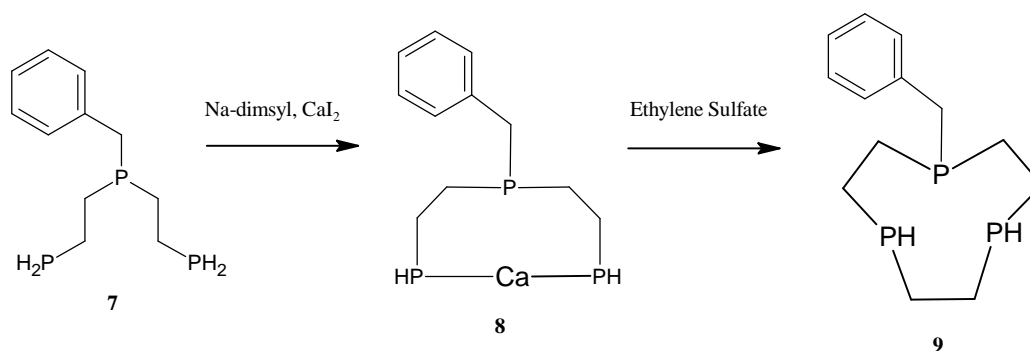
**Scheme 3.3**: Proposed synthesis of [9]aneP$_3$Bz, **9**

## 3.3 Synthesis of BzPH$_2$, 3

The formation of benzyl phosphine, **3**, was achieved through the synthesis of the Grignard reagent, followed by the formation of the phosphorus dichloride before being reduced by lithium aluminium hydride reduction mixture, illustrated in **Scheme 3.4** below.
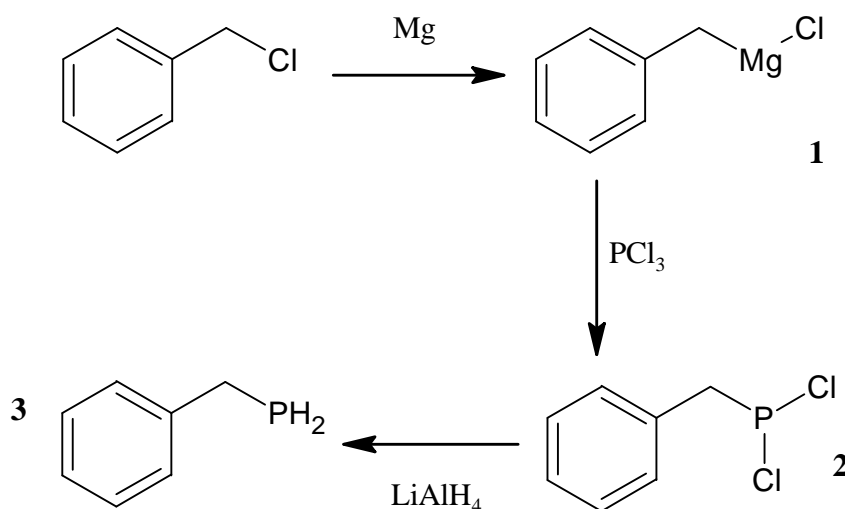


**Scheme 3.4**: Proposed synthesis of BzPH$_2$, **3**

The synthesis of BzMgCl, **1**, was conducted using a standard synthesis for Grignard reagents. Magnesium turnings were placed in a 3L round bottomed flask with 1L of diethyl ether and benzyl chloride added dropwise until the exotherm is established. The addition is then tempered according to the exotherm so that a steady reflux is

maintained. The reflux eventually subsides as the mixture changes colour from colourless to a dark yellow, which is due to the synthesis of the Grignard and the formation of colloidal magnesium. The mixture is then filtered and the strength of the Grignard was determined via titration using 0.1M HCl solution.

BzPCl$_2$, **2**, was prepared according to an adapted literature method from Weil et al[51]. The solution of **1** was added to a 3L round bottomed flask equipped with a mechanical stirrer and anhydrous zinc chloride powder added in small portions at 0 $^O$C. The mixture, warmed to room temperature, was then stirred for an hour. The white suspension was next cooled to -80 $^O$C and phosphorus trichloride added quickly before warming slowly to room temperature before stirring for 10 hours. The copious white precipitate was allowed to settle and the diethyl ether filtered off, the precipitate was washed with ether, the filtrates combined before distilling off the volatiles and characterising by $^1$H and $^{31}$P{$^1$H} NMR spectroscopy. The $^1$H NMR spectrum shows a five proton multiplet at δ 7.33 ppm relating to the aromatic hydrogens, which was too broad to determine individual proton environments. A doublet at δ 3.72 ppm (d, $^1J_{C-H}$ = 15.39 Hz) was also observed relating to the CH$_2$ hydrogens. In the $^{31}$P{$^1$H} NMR spectrum an individual singlet was observed at δ 179.07 ppm which is typical of phosphorus chlorides.

The formation of benzyl phosphine, **3**, was achieved through a standard lithium aluminium hydride reduction. **3**, was added to a mixture of LiAlH$_4$ and diethyl ether at ice temperature and then, once warmed to room temperature, refluxed for 1 hour. Conventional work up followed by distillation afforded the phosphine in a good reproducible yield. Benzyl phosphine was characterised by $^1$H, $^{13}$C{$^1$H} and $^{31}$P{$^1$H} NMR spectroscopy. A singlet resonance was seen in the $^{31}$P{$^1$H} NMR spectrum at δ -120.9ppm, which is typical of primary phosphines and markedly different to the singlet observed with the benzyl dichlorophosphine. The $^1$H NMR spectrum reveals a similarly broad aromatic hydrogen region but now also shows a multiplet at δ 2.91 ppm for the CH$_2$ hydrogens and a triplet of doublets at δ 3.37 ppm (t, 1H, $^1J_{P-H}$ = 7.47Hz) and  δ 2.72 ppm (t, 1H, $^1J_{P-H}$ = 7.5Hz) produced by the phosphine hydrogens. This splitting is due to the ½ spin nuclei of phosphorus, which normally splits its own hydrogens into a triplet, but being influenced by the two hydrogens on the CH$_2$ instead produces a triplet of doublets.

## 3.4 Synthesis of PO(OEt)₂(vinyl), 5

The formation of the vinyl phosphonate was performed via a simple Arbusov – Michaelis reaction of triethyl phosphite and 1,2-dibromoethane before dehydrobromination to give the vinyl phosphonate as shown in **Scheme 3.5**.
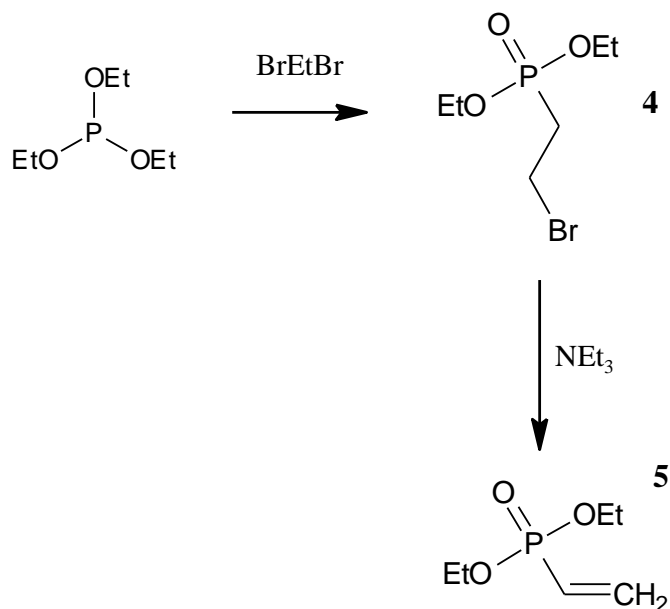


**Scheme 3.5**: Proposed synthesis of PO(OEt)₂(vinyl), **5**

The synthesis of bromoethyl phosphonate was achieved though an adapted literature method of Bride et al[52], which used triethyl phosphite and 1,2-dibromoethane. The phosphite was added dropwise to five equivalents of the 1,2-dibromoethane in a standard distillation apparatus under an inert atmosphere at 140 $^O$C. The reaction was designated as completed once the ethyl bromide had finished distilling over, the product was then obtained as a clear colourless liquid by distilling in vacuo and was characterised by $^1$H, $^{13}$C{$^1$H} and $^{31}$P{$^1$H} NMR spectroscopy. The $^1$H NMR spectrum showed four differing hydrogen environments as expected, the esteric protons produced a multiplet at δ 4.01 ppm and the terminal hydrogens adjacent to them produced a triplet at δ 1.23 ppm ($^1J_{H-H}$ = 7.05 Hz). The hydrogens on the same carbon as the bromide showed a quartet at δ 3.42 ppm ($^1J_{H-H}$ = 8.55 Hz) while the CH₂ group adjacent to it showed a multiplet at δ 2.28 ppm. In the $^{13}$C{$^1$H} NMR spectrum, the addition of the ethyl bromide chain to the phosphite was further confirmed by a

doublet δ 30.97 ppm ($^1J_{C-P}$ = 540.48 Hz). The $^{31}P\{^1H\}$ NMR spectrum showed one singlet resonance at δ 26.14 ppm confirming there was no starting material remaining.

The synthesis of the vinyl phosphonate was again achieved through an adapted literature method of Bride at al. The ethyl bromide phosphonate was placed in a round bottomed flask, put under nitrogen and cooled to -30 $^O$C. A solution of triethylamine and toluene was then added slowly, with stirring, and allowed to warm to room temperature. The solution was then stirred for 72 hours whereupon the triethylamine hydrobromide solid produced was filtered off, the vinyl phosphonate isolated by vacuum transfer and then characterised by $^1H$, $^{13}C\{^1H\}$ and $^{31}P\{^1H\}$ NMR spectroscopy. The $^1H$ NMR spectrum showed the same shifts for the esteric protons as in the ethyl bromide phosphonate, a doublet of quartets overlapping each other at δ 3.92 ppm ($^1J_{H-H}$ = 7.26 Hz) and a triplet at δ 1.16 ppm ($^1J_{H-H}$ = 7.02 Hz). The vinyl hydrogens produced two different envrionments with multiplets at δ 6.08 ppm (CH$_2$C**H**) and δ 5.88 ppm (C**H$_2$**CH). This was further confirmed by $^{13}C\{^1H\}$ NMR spectrum which showed a singlet at δ 135.67 ppm and doublet at δ 126.18 ppm ($^1J_{C=C}$ = 732.9 Hz). The $^{31}P\{^1H\}$ NMR spectrum produced an individual singlet at δ 17.83 ppm determing that the reaction was complete.

## 3.5 Synthesis of BzP(CHCH$_2$PH$_2$)$_2$, 7

The synthesis of BzP(CHCH$_2$P(O)(OEt)$_2$)$_2$ was accomplished by a novel coupling reaction using potassium *tert*-butoxide. A solution of benzyl phosphine and vinyl phosphonate in tetrahydrofuran were added to a round bottomed flask under a nitrogen atmosphere. A suspension of potassium *tert*-butoxide in tetrahydrofuran was then added from a pressure equalised dropping funnel while the heat was increased, this was done in such a way that reflux was obtained as the addition finished. During the addition the reaction mixture turned straw yellow and cloudy. The colour intensified as the addition progresses turning orange on completion. The reflux is then maintained for three hours, the end of which sees the reaction mixture becomes a viscous clear straw yellow solution. The reaction can be followed by $^{31}P\{^1H\}$ NMR spectroscopy, where the benzyl phosphine can be seen turning from a primary phosphine, to a secondary and finally tertiary phosphine (**Figure 3.1**).
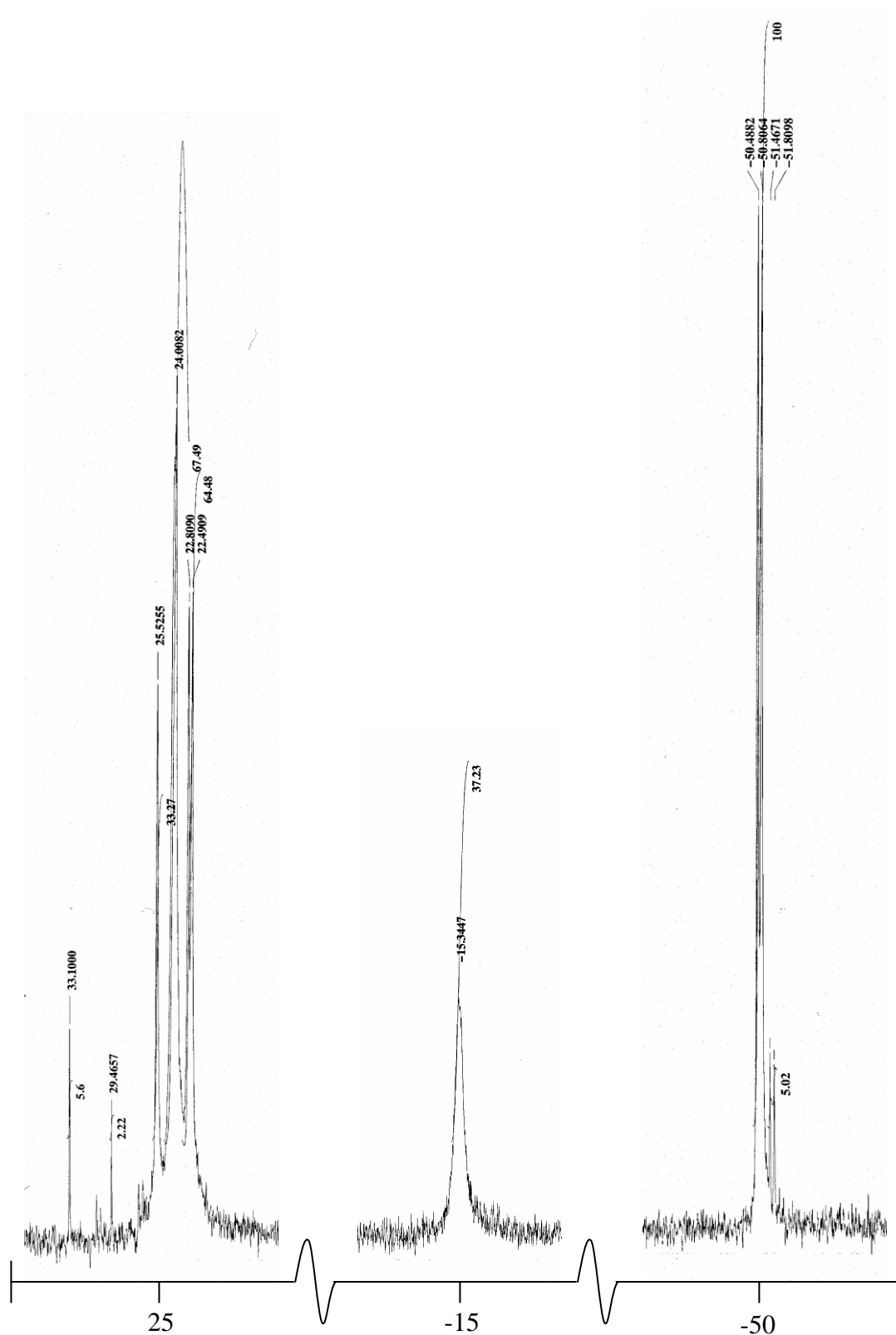
**Figure 3.1**: $^{31}P$ NMR spectrum of BzP(EtP(O)(OEt)$_2$)$_2$, **6**, mid-reaction illustrating the mono-coupled (A) and di-coupled (B) species

The free phosphine is seen at δ -120.9 ppm, the secondary at approximately δ -50.8 ppm and the tertiary at approximately δ -15.3 ppm. A complex series of multiplets are also seen between δ 22-26 ppm, which are attributed to the phosphonate phosphorus environment.

Following workup, the product was reduced utilising a standard lithium aluminium hydride reduction. The phosphonate was added drop wise to a reducing mixture of lithium aluminium hydride and diethyl ether in an inert atmosphere and at ice bath temperature. Once warmed to room temperature the mixture was refluxed for an hour the mixture was hydrolysed, the organic and aqueous layers separated and the volatiles removed to give the triphosphine as a clear colourless oil. The triphosphine was characterised by $^{31}P\{^1H\}$ and $^{31}P$ NMR spectroscopy, which showed two distinct environments for the tertiary and primary phosphine. The tertiary phosphine was observed as a singlet at δ -19.3 ppm (s, Bz**P**) in both spectra confirming there are no hydrogens bonded to the phosphorus atom, whereas the terminal phosphines produced a singlet at δ -128.3 ppm in the hydrogen decoupled spectrum and a triplet (t, **P**H$_2$, $^2J_{P-H}$ = 525.96 Hz) in the $^{31}P$ NMR spectrum, thus confirming the terminal phosphines as primary as shown in **Figure 3.2**.

The reduction of the phosphonate, **6**, was not a simple procedure, the conditions of which, having a clear effect on the outcome. Cleavage between the benzyl and tertiary phosphine was particularly common thereby producing a chain of two primary and one secondary phosphine, which was confirmed by $^{31}P\{^1H\}$ and $^{31}P$ NMR spectra and is illustrated in **Figure 3.3**. In the $^{31}P\{^1H\}$ NMR spectrum the tertiary phosphine singlet had shifted from δ -19.3 ppm to δ -62.8 ppm and furthermore the $^{31}P$ NMR spectrum showed a change from a singlet to a doublet δ -63.1 ppm (d, C**P**C, $^2J_{P-H}$ = 495.57 Hz). The $^1H$ NMR spectrum also confirmed that there were no aromatic hydrogens present thereby proving that the cleavage occured between the benzyl CH$_2$ and the tertiary phosphorus atom.
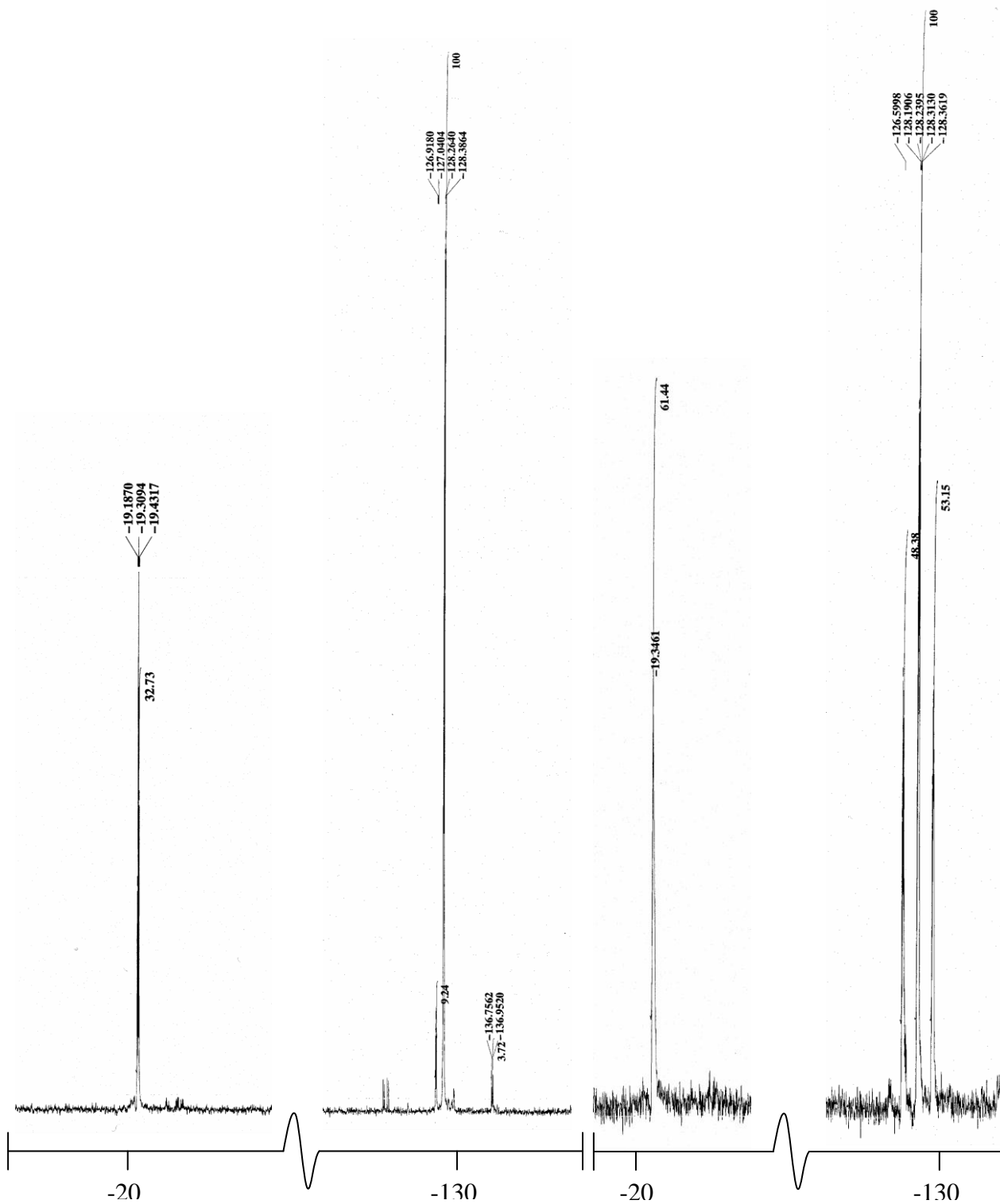
**Figure 3.2**: $^{31}P\{^{1}H\}$ NMR spectrum (left) and $^{31}P$ NMR spectrum (right) of BzP(EtPH$_2$)$_2$, **7**
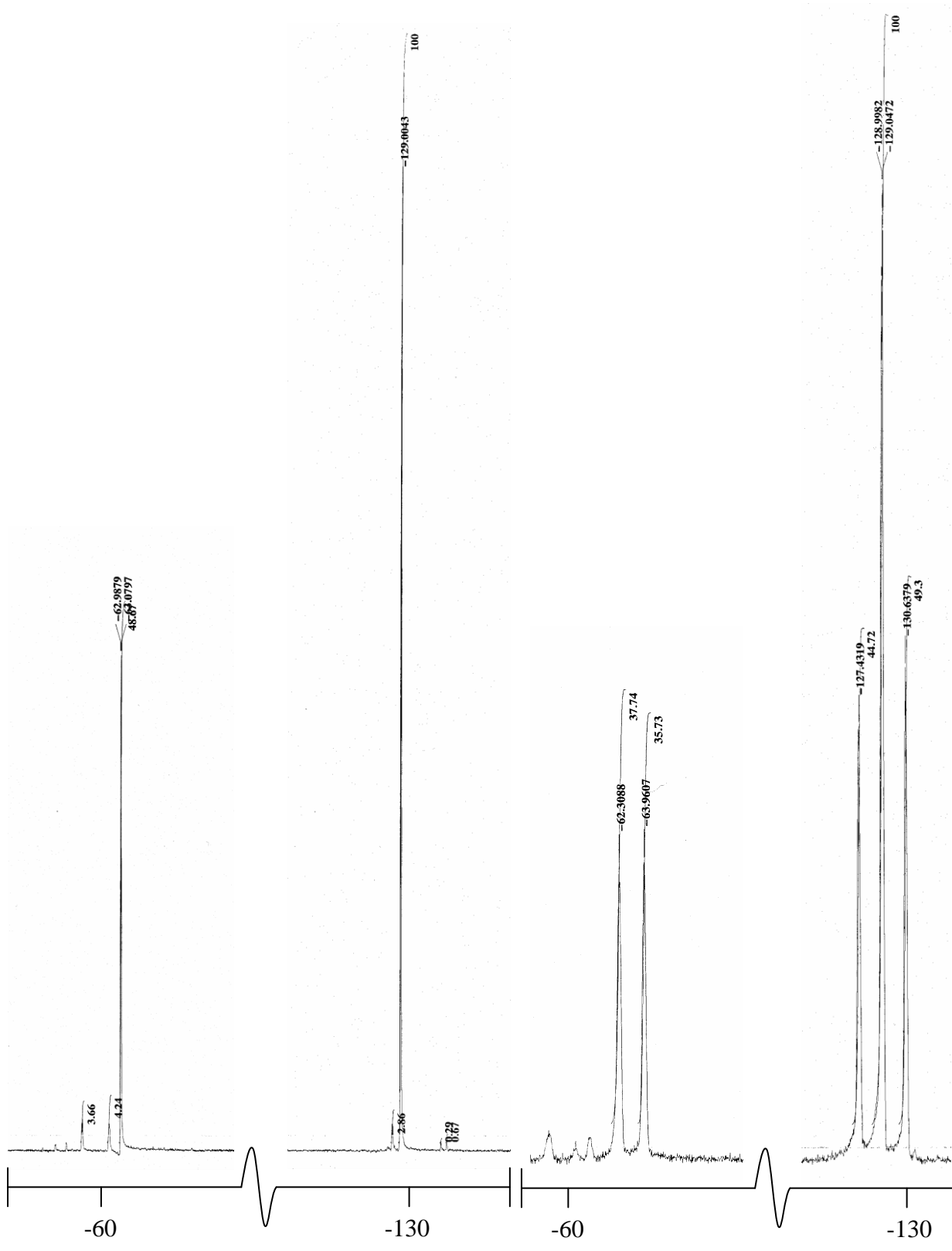
**Figure 3.3**: $^{31}P\{^{1}H\}$ NMR spectrum (left) and $^{31}P$ NMR spectrum (right) of HP(EtPH$_2$)$_2$, **10**

## 3.6 Attempted synthesis of [9]aneP$_3$Bz, 9

This synthesis was attempted in a sealed flask containing BzP(CHCH$_2$PH$_2$)$_2$ and dimethyl sulfoxide. Sodium dimsyl was added drop wise with stirring, under a nitrogen atmosphere at -78 $^O$C. After addition the solution was warmed to room temperature in a water bath for 5 minutes where a dark grey solution was observed and was then cooled down to -78 $^O$C. Calcium iodide was added as a suspension in dimethyl sulfoxide and the mixture was again warmed to room temperature in a water bath whereupon the suspension dissolved. The solution was cooled down to -78 $^O$C and ethylene sulfate in dimethyl sulfoxide was added before once again being warmed to room temperature. It was hoped at this point a precipitate of calcium sulfate would form indicating that the ring closure had been successful, however no precipitate was forthcoming and upon inspection by $^{31}$P{$^1$H} NMR spectroscopy and mass spectrometry no macrocycle was found.

## 3.7 Experimental

### 3.7.1 General Procedures

All synthetic procedures were carried out under an atmosphere of dry nitrogen using standard Schlenk line techniques. All solvents were freshly distilled under nitrogen from sodium (diethyl ether, petroleum ether and tetrahydrofuran) or calcium hydride (acetonitrile, dichloromethane and chloroform) before use. $^1$H NMR spectra were obtained using Bruker 250, 400 and 500 MHz spectrometers referenced to tetramethylsilane ($\delta$= 0 ppm). $^{31}$P{$^1$H} (and $^{31}$P), $^{19}$F{$^1$H} and $^{13}$C{$^1$H} NMR spectra were recorded on a Jeol Eclipse 300 MHz spectrometer operating at 121.17 MHz, 282.8 MHz and 75.6 MHz respectively. $^{31}$P{$^1$H} and $^{19}$F{$^1$H} chemical shifts are referenced to external $H_3PO_4$ ($\delta$= 0 ppm) and external $CFCl_3$ respectively. All NMR spectra were recorded at 293 K unless otherwise stated. Infrared spectra were recorded from the pure solid on a Shimadzu IRAffinity-1 FTIR spectrometer. Mass spectra were obtained using a Waters LCT Premier XE mass spectrometer.

### 3.7.2 BzMgCl, 1

To a 3 L round bottomed flask equipped with a pressure equalised dropping funnel, condenser with nitrogen inlet and mechanical stirrer was added heated magnesium turnings (56 g, 2.3 mol). The turnings were stirred for an hour and then diethyl ether (2 L) was added. Benzyl chloride, **1**, (253 g, 2 mol) was then added dropwise, the rate of addition being determined by the vigour of the reflux. The solution was filtered and the concentration determined by titration against 0.1 M HCl using phenolphthalein indictor.

### 3.7.3 BzPCl$_2$, 2

BzMgCl, **2**, (700 ml, 1.0 mol) was added to a 3 L round bottomed multi-necked flask equipped with a mechanical stirrer, reflux condenser and nitrogen inlet and solid addition funnel. Diethyl ether (500 ml) was added and then cooled to 0 $^O$C and then anhydrous ZnCl$_2$ (136 g, 1.0 mol) was added in small portions. Once the addition was complete the mixture was warmed to room temperature and stirred for 1 hour. The

white suspension was then cooled to -80 $^O$C and PCl$_3$ (260 ml, 3.0 mol) was added quickly from a pressure equalised dropping funnel. The mixture was allowed to warm to room temperature and then stirred for 10 hours. The copious white precipitate was allowed to settle and the Et$_2$O filtered off. The precipitate was washed with Et$_2$O (2 x 200 ml) and the filtrates combined. The ether was then removed through distillation and the title compound was obtained as a clear colourless liquid. Yield 121.11 g (63%) $^1$H-NMR (CDCl$_3$): δ 7.33 (m, 5H, H$_{AR}$) 3.72 (d, 2H, $^1$J$_{H\text{-}H}$ = 15.39Hz) $^{31}$P{$^1$H}-NMR (CDCl$_3$): δ 179.07

### 3.7.4 BzPH$_2$, 3

To a stirred mixture of LiAlH$_4$ (3.80 g, 0.1 mol) in diethyl ether (200 ml) add BzPCl$_2$, **2**, (19.3 g, 0.1 mol) dropwise in an inert atmosphere while being cooled in ice. Warm to room temperature and then reflux for 1 hour. The mixture was then hydrolysed with water (2 ml) followed by a 15% NaOH solution (2 ml) and finally water (6 ml). The aqueous and organic layers were separated with the aqueous layer being washed with diethyl ether (2 x 20 ml) and the title compound was distilled from solution as clear colourless liquid. Yield 12.09 g (97%) $^1$H-NMR (CDCl$_3$): δ 7.28 (m, 5H, H$_{AR}$) 3.37 (t, 1H, $^1$J$_{P\text{-}H}$ = 7.5 Hz) 2.91 (m, 2H, C**H$_2$**) 2.72 (t, 1H, $^1$J$_{P\text{-}H}$ = 7.5 Hz) $^{13}$C{$^1$H}-NMR (CDCl$_3$): δ 142.81 (s) 128.78 (s) 127.88 (s) 125.88 (s) 65.98 (s) 21.03 (d, 2H, $^1$J$_{CH}$ = 41.22 Hz) $^{31}$P{$^1$H}-NMR (CDCl$_3$): δ -120.95

### 3.7.5 PO(OEt)$_2$(EtBr), 4

In a distillation apparatus equipped with a pressure equalised dropping funnel, Triethyl phosphite (133 g, 0.8 mol) was added drop wise to 5 equivalents of 1,2-dibromoethane (752, 4 mol) at 140 $^O$C under a nitrogen atmosphere. Once the distillation of ethyl bromide was completed the product was distilled in vacuo to give the title compound as a clear colourless liquid. Yield 134.97 g (69%) $^1$H-NMR (CDCl$_3$): δ 4.01 (m, 4H, OC**H$_2$**) 3.42 (q, 2H, $^1$J$_{H\text{-}H}$ = 8.55 Hz) 2.28 (m, 2H, PC**H$_2$**) 1.23 (t, 6H, $^1$J$_{H\text{-}H}$ = 7.05 Hz) $^{13}$C{$^1$H}-NMR (CDCl$_3$): δ 63.25 (s) 30.97 (d, $^1$J$_{C\text{-}Br}$ = 540.48 Hz) 24.06 (s) 16.66 (s) $^{31}$P{$^1$H}-NMR (CDCl$_3$): δ 26.14

### 3.7.6 PO(OEt)₂(vinyl), 5

In a round bottomed flask equipped with a magnetic stirrer bar, containing PO(OEt)₂(EtBr), **4**, (24.50 g, 0.1 mol), a solution of Triethylamine (15.3 ml, 0.11 mol) in Toluene (50 ml) was added at -30 $^O$C under nitrogen and stirred for 72 hours. Solid ammonium bromide precipitated out and the solution was then filtered and the title compound was obtained by vacuum transfer to afford a straw coloured clear solution. Yield 14.07 g (86%) $^1$H-NMR (CDCl₃): δ 6.08 (m, 1H, CH₂C**H**) 5.88 (m, 2H, C**H₂**CH) 3.92 (dq, 4H, $^1$J$_{H-H}$ = 7.26 Hz) 1.16 (t, 6H, $^1$J$_{H-H}$ = 7.02 Hz) $^{13}$C{$^1$H}-NMR (CDCl₃): δ 135.67 (s) 126.18 (d, $^1$J$_{C-P}$ = 732.9 Hz) 62.07 (s) 16.60 (s) $^{31}$P{$^1$H}-NMR (CDCl₃): δ 17.83

### 3.7.7 BzP(EtPO(OEt)₂)₂, 6

Benzyl phosphine, **3**, (1.24 g, 0.01 mol) was added to a multi-necked round bottomed flask equipped with a condenser, dropping funnel and nitrogen inlet containing THF (20ml) and PO(OEt)₂(vinyl), **5**, (3.61 g, 0.022 mol) at room temperature. Potassium *t*-butoxide (2.24 g, 0.02 mol) in solution with THF was the added dropwise with increasing temperature so that reflux is obtained as the addition finishes. The mixture was refluxed for 2 hours then filtered and the title compound was distilled from solution as a clear colourless liquid. Yield 2.88 g (64%) $^{31}$P{$^1$H}-NMR (CDCl₃): δ -15.40 (s, 1P, Bz**P**) 31.26 (s, 2P, **P**O)

### 3.7.8 BzP(EtPH₂)₂, 7

To a multi-necked round bottomed flask equipped with a condenser and nitrogen inlet containing lithium aluminium hydride (5.0 g, 0.132 M) in diethyl ether (100 ml) add BzP(EtPO(OEt)₂)₂, **6**, (14.93 g, 0.033 M) dropwise at ice bath temperature. Once the addition is completed the mixture is refluxed for 1 hour. The mixture was then hydrolysed with water (2 ml) followed by a 15% NaOH solution (2 ml) and finally water (6 ml). The aqueous and organic layers were separated with the aqueous layer

being washed with diethyl ether (2 x 20 ml) and the title compound was distilled from solution as clear colourless liquid. Yield 2.57 g (32%) $^{31}$P{$^1$H}-NMR (CDCl$_3$): δ -19.31 (s, 1P, Bz**P**) -128.26 (s, 1P, **P**H$_2$) $^{31}$P-NMR(CDCl$_3$): δ -19.31 (s, 1P, Bz**P**) -128.31 (t, 2P, **P**H$_2$, $^2$J$_{\text{P-H}}$ = 525.96 Hz)

### 3.7.9 HP(EtPH$_2$)$_2$ (bi-product), 10

This triphosphine regularly occured as a bi-product during the synthesis of BzP(EtPH$_2$)$_2$, of which the obtained data follows. $^1$H-NMR (CDCl$_3$): δ 3.66 (m, 5H, P**H**) 1.76 (m, 4H, C**H$_2$**PH) 1.18 (m, 4H, C**H$_2$**PH$_2$) $^{13}$C{$^1$H}-NMR (CDCl$_3$): δ 23.91 (s) 12.99 $^{31}$P{$^1$H}-NMR (CDCl$_3$): δ -63.08 (s), -129.00 (s) $^{31}$P-NMR(CDCl$_3$): δ 63.1 ppm (d, C**P**C, $^2$J$_{\text{P-H}}$ = 495.57Hz) -129.00 (t, 2P, **P**H$_2$, $^2$J$_{\text{P-H}}$ = 484.59 Hz)

### 3.7.10 [9]aneP$_3$Bz (attempted), 9

In a sealed flask containing BzP(EtPH$_2$)$_2$ (0.1 g, 6.5 x 10$^{-4}$ mol) and dimethyl sulfoxide (10 ml) was added sodium dimsyl (1.1 ml, 1.3 x 10$^{-3}$ mol) dropwise with stirring, under a nitrogen atmosphere at -78 $^O$C. After addition the solution was warmed to room temperature in a water bath for 5 minutes and then cooled back down to -78 $^O$C where calcium iodide (0.19 g, 6.5 x 10$^{-4}$ mol) was added as a suspension in dimethyl sulfoxide. The mixture was again warmed to room temperature in a water bath whereupon the suspension dissolved. The solution was cooled down to -78 $^O$C and ethylene sulfate (0.08 g, 6.5 x 10$^{-4}$ mol) in dimethyl sulfoxide was added. It was hoped at this point a precipitate of calcium sulfate would form indicating that the ring closure had been successful, however no precipitate was forthcoming and upon inspection by $^{31}$P{$^1$H} NMR spectroscopy and mass spectrometry no macrocycle was found.

## 3. 8 Conclusion

In conclusion, our new synthesis to the linear triphosphine ligand, **7**, has been moderately successful. The coupling of the benzyl phosphine, **3**, with two equivalents of vinyl phosphonate, **5**, is an simple synthesis for forming the triphosphine precursor, **6**, and can be reduced to the tridentate ligand immediately after filtering. However this does cause cleavage of the benzyl C-P bond resulting in two triphosphine ligands, **7** and **10**. To combat this the precursor, **6**, can be distilled and the reduction conducted using diethyl ether as the solvent (as described in the experimental **3.7.8**). Unfortunately our ring closure utilising a ring closing metathesis with ethylene sulfate failed to work. Further investigation could be done to see with a different substituent would be more successful, for example an ethyl dihalide. Alternatively the calcium source could be used as the base to deprotonate the diphosphine by using calcium bis(trimethylsilyl)amine.

# References

## Chapter 1

[1]     J. P. Collman, L. S. Hegedus, J . R. Norton and R. G. Finke, *Principles and applications of organotransition metal chemistry, 2$^{nd}$ ed., University Science Books¸* Mill Valley, California, 1987

[2]     J. A. Osborn, F. H. Jardine, J. F. Young and G. Wilkinson, *J.Chem. Soc.A*, 1966, 1711

[3]     G. T. Woolley, S. L. Kitson and R. G. Reid, *J. Labelled Compd. Radiopharm.*, 2006, **50**, 468

[4]     R.H. Crabtree, *The Organometallic Chemistry of the Transition Metals*, 4$^{th}$ ed., John Wiley & Son, 2005

[5]     N. N. Greenwood, A. Earnshaw, *Chemistry of the Elements*, 2$^{nd}$ ed., Butterworth-Heinemann, 1997

[6]     K. F. Purcell, J. C. Kotz, *Inorganic Chemistry*, W. B. Saunders, 1997

[7]     A. G. Orpen & N. G. Connelly, *Chem. Commun.*, 1985, 1310

[8]     C. A. Tolman, *Chem. Rev.*, 1977, **77**,313

[9]     P. G. Edwards, J. S. Fleming, S. S. Liyanage, *Inorg. Chem.*, 1996, **35**, 4563

[10]    N. Fey, A. C. Tsipis, S. E. Harris, J. N. Harvey, A. G. Orpen, and R. A. Mansson, *Chem. Eur. J.*, 2006, **12**, 291

[11]    N. Fey, A. G. Orpen, and J. N. Harvey, *Coordination Chemistry Reviews*, 2009, **253**, 704

[12]    G. Schwarzenbach, *Helv. Chim. Acta.* 1952, **35**, 2344

[13]    A. E. Martell, R. D. Hancock, R. J. Motekaitis, *Coord. Chem. Rev.*, 1994, **133**, 39

[14]    F. P. Hinz & D. W. Margerum, *Inorg. Chem.*, 1974, **13**, 2941

[15]    R. D. Hancock, M. P. Ngwenya, *J. Chem. Soc. Dalton. Trans.*, 1987, **12**, 2911

[16]    A. M. Caminade, J. P. Majoral, *Chem. Rev.*, 1994, **94**, 1183

[17]    E. P. Kyba, A. M. John, S. B. Brown, C. W. Hudson, M. J. McPhaul, A. Harding, K. Larsen, S. Niedzwiecki, R. E. Davis, *J. Am. Chem. Soc.*, 1980, **102**,139

[18]    E. P. Kyba & S. S. P. Chou, *J. Am. Chem. Soc.*, 1980, **102**, 7012

[19]    M. A. Fox, K. A. Campbell & E. P. Kyba, *Inorg. Chem.*, 1981, **20**, 4163

[20]    E. P. Kyba, C. N. Clubb, S. B. Larson, V. J. Schueler, R. E. Davis, *J. Am. Chem. Soc.*, 1985, **107**, 2141

[21]    W. Marty, G. Schwarzenbach, *Chimia*, 1970, **24**, 431

[22]    T. A. Deldonno and W. Rosen, *J. Am. Chem. Soc.*, 1977, **99**, 8051

[23]    R. Bartsch, S. Hietkamp, S. Morton, H. Peters and O. Stelzer, *Inorg. Chem.*, 1983, **22**, 3624

[24]  B. N. Diel, P. F. Brandt, R. C. Haltiwanger & A. D. Norman, *J. Am. Chem. Soc.*, 1982, **104**, 4700

[25]  B. N. Diel, P. F. Brandt, R. C. Haltiwanger M. L. J. Hackney, and A. D. Norman, *Inorg. Chem. Soc.*, 1989, **28**, 2811

[26]  D. J. Jones, P. G. Edwards, R. P. Tooze and T. Albers, *J. Chem. Soc., Dalton Trans.,* 1999, 1045

[27]  P. G. Edwards, J. S. Fleming and S. S. Liyange, *Inorg. Chem.,* 1996, **35**, 4563

[28]  T. Albers & P. G. Edwards, *Chem. Comm.*, 2007, **8**, 858

[29]  B. Lambert & J. F. Desreux, *Synthesis*, 2000, **12**, 1668

**Chapter 2**

[30]  T. Albers and P. G. Edwards, *Chem. Commum.*, 2007, **858**

[31]  J. Johnstone, *Ph.D Thesis*, Cardiff University, 2004

[32]  E. Reixach, *Ph.D Thesis*, Cardiff University, 2006

[33]  W. Zhang, *Ph.D Thesis*, Cardiff University, 2005

[34]  G. Tavs, *Chem. Ber.*, 1970, **103**, 2428

[35]  E. P. Kyba, S. T. Liu, R. L. Harris, *Organometallics*, 1983, **2**, 1877

[36]  T. Campbell, A. M. Gibson, R. Hart, S. D. Orchard, S. J.A. Pope, G. Reid, *J. Org. Chem.¸*1999, **592**, 296

[37]  H. Luth, M. R. Truter and A. Robson, *J. Chem. Soc. A*, 1969, 28

[38]  G. Albetin, E. Bordignon, & F. Tonel, *J. Organometallic Chem.*, 2002, **660**, 55

[39]  P. G. Edwards, M. L. Whatton amd R. Haigh., *Organometallics*, 2000, **19**, 2652

[40]  D. Catheline and D. Astruc, *Organometallics*, 1984, **3**, 1094

[41]  A. Dulai, C. L. McMullin, K. Tenza, and D. F. Wass, *Organometallics*, 2011, **30**, 935

[42]  A. M. Bond, S. W. Carr and R. Colton, *Inorg. Chem.*, 1984, **23**, 2343

[43]  J. Connolly, A. R. J. Genge, W. Levason, S. D. Orchard, S. J. A. Pope, G. Reid, *J. Chem. Soc. Dalton Trans.*, 1999, 2343

[44]  P. M. Triechel, W. K. Dean, W. M. Douglas, *J. Organometallic Chem.*, 1972, **42**, 145

[45]  T. Campbell, A. M. Gibson, R. Hart, S. D. Orchard, S. J.A. Pope, G. Reid, *J. Organometallic Chem.*, 1999, **592**, 296

[46]  J. A. Bowden, R. Colton, C. J. Commons, *Aust. J. Chem.*, 1973, **26**, 655

**Chapter 3**

[47]  D. J. Lowry and M. L. Helm, *Inorg. Chem.*, 2010, **49**, 4732

[48]  R. B. King and J. C. Cloyd, *J. Am. Chem. Soc.*, 1975, **97**, 46

[49]  D. Romo, A. I. Myers, *j. Org. Chem*, 1992, **57**, 6265

[50] J. Paterova, M. Skalicky, M. Rybackova, M. Kvicalova, J. Cvacka and J. Kvicala, *J. Flourine Chem.*, 2010, **131**, 1338

[51] T. H. Weil, B. Prijs, H. Erlenmeyer, *Helv. Chim. Acta.*, 1952, **35**, 1412

[52] M. H. Bride, W. A. W. Cummings and W. Pickles, *J. Appl. Chem.*, 1961, **9**, 352

# Appendix

**Appendix**

## 1. Air Sensitive Techniques

### 1.1 Schlenk Line

Schlenk lines generally consist of a glass manifold containing two-way taps which can be set to a vacuum of inert gases, applying these states to reaction vessels. Therefore Schlenk lines can be used for the removal of solvents, drying of products and the handling of air sensitive chemicals. The major hazards associated with Schlenk line use are:

- Implosions – usually as a result of weakness or fractures in the glassware
- Explosions – from condensation of liquid oxygen within the solvent trap and reaction with volatiles/grease therein

Both scenarios would result in extensive glass fragmentation contaminated with potentially toxic chemicals, resulting in serious risk. To minimise these risks the following precautions should be adhered to:

- Ensure that all equipment (both line and reaction vessels) are free from cracks and impact damage (star cracks)
- Ensure that all joints and taps on the Schlenk line are well greased using high quality Apiezon vacuum grease and reaction vessels are also well sealed with standard grease.
- Ensure that the Schlenk line solvent trap is empty of solvent before use.
- Do not allow air to be drawn into the solvent trap when cooled in liquid nitrogen, this will condense liquid oxygen which is highly explosive
- When switching off the line, liquid nitrogen should be removed before admitting air into the system.
- If liquid oxygen is observed in the solvent trap (identified as a blue coloured liquid) then the Dewar should be removed, the pump switched off and all taps opened before evacuating the laboratory.

Reactions in an inert atmosphere can be achieved through the use of a Schlenk line by first evacuating the reaction vessel and then reintroducing an inert atmosphere (in our case, nitrogen but argon is also available) repeating three times. The rate of gas flow into the Schlenk line can be monitored via the oil and gas bubblers exiting the Schlenk line. Thick pressure tubing is used throughout the system to connect the nitrogen supply to the vacuum and subsequently the four channels through which reaction vessels can be connected.

**1.2 Glove Box**

The inert atmosphere glove box was primarily used for the weighing of air sensitive solids into reaction vessels for reaction on the Schlenk line. The workspace is typically filled with nitrogen (argon and other inert gases may also be used) providing a dry air-free environment. An antechamber, which can be evacuated and flooded with inert gas allows the introduction of materials or equipment from outside the glove box.

Prior to entering the glove box, the antechamber was placed under vacuum and purged with nitrogen three times, ensuring there was free flow of gas through all glassware. Any sealed flasks or containers were evacuated before being placed within the antechamber to prevent explosions. The gloves were also evacuated and purged with nitrogen three times before used.

**2. Safety**

Due to the toxicity and malodorous nature of primary phosphines, certain safety measures were adhered to so that a safe working environment was maintained. Thes included:

- Carrying out all experiments within a fume cupboard and under nitrogen, avoiding prolonged exposures to the vapours, avoiding skin contact by wearing latex gloves and receiving pseudocholinesterase blood tests every six months.

- Any phosphine gas produced were absorbed by bubbling all exhaust gases from the Schlenk line through a rig of four Dreschel bottles, connected in series, containing concentrated ammonia solution in an aqueous solution of copper (II) sulfate. Over time, phosphines form a grey/black precipitate within the Dreschel bottles, which can be safely destroyed using nitric acid.

- All glassware was submerged and soaked in a bleach bath within the fume cupboard overnight to oxidise any remaining phosphines before normal cleaning procedures can be undertaken. Cannulae were cleaned by passing bleach, then water and finally acetone through them.

- Any phosphine spills were cleaned by immediately pouring bleach on the affected area, scrubbing, and then leaving for half hour before being washed and dried.

## 1.3 X- Ray Crystallograpy Tables

### [Mo(CO)$_3$(2-fpp)$_3$] (Compound 10, Chapter 2)

Table 1. Crystal data and structure refinement for pge1312.

| | | | |
|---|---|---|---|
| Identification code | pge1312 | | |
| Empirical formula | C21 H18 F3 Mo O3 P3 | | |
| Formula weight | 564.20 | | |
| Temperature | 150(2) K | | |
| Wavelength | 1.54180 Å | | |
| Crystal system | Triclinic | | |
| Space group | P-1 | | |
| Unit cell dimensions | a = 7.1167(3) Å | $\alpha$= 78.187(3)°. | |
| | b = 11.1574(4) Å | $\beta$= 80.867(3)°. | |
| | c = 15.2192(5) Å | $\gamma$ = 77.748(4)°. | |
| Volume | 1147.50(7) Å$^3$ | | |
| Z | 2 | | |
| Density (calculated) | 1.633 Mg/m$^3$ | | |
| Absorption coefficient | 7.067 mm$^{-1}$ | | |
| F(000) | 564 | | |
| Crystal size | 0.34 x 0.28 x 0.19 mm$^3$ | | |
| Theta range for data collection | 2.99 to 74.24°. | | |
| Index ranges | -8<=h<=8, -13<=k<=11, -15<=l<=18 | | |
| Reflections collected | 7862 | | |
| Independent reflections | 4473 [R(int) = 0.0175] | | |
| Completeness to theta = 74.24° | 96.0 % | | |
| Max. and min. transmission | 0.3470 and 0.1973 | | |
| Refinement method | Full-matrix least-squares on F$^2$ | | |
| Data / restraints / parameters | 4473 / 2 / 303 | | |
| Goodness-of-fit on F$^2$ | 1.096 | | |
| Final R indices [I>2sigma(I)] | R1 = 0.0256, wR2 = 0.0650 | | |
| R indices (all data) | R1 = 0.0264, wR2 = 0.0659 | | |
| Largest diff. peak and hole | 0.401 and -0.851 e.Å$^{-3}$ | | |

Table 2. Atomic coordinates ( x $10^4$) and equivalent isotropic displacement parameters ($\text{Å}^2$x $10^3$) for pge1312. U(eq) is defined as one third of the trace of the orthogonalized $U^{ij}$ tensor.

| | x | y | z | U(eq) |
|---|---|---|---|---|
| C(1) | 3512(3) | 1952(2) | -139(1) | 23(1) |
| C(2) | 5104(3) | 1560(2) | -736(2) | 28(1) |
| C(3) | 5006(4) | 946(2) | -1419(2) | 34(1) |
| C(4) | 3231(4) | 698(2) | -1512(2) | 34(1) |
| C(5) | 1599(4) | 1056(2) | -925(2) | 32(1) |
| C(6) | 1747(3) | 1680(2) | -244(2) | 28(1) |
| C(7) | 2738(3) | 5783(2) | 2652(2) | 27(1) |
| C(8) | 1813(4) | 5839(2) | 3518(2) | 33(1) |
| C(8A) | 1813(4) | 5839(2) | 3518(2) | 33(1) |
| C(9) | 2675(5) | 6076(3) | 4196(2) | 45(1) |
| C(10) | 4546(5) | 6283(3) | 4003(2) | 51(1) |
| C(11) | 5521(4) | 6239(3) | 3148(2) | 49(1) |
| C(12) | 4632(4) | 5984(2) | 2482(2) | 38(1) |
| C(12A) | 4632(4) | 5984(2) | 2482(2) | 38(1) |
| C(13) | 2939(3) | 1433(2) | 4125(1) | 24(1) |
| C(14) | 3132(3) | 159(2) | 4189(2) | 28(1) |
| C(14A) | 3132(3) | 159(2) | 4189(2) | 28(1) |
| C(15) | 2646(3) | -620(2) | 4981(2) | 32(1) |
| C(16) | 1917(3) | -103(3) | 5743(2) | 38(1) |
| C(17) | 1675(4) | 1166(3) | 5709(2) | 39(1) |
| C(18) | 2190(3) | 1922(2) | 4901(2) | 33(1) |
| C(18A) | 2190(3) | 1922(2) | 4901(2) | 33(1) |
| C(19) | -928(3) | 3334(2) | 3050(2) | 24(1) |
| C(20) | 588(3) | 1446(2) | 2066(1) | 26(1) |
| C(21) | -970(4) | 3840(2) | 1167(2) | 30(1) |
| F(1) | 6840(2) | 1818(2) | -651(1) | 40(1) |
| F(2) | -14(3) | 5639(2) | 3710(1) | 51(1) |
| F(2A) | 5780(40) | 5820(30) | 1725(14) | 89(12) |
| F(3) | 3807(3) | -314(2) | 3445(1) | 37(1) |
| F(3A) | 1972(11) | 3104(5) | 4798(5) | 42(2) |
| Mo(1) | 1062(1) | 3154(1) | 1985(1) | 19(1) |
| O(1) | -2082(2) | 3378(2) | 3671(1) | 33(1) |
| O(2) | 261(3) | 463(2) | 2110(1) | 37(1) |

| | | | |
|---|---|---|---|
| O(3) | -2183(3) | 4255(2) | 715(2) | 50(1) |
| P(1) | 3731(1) | 2791(1) | 742(1) | 24(1) |
| P(2) | 1575(1) | 5330(1) | 1819(1) | 30(1) |
| P(3) | 3548(1) | 2414(1) | 3051(1) | 26(1) |

Table 3.   Bond lengths [Å] and angles [°] for pge1312.

| | | | |
|---|---|---|---|
| C(1)-C(2) | 1.388(3) | C(15)-H(15) | 0.9500 |
| C(1)-C(6) | 1.393(3) | C(16)-C(17) | 1.380(4) |
| C(1)-P(1) | 1.827(2) | C(16)-H(16) | 0.9500 |
| C(2)-F(1) | 1.357(3) | C(17)-C(18) | 1.386(4) |
| C(2)-C(3) | 1.375(3) | C(17)-H(17) | 0.9500 |
| C(3)-C(4) | 1.383(4) | C(18)-H(18) | 0.9500 |
| C(3)-H(3) | 0.9500 | C(19)-O(1) | 1.152(3) |
| C(4)-C(5) | 1.388(3) | C(19)-Mo(1) | 1.988(2) |
| C(4)-H(4) | 0.9500 | C(20)-O(2) | 1.155(3) |
| C(5)-C(6) | 1.390(3) | C(20)-Mo(1) | 1.980(2) |
| C(5)-H(5) | 0.9500 | C(21)-O(3) | 1.150(3) |
| C(6)-H(6) | 0.9500 | C(21)-Mo(1) | 1.984(2) |
| C(7)-C(8) | 1.383(3) | Mo(1)-P(3) | 2.4870(6) |
| C(7)-C(12) | 1.389(3) | Mo(1)-P(2) | 2.4878(6) |
| C(7)-P(2) | 1.822(2) | Mo(1)-P(1) | 2.4902(6) |
| C(8)-F(2) | 1.343(3) | P(1)-H(1A) | 1.2996 |
| C(8)-C(9) | 1.376(4) | P(1)-H(1B) | 1.2996 |
| C(9)-C(10) | 1.375(5) | P(2)-H(2A) | 1.3026 |
| C(9)-H(9) | 0.9500 | P(2)-H(2B) | 1.3026 |
| C(10)-C(11) | 1.378(5) | P(3)-H(3A) | 1.3146 |
| C(10)-H(10) | 0.9500 | P(3)-H(3B) | 1.3146 |
| C(11)-C(12) | 1.381(4) | | |
| C(11)-H(11) | 0.9500 | | |
| C(12)-H(12) | 0.9500 | | |
| C(13)-C(14) | 1.383(3) | | |
| C(13)-C(18) | 1.384(3) | | |
| C(13)-P(3) | 1.818(2) | | |
| C(14)-F(3) | 1.326(3) | | |
| C(14)-C(15) | 1.376(3) | | |
| C(15)-C(16) | 1.380(4) | | |

| | | | |
|---|---|---|---|
| C(2)-C(1)-C(6) | 117.0(2) | C(18)-C(13)-P(3) | 122.06(18) |
| C(2)-C(1)-P(1) | 121.24(17) | F(3)-C(14)-C(15) | 119.4(2) |
| C(6)-C(1)-P(1) | 121.77(16) | F(3)-C(14)-C(13) | 117.5(2) |
| F(1)-C(2)-C(3) | 118.3(2) | C(15)-C(14)-C(13) | 123.1(2) |
| F(1)-C(2)-C(1) | 118.2(2) | C(14)-C(15)-C(16) | 118.3(2) |
| C(3)-C(2)-C(1) | 123.4(2) | C(14)-C(15)-H(15) | 120.8 |
| C(2)-C(3)-C(4) | 118.3(2) | C(16)-C(15)-H(15) | 120.8 |
| C(2)-C(3)-H(3) | 120.9 | C(17)-C(16)-C(15) | 120.6(2) |
| C(4)-C(3)-H(3) | 120.9 | C(17)-C(16)-H(16) | 119.7 |
| C(3)-C(4)-C(5) | 120.6(2) | C(15)-C(16)-H(16) | 119.7 |
| C(3)-C(4)-H(4) | 119.7 | C(16)-C(17)-C(18) | 119.4(2) |
| C(5)-C(4)-H(4) | 119.7 | C(16)-C(17)-H(17) | 120.3 |
| C(4)-C(5)-C(6) | 119.7(2) | C(18)-C(17)-H(17) | 120.3 |
| C(4)-C(5)-H(5) | 120.2 | C(13)-C(18)-C(17) | 121.4(2) |
| C(6)-C(5)-H(5) | 120.2 | C(13)-C(18)-H(18) | 119.3 |
| C(5)-C(6)-C(1) | 121.1(2) | C(17)-C(18)-H(18) | 119.3 |
| C(5)-C(6)-H(6) | 119.5 | O(1)-C(19)-Mo(1) | 176.66(19) |
| C(1)-C(6)-H(6) | 119.5 | O(2)-C(20)-Mo(1) | 178.2(2) |
| C(8)-C(7)-C(12) | 116.6(2) | O(3)-C(21)-Mo(1) | 177.8(2) |
| C(8)-C(7)-P(2) | 120.80(18) | C(20)-Mo(1)-C(21) | 90.76(10) |
| C(12)-C(7)-P(2) | 122.36(19) | C(20)-Mo(1)-C(19) | 88.41(9) |
| F(2)-C(8)-C(9) | 118.2(2) | C(21)-Mo(1)-C(19) | 89.95(9) |
| F(2)-C(8)-C(7) | 118.4(2) | C(20)-Mo(1)-P(3) | 92.19(7) |
| C(9)-C(8)-C(7) | 123.4(3) | C(21)-Mo(1)-P(3) | 176.42(7) |
| C(10)-C(9)-C(8) | 118.5(3) | C(19)-Mo(1)-P(3) | 88.12(6) |
| C(10)-C(9)-H(9) | 120.8 | C(20)-Mo(1)-P(2) | 177.29(6) |
| C(8)-C(9)-H(9) | 120.8 | C(21)-Mo(1)-P(2) | 86.64(7) |
| C(9)-C(10)-C(11) | 120.1(3) | C(19)-Mo(1)-P(2) | 92.39(6) |
| C(9)-C(10)-H(10) | 120.0 | P(3)-Mo(1)-P(2) | 90.43(2) |
| C(11)-C(10)-H(10) | 120.0 | C(20)-Mo(1)-P(1) | 89.70(6) |
| C(10)-C(11)-C(12) | 120.4(3) | C(21)-Mo(1)-P(1) | 94.68(7) |
| C(10)-C(11)-H(11) | 119.8 | C(19)-Mo(1)-P(1) | 175.02(6) |
| C(12)-C(11)-H(11) | 119.8 | P(3)-Mo(1)-P(1) | 87.355(19) |
| C(11)-C(12)-C(7) | 121.1(3) | P(2)-Mo(1)-P(1) | 89.71(2) |
| C(11)-C(12)-H(12) | 119.5 | C(1)-P(1)-Mo(1) | 121.40(7) |
| C(7)-C(12)-H(12) | 119.5 | C(1)-P(1)-H(1A) | 107.0 |
| C(14)-C(13)-C(18) | 117.1(2) | Mo(1)-P(1)-H(1A) | 107.0 |
| C(14)-C(13)-P(3) | 120.80(17) | C(1)-P(1)-H(1B) | 107.0 |

| | | | |
|---|---|---|---|
| Mo(1)-P(1)-H(1A) | 107.0 | Mo(1)-P(2)-H(2B) | 107.1 |
| C(1)-P(1)-H(1B) | 107.0 | H(2A)-P(2)-H(2B) | 106.8 |
| Mo(1)-P(1)-H(1B) | 107.0 | C(13)-P(3)-Mo(1) | 118.53(7) |
| H(1A)-P(1)-H(1B) | 106.7 | C(13)-P(3)-H(3A) | 107.7 |
| C(7)-P(2)-Mo(1) | 120.76(7) | Mo(1)-P(3)-H(3A) | 107.7 |
| C(7)-P(2)-H(2A) | 107.1 | C(13)-P(3)-H(3B) | 107.7 |
| Mo(1)-P(2)-H(2A) | 107.1 | Mo(1)-P(3)-H(3B) | 107.7 |
| C(7)-P(2)-H(2B) | 107.1 | H(3A)-P(3)-H(3B) | 107.1 |

Symmetry transformations used to generate equivalent atoms:

## Fe(Cp)(2-fpp)$_3$]PF$_6$ (Compound 11, Chapter 2)

Table 1. Crystal data and structure refinement for pge1315.

| | |
|---|---|
| Identification code | pge1315 |
| Empirical formula | C23 H23 F9 Fe P4 |
| Formula weight | 650.14 |
| Temperature | 150(2) K |
| Wavelength | 1.54184 Å |
| Crystal system | Monoclinic |
| Space group | P21/n |
| Unit cell dimensions | a = 9.86250(10) Å $\alpha$= 90°. |
| | b = 15.4290(2) Å $\beta$= 97.2470(10)°. |
| | c = 17.1595(2) Å $\gamma$ = 90°. |
| Volume | 2590.28(5) Å$^3$ |
| Z | 4 |
| Density (calculated) | 1.667 Mg/m$^3$ |
| Absorption coefficient | 7.734 mm$^{-1}$ |
| F(000) | 1312 |
| Crystal size | 0.29 x 0.17 x 0.09 mm$^3$ |
| Theta range for data collection | 3.87 to 73.44°. |
| Index ranges | -12<=h<=8, -19<=k<=18, -21<=l<=19 |
| Reflections collected | 19024 |
| Independent reflections | 5152 [R(int) = 0.0186] |
| Completeness to theta = 73.44° | 98.9 % |
| Max. and min. transmission | 0.5428 and 0.2126 |
| Refinement method | Full-matrix least-squares on F$^2$ |

| | | | | |
|---|---|---|---|---|
| Data / restraints / parameters | | | 5152 / 582 / 466 | |
| Goodness-of-fit on $F^2$ | | | 1.050 | |
| Final R indices [I>2sigma(I)] | | | R1 = 0.0327, wR2 = 0.0872 | |
| R indices (all data) | | | R1 = 0.0341, wR2 = 0.0882 | |
| Largest diff. peak and hole | | | 0.550 and -0.445 e.Å$^{-3}$ | |

Table 2. Atomic coordinates ( x $10^4$) and equivalent isotropic displacement parameters (Å$^2$x $10^3$) for pge1315. U(eq) is defined as one third of the trace of the orthogonalized U$^{ij}$ tensor.

| | x | y | z | U(eq) |
|---|---|---|---|---|
| C(1) | 5695(2) | 4176(2) | 1720(1) | 25(1) |
| C(2) | 6360(2) | 4516(2) | 1129(1) | 27(1) |
| C(3) | 6048(3) | 5304(2) | 779(1) | 32(1) |
| C(4) | 5002(3) | 5786(2) | 1035(2) | 35(1) |
| C(5) | 4297(3) | 5470(2) | 1623(2) | 36(1) |
| C(6) | 4630(3) | 4668(2) | 1960(2) | 32(1) |
| C(7) | 5851(2) | 1207(2) | 3422(1) | 24(1) |
| C(8) | 6389(2) | 1801(2) | 3973(1) | 26(1) |
| C(9) | 5938(3) | 1910(2) | 4696(2) | 32(1) |
| C(10) | 4878(3) | 1391(2) | 4875(2) | 38(1) |
| C(11) | 4300(3) | 783(2) | 4337(2) | 41(1) |
| C(12) | 4777(3) | 688(2) | 3618(2) | 34(1) |
| C(13) | 4212(2) | 1033(2) | 1023(2) | 35(1) |
| C(14) | 4583(3) | 1584(2) | 426(2) | 38(1) |
| C(15) | 4238(3) | 2444(2) | 607(2) | 37(1) |
| C(16) | 3637(2) | 2422(2) | 1316(2) | 35(1) |
| C(17) | 3625(2) | 1557(2) | 1572(2) | 36(1) |
| F(1) | 7389(2) | 4041(1) | 884(1) | 41(1) |
| F(2) | 7447(2) | 2297(1) | 3800(1) | 36(1) |
| C(18) | 8437(11) | 877(5) | 957(4) | 22(1) |
| C(19) | 9858(7) | 819(4) | 1000(4) | 26(1) |
| C(20) | 10551(7) | 45(4) | 975(3) | 27(1) |
| C(21) | 9782(8) | -712(4) | 881(4) | 30(1) |
| C(22) | 8373(6) | -679(5) | 832(4) | 28(1) |
| C(23) | 7719(6) | 105(5) | 866(3) | 27(1) |
| F(3) | 10596(2) | 1570(1) | 1066(1) | 37(1) |
| C(18A) | 8480(20) | 985(10) | 930(8) | 23(3) |

| | | | | |
|---|---|---|---|---|
| C(19A) | 7874(11) | 196(10) | 695(4) | 26(2) |
| C(20A) | 8587(12) | -579(9) | 689(7) | 29(2) |
| C(21A) | 9996(14) | -552(8) | 934(8) | 26(2) |
| C(22A) | 10616(14) | 220(8) | 1169(7) | 28(2) |
| C(23A) | 9879(15) | 970(9) | 1168(8) | 25(2) |
| F(3A) | 6499(4) | 178(3) | 456(3) | 43(2) |
| F(4) | 7641(6) | 1857(4) | -2012(4) | 79(2) |
| F(5) | 5568(8) | 1844(7) | -2706(5) | 127(3) |
| F(6) | 4738(7) | 1162(5) | -1684(5) | 71(2) |
| F(7) | 6781(4) | 1215(4) | -1019(2) | 61(1) |
| F(8) | 5738(8) | 2405(3) | -1523(6) | 128(3) |
| F(9) | 6597(5) | 591(3) | -2157(3) | 54(1) |
| P(4) | 6125(8) | 1545(6) | -1932(5) | 40(1) |
| F(4A) | 7344(11) | 2203(8) | -2124(7) | 120(4) |
| F(5A) | 5686(12) | 1547(5) | -2952(4) | 102(3) |
| F(6A) | 4748(10) | 1064(7) | -1970(7) | 81(3) |
| F(7A) | 6452(11) | 1720(8) | -1124(4) | 106(3) |
| F(8A) | 5172(10) | 2474(4) | -2090(7) | 108(3) |
| F(9A) | 6935(11) | 833(8) | -2056(7) | 127(4) |
| P(4A) | 6099(14) | 1657(10) | -1928(9) | 59(2) |
| P(1) | 6171(1) | 3130(1) | 2166(1) | 24(1) |
| P(2) | 6474(1) | 1122(1) | 2471(1) | 26(1) |
| P(3) | 7550(1) | 1937(1) | 1011(1) | 25(1) |
| P(3A) | 7550(1) | 1937(1) | 1011(1) | 25(1) |
| Fe(1) | 5631(1) | 1955(1) | 1507(1) | 20(1) |

Table 3.   Bond lengths [Å] and angles [°] for pge1315.

| | | | |
|---|---|---|---|
| C(1)-C(2) | 1.380(3) | C(19)-F(3) | 1.366(7) |
| C(1)-C(6) | 1.400(3) | C(19)-C(20) | 1.378(8) |
| C(1)-P(1) | 1.822(2) | C(20)-C(21) | 1.392(8) |
| C(2)-F(1) | 1.360(3) | C(20)-H(20) | 0.9500 |
| C(2)-C(3) | 1.373(4) | C(21)-C(22) | 1.383(8) |
| C(3)-C(4) | 1.388(4) | C(21)-H(21) | 0.9500 |
| C(3)-H(3) | 0.9500 | C(22)-C(23) | 1.376(8) |
| C(4)-C(5) | 1.384(4) | C(22)-H(22) | 0.9500 |
| C(4)-H(4) | 0.9500 | C(23)-H(23) | 0.9500 |
| C(5)-C(6) | 1.388(4) | C(18A)-C(23A) | 1.387(16) |

| | | | |
|---|---|---|---|
| C(5)-H(5) | 0.9500 | C(18A)-C(19A) | 1.395(15) |
| C(6)-H(6) | 0.9500 | C(19A)-F(3A) | 1.367(11) |
| C(7)-C(8) | 1.373(3) | C(19A)-C(20A) | 1.388(12) |
| C(7)-C(12) | 1.403(3) | C(20A)-C(21A) | 1.400(12) |
| C(7)-P(2) | 1.820(2) | C(20A)-H(20A) | 0.9500 |
| C(8)-F(2) | 1.357(3) | C(21A)-C(22A) | 1.375(11) |
| C(8)-C(9) | 1.381(3) | C(21A)-H(21A) | 0.9500 |
| C(9)-C(10) | 1.383(4) | C(22A)-C(23A) | 1.367(12) |
| C(9)-H(9) | 0.9500 | C(22A)-H(22A) | 0.9500 |
| C(10)-C(11) | 1.387(4) | C(23A)-H(23A) | 0.9500 |
| C(10)-H(10) | 0.9500 | F(4)-P(4) | 1.594(10) |
| C(11)-C(12) | 1.382(4) | F(5)-P(4) | 1.447(10) |
| C(11)-H(11) | 0.9500 | F(6)-P(4) | 1.597(11) |
| C(12)-H(12) | 0.9500 | F(7)-P(4) | 1.697(9) |
| C(13)-C(14) | 1.414(4) | F(8)-P(4) | 1.571(10) |
| C(13)-C(17) | 1.418(4) | F(9)-P(4) | 1.605(10) |
| C(13)-Fe(1) | 2.092(2) | F(4A)-P(4A) | 1.560(17) |
| C(13)-H(13) | 0.9500 | F(5A)-P(4A) | 1.761(17) |
| C(14)-C(15) | 1.414(4) | F(6A)-P(4A) | 1.611(17) |
| C(14)-Fe(1) | 2.087(2) | F(7A)-P(4A) | 1.384(16) |
| C(14)-H(14) | 0.9500 | F(8A)-P(4A) | 1.561(16) |
| C(15)-C(16) | 1.419(4) | F(9A)-P(4A) | 1.546(16) |
| C(15)-Fe(1) | 2.075(2) | P(1)-Fe(1) | 2.1667(7) |
| C(15)-H(15) | 0.9500 | P(1)-H(1A) | 1.2944 |
| C(16)-C(17) | 1.406(4) | P(1)-H(1B) | 1.2944 |
| C(16)-Fe(1) | 2.081(2) | P(2)-Fe(1) | 2.1750(6) |
| C(16)-H(16) | 0.9500 | P(2)-H(2A) | 1.2996 |
| C(17)-Fe(1) | 2.087(2) | P(2)-H(2B) | 1.2996 |
| C(17)-H(17) | 0.9500 | P(3)-Fe(1) | 2.1715(6) |
| C(18)-C(23) | 1.384(11) | P(3)-H(3A) | 1.2955 |
| C(18)-C(19) | 1.397(10) | P(3)-H(3B) | 1.2955 |
| C(18)-P(3) | 1.863(7) | | |

| | | | |
|---|---|---|---|
| C(2)-C(1)-C(6) | 117.0(2) | F(3A)-C(19A)-C(18A) | 118.6(12) |
| C(2)-C(1)-P(1) | 121.62(18) | C(20A)-C(19A)-C(18A) | 123.7(10) |
| C(6)-C(1)-P(1) | 121.36(18) | C(19A)-C(20A)-C(21A) | 117.2(10) |
| F(1)-C(2)-C(3) | 118.5(2) | C(19A)-C(20A)-H(20A) | 121.4 |
| F(1)-C(2)-C(1) | 117.7(2) | C(21A)-C(20A)-H(20A) | 121.4 |

| | | | |
|---|---|---|---|
| C(3)-C(2)-C(1) | 123.8(2) | C(22A)-C(21A)-C(20A) | 120.1(9) |
| C(2)-C(3)-C(4) | 118.1(2) | C(22A)-C(21A)-H(21A) | 120.0 |
| C(2)-C(3)-H(3) | 120.9 | C(20A)-C(21A)-H(21A) | 120.0 |
| C(4)-C(3)-H(3) | 120.9 | C(23A)-C(22A)-C(21A) | 121.1(11) |
| C(5)-C(4)-C(3) | 120.2(2) | C(23A)-C(22A)-H(22A) | 119.4 |
| C(5)-C(4)-H(4) | 119.9 | C(21A)-C(22A)-H(22A) | 119.5 |
| C(3)-C(4)-H(4) | 119.9 | C(22A)-C(23A)-C(18A) | 121.5(11) |
| C(4)-C(5)-C(6) | 120.3(2) | C(22A)-C(23A)-H(23A) | 119.2 |
| C(4)-C(5)-H(5) | 119.9 | C(18A)-C(23A)-H(23A) | 119.2 |
| C(6)-C(5)-H(5) | 119.9 | F(5)-P(4)-F(8) | 93.1(6) |
| C(5)-C(6)-C(1) | 120.5(2) | F(5)-P(4)-F(4) | 94.4(7) |
| C(5)-C(6)-H(6) | 119.7 | F(8)-P(4)-F(4) | 93.8(6) |
| C(1)-C(6)-H(6) | 119.7 | F(5)-P(4)-F(6) | 97.1(6) |
| C(8)-C(7)-C(12) | 117.0(2) | F(8)-P(4)-F(6) | 85.9(6) |
| C(8)-C(7)-P(2) | 121.37(18) | F(4)-P(4)-F(6) | 168.5(7) |
| C(12)-C(7)-P(2) | 121.61(18) | F(5)-P(4)-F(9) | 99.2(7) |
| F(2)-C(8)-C(7) | 117.8(2) | F(8)-P(4)-F(9) | 167.5(7) |
| F(2)-C(8)-C(9) | 118.1(2) | F(4)-P(4)-F(9) | 87.3(5) |
| C(7)-C(8)-C(9) | 124.0(2) | F(6)-P(4)-F(9) | 90.5(6) |
| C(8)-C(9)-C(10) | 117.9(2) | F(5)-P(4)-F(7) | 178.8(8) |
| C(8)-C(9)-H(9) | 121.1 | F(8)-P(4)-F(7) | 85.8(6) |
| C(10)-C(9)-H(9) | 121.1 | F(4)-P(4)-F(7) | 85.3(4) |
| C(9)-C(10)-C(11) | 120.1(2) | F(6)-P(4)-F(7) | 83.2(6) |
| C(9)-C(10)-H(10) | 119.9 | F(9)-P(4)-F(7) | 81.9(4) |
| C(11)-C(10)-H(10) | 119.9 | F(7A)-P(4A)-F(9A) | 97.3(10) |
| C(12)-C(11)-C(10) | 120.6(2) | F(7A)-P(4A)-F(4A) | 94.1(10) |
| C(12)-C(11)-H(11) | 119.7 | F(9A)-P(4A)-F(4A) | 88.0(10) |
| C(10)-C(11)-H(11) | 119.7 | F(7A)-P(4A)-F(8A) | 100.9(11) |
| C(11)-C(12)-C(7) | 120.3(2) | F(9A)-P(4A)-F(8A) | 161.7(13) |
| C(11)-C(12)-H(12) | 119.8 | F(4A)-P(4A)-F(8A) | 89.1(9) |
| C(7)-C(12)-H(12) | 119.8 | F(7A)-P(4A)-F(6A) | 100.8(11) |
| C(14)-C(13)-C(17) | 107.7(2) | F(9A)-P(4A)-F(6A) | 88.8(9) |
| C(14)-C(13)-Fe(1) | 70.04(14) | F(4A)-P(4A)-F(6A) | 165.1(13) |
| C(17)-C(13)-Fe(1) | 69.98(14) | F(8A)-P(4A)-F(6A) | 89.3(9) |
| C(14)-C(13)-H(13) | 126.2 | F(7A)-P(4A)-F(5A) | 178.1(12) |
| C(17)-C(13)-H(13) | 126.2 | F(9A)-P(4A)-F(5A) | 80.7(9) |
| Fe(1)-C(13)-H(13) | 125.4 | F(4A)-P(4A)-F(5A) | 85.8(9) |
| C(15)-C(14)-C(13) | 108.2(2) | F(8A)-P(4A)-F(5A) | 81.0(8) |

| | | | |
|---|---|---|---|
| C(15)-C(14)-Fe(1) | 69.68(14) | F(6A)-P(4A)-F(5A) | 79.3(8) |
| C(13)-C(14)-Fe(1) | 70.40(14) | C(1)-P(1)-Fe(1) | 119.29(7) |
| C(15)-C(14)-H(14) | 125.9 | C(1)-P(1)-H(1A) | 107.5 |
| C(13)-C(14)-H(14) | 125.9 | Fe(1)-P(1)-H(1A) | 107.5 |
| Fe(1)-C(14)-H(14) | 125.6 | C(1)-P(1)-H(1B) | 107.5 |
| C(14)-C(15)-C(16) | 107.7(2) | Fe(1)-P(1)-H(1B) | 107.5 |
| C(14)-C(15)-Fe(1) | 70.59(14) | H(1A)-P(1)-H(1B) | 107.0 |
| C(16)-C(15)-Fe(1) | 70.27(13) | C(7)-P(2)-Fe(1) | 119.94(7) |
| C(14)-C(15)-H(15) | 126.1 | C(7)-P(2)-H(2A) | 107.3 |
| C(16)-C(15)-H(15) | 126.1 | Fe(1)-P(2)-H(2A) | 107.3 |
| Fe(1)-C(15)-H(15) | 124.6 | C(7)-P(2)-H(2B) | 107.3 |
| C(17)-C(16)-C(15) | 108.1(2) | Fe(1)-P(2)-H(2B) | 107.3 |
| C(17)-C(16)-Fe(1) | 70.52(14) | H(2A)-P(2)-H(2B) | 106.9 |
| C(15)-C(16)-Fe(1) | 69.80(14) | C(18)-P(3)-Fe(1) | 118.0(3) |
| C(17)-C(16)-H(16) | 126.0 | Fe(1)-P(3)-H(3A) | 107.8 |
| C(15)-C(16)-H(16) | 126.0 | Fe(1)-P(3)-H(3B) | 107.8 |
| Fe(1)-C(16)-H(16) | 125.3 | C(15)-Fe(1)-C(16) | 39.93(11) |
| C(16)-C(17)-C(13) | 108.3(2) | C(15)-Fe(1)-C(14) | 39.73(12) |
| C(16)-C(17)-Fe(1) | 70.06(14) | C(16)-Fe(1)-C(14) | 66.60(11) |
| C(13)-C(17)-Fe(1) | 70.34(14) | C(15)-Fe(1)-C(17) | 66.65(10) |
| C(16)-C(17)-H(17) | 125.9 | C(16)-Fe(1)-C(17) | 39.42(11) |
| C(13)-C(17)-H(17) | 125.9 | C(14)-Fe(1)-C(17) | 66.43(11) |
| Fe(1)-C(17)-H(17) | 125.3 | C(15)-Fe(1)-C(13) | 66.72(10) |
| C(23)-C(18)-C(19) | 116.5(5) | C(16)-Fe(1)-C(13) | 66.53(11) |
| C(23)-C(18)-P(3) | 121.6(7) | C(14)-Fe(1)-C(13) | 39.56(11) |
| C(19)-C(18)-P(3) | 121.9(7) | C(17)-Fe(1)-C(13) | 39.68(11) |
| F(3)-C(19)-C(20) | 118.5(5) | C(15)-Fe(1)-P(1) | 100.39(8) |
| F(3)-C(19)-C(18) | 118.0(6) | C(16)-Fe(1)-P(1) | 87.57(8) |
| C(20)-C(19)-C(18) | 123.5(5) | C(14)-Fe(1)-P(1) | 139.02(9) |
| C(19)-C(20)-C(21) | 117.8(5) | C(17)-Fe(1)-P(1) | 113.00(9) |
| C(19)-C(20)-H(20) | 121.1 | C(13)-Fe(1)-P(1) | 152.12(8) |
| C(21)-C(20)-H(20) | 121.1 | C(15)-Fe(1)-P(3) | 103.94(8) |
| C(22)-C(21)-C(20) | 120.3(5) | C(16)-Fe(1)-P(3) | 142.72(8) |
| C(22)-C(21)-H(21) | 119.9 | C(14)-Fe(1)-P(3) | 90.37(8) |
| C(20)-C(21)-H(21) | 119.9 | C(17)-Fe(1)-P(3) | 153.61(9) |
| C(23)-C(22)-C(21) | 120.2(5) | C(13)-Fe(1)-P(3) | 114.08(8) |
| C(23)-C(22)-H(22) | 119.9 | P(1)-Fe(1)-P(3) | 92.64(2) |
| C(21)-C(22)-H(22) | 119.9 | C(15)-Fe(1)-P(2) | 159.12(8) |

| | | | |
|---|---|---|---|
| C(22)-C(23)-C(18) | 121.7(6) | C(16)-Fe(1)-P(2) | 126.00(8) |
| C(22)-C(23)-H(23) | 119.1 | C(14)-Fe(1)-P(2) | 127.76(9) |
| C(18)-C(23)-H(23) | 119.1 | C(17)-Fe(1)-P(2) | 93.44(7) |
| C(23A)-C(18A)-C(19A) | 116.5(9) | C(13)-Fe(1)-P(2) | 94.15(8) |
| F(3A)-C(19A)-C(20A) | 117.7(11) | P(1)-Fe(1)-P(2) | 93.04(2) |
| | | P(3)-Fe(1)-P(2) | 91.23(3) |

Symmetry transformations used to generate equivalent atoms:

## [Cr(CO) $_3$ (2-fpp)$_3$] (Compound 12, Chapter 2)

Table 1. Crystal data and structure refinement for pge1313.

| | |
|---|---|
| Identification code | pge1313 |
| Empirical formula | C21 H18 Cr F3 O3 P3 |
| Formula weight | 520.26 |
| Temperature | 150(2) K |
| Wavelength | 1.54180 Å |
| Crystal system | Triclinic |
| Space group | P-1 |
| Unit cell dimensions | a = 9.4359(5) Å $\quad$ $\alpha$= 70.009(5)°. |
| | b = 10.0929(6) Å $\quad$ $\beta$= 70.828(4)°. |
| | c = 14.3430(7) Å $\quad$ $\gamma$ = 64.925(5)°. |
| Volume | 1135.33(11) Å$^3$ |
| Z | 2 |
| Density (calculated) | 1.522 Mg/m$^3$ |
| Absorption coefficient | 6.561 mm$^{-1}$ |
| F(000) | 528 |
| Crystal size | 0.26 x 0.23 x 0.17 mm$^3$ |
| Theta range for data collection | 3.36 to 73.49°. |
| Index ranges | -11<=h<=11, -12<=k<=11, -12<=l<=17 |
| Reflections collected | 7557 |
| Independent reflections | 4392 [R(int) = 0.0166] |
| Completeness to theta = 73.49° | 96.0 % |
| Max. and min. transmission | 0.4017 and 0.2803 |
| Refinement method | Full-matrix least-squares on F$^2$ |
| Data / restraints / parameters | 4392 / 2 / 303 |
| Goodness-of-fit on F$^2$ | 1.056 |
| Final R indices [I>2sigma(I)] | R1 = 0.0282, wR2 = 0.0760 |

R indices (all data)                                     R1 = 0.0290, wR2 = 0.0767

Largest diff. peak and hole                      0.321 and -0.456 e.$\text{Å}^{-3}$

Table 2.  Atomic coordinates ( x $10^4$) and equivalent isotropic displacement parameters ($\text{Å}^2$x $10^3$) for pge1313.  U(eq) is defined as one third of the trace of the orthogonalized $U^{ij}$ tensor.

| | x | y | z | U(eq) |
|---|---|---|---|---|
| C(1) | 7782(2) | 5421(2) | 506(1) | 24(1) |
| C(2) | 7502(2) | 6428(2) | -405(1) | 30(1) |
| C(3) | 7143(2) | 6121(2) | -1148(1) | 38(1) |
| C(4) | 7039(2) | 4721(2) | -963(2) | 38(1) |
| C(5) | 7311(2) | 3673(2) | -64(2) | 38(1) |
| C(6) | 7680(2) | 4015(2) | 668(1) | 30(1) |
| C(7) | 8683(2) | 5091(2) | 4054(1) | 23(1) |
| C(8) | 10247(2) | 5036(2) | 3640(1) | 28(1) |
| C(8A) | 10247(2) | 5036(2) | 3640(1) | 28(1) |
| C(9) | 11553(2) | 3740(2) | 3826(1) | 33(1) |
| C(10) | 11284(2) | 2445(2) | 4447(1) | 33(1) |
| C(11) | 9739(3) | 2449(2) | 4873(2) | 36(1) |
| C(12) | 8456(2) | 3765(2) | 4671(2) | 32(1) |
| C(12A) | 8456(2) | 3765(2) | 4671(2) | 32(1) |
| C(13) | 7699(2) | 10144(2) | 2114(1) | 26(1) |
| C(14) | 6900(2) | 10876(2) | 2899(1) | 30(1) |
| C(14A) | 6900(2) | 10876(2) | 2899(1) | 30(1) |
| C(15) | 7648(3) | 11321(2) | 3359(2) | 35(1) |
| C(16) | 9280(3) | 11008(2) | 3024(2) | 38(1) |
| C(17) | 10130(2) | 10268(2) | 2252(2) | 38(1) |
| C(18) | 9348(2) | 9838(2) | 1807(1) | 32(1) |
| C(18A) | 9348(2) | 9838(2) | 1807(1) | 32(1) |
| C(19) | 4025(2) | 8629(2) | 3185(1) | 27(1) |
| C(20) | 4681(2) | 8061(2) | 1423(1) | 26(1) |
| C(21) | 5170(2) | 5823(2) | 2980(1) | 28(1) |
| Cr(1) | 5811(1) | 7473(1) | 2421(1) | 18(1) |
| F(1) | 7585(2) | 7806(1) | -573(1) | 46(1) |
| F(2) | 10467(2) | 6297(2) | 2986(1) | 42(1) |
| F(2A) | 6952(4) | 3766(4) | 4851(3) | 38(1) |
| F(3) | 5310(2) | 11157(2) | 3224(1) | 45(1) |

| | | | |
|---|---|---|---|
| F(3A) | 10093(11) | 9089(14) | 1082(8) | 57(4) |
| O(1) | 2900(2) | 9331(2) | 3678(1) | 43(1) |
| O(2) | 3908(2) | 8416(2) | 840(1) | 40(1) |
| O(3) | 4749(2) | 4799(2) | 3301(1) | 45(1) |
| P(1) | 8092(1) | 5971(1) | 1488(1) | 23(1) |
| P(2) | 6999(1) | 6818(1) | 3777(1) | 24(1) |
| P(3) | 6663(1) | 9516(1) | 1573(1) | 26(1) |

Table 3.   Bond lengths [Å] and angles [°] for pge1313.

| | | | |
|---|---|---|---|
| C(1)-C(2) | 1.379(2) | C(13)-P(3) | 1.8232(17) |
| C(1)-C(6) | 1.397(2) | C(14)-F(3) | 1.350(2) |
| C(1)-P(1) | 1.8218(17) | C(14)-C(15) | 1.383(3) |
| C(2)-F(1) | 1.360(2) | C(15)-C(16) | 1.381(3) |
| C(2)-C(3) | 1.378(3) | C(15)-H(15) | 0.9500 |
| C(3)-C(4) | 1.386(3) | C(16)-C(17) | 1.380(3) |
| C(3)-H(3) | 0.9500 | C(16)-H(16) | 0.9500 |
| C(4)-C(5) | 1.380(3) | C(17)-C(18) | 1.381(3) |
| C(4)-H(4) | 0.9500 | C(17)-H(17) | 0.9500 |
| C(5)-C(6) | 1.389(3) | C(18)-H(18) | 0.9500 |
| C(5)-H(5) | 0.9500 | C(19)-O(1) | 1.158(2) |
| C(6)-H(6) | 0.9500 | C(19)-Cr(1) | 1.8438(17) |
| C(7)-C(8) | 1.382(2) | C(20)-O(2) | 1.155(2) |
| C(7)-C(12) | 1.389(2) | C(20)-Cr(1) | 1.8499(17) |
| C(7)-P(2) | 1.8208(16) | C(21)-O(3) | 1.157(2) |
| C(8)-F(2) | 1.350(2) | C(21)-Cr(1) | 1.8445(18) |
| C(8)-C(9) | 1.383(3) | Cr(1)-P(2) | 2.3248(5) |
| C(9)-C(10) | 1.379(3) | Cr(1)-P(3) | 2.3296(5) |
| C(9)-H(9) | 0.9500 | Cr(1)-P(1) | 2.3344(5) |
| C(10)-C(11) | 1.383(3) | P(1)-H(1A) | 1.2833 |
| C(10)-H(10) | 0.9500 | P(1)-H(1B) | 1.2833 |
| C(11)-C(12) | 1.385(3) | P(2)-H(2A) | 1.2939 |
| C(11)-H(11) | 0.9500 | P(2)-H(2B) | 1.2939 |
| C(12)-H(12) | 0.9500 | P(3)-H(3A) | 1.3046 |
| C(13)-C(14) | 1.386(3) | P(3)-H(3B) | 1.3046 |
| C(13)-C(18) | 1.395(3) | | |

| | | | |
|---|---|---|---|
| C(2)-C(1)-C(6) | 116.75(16) | C(17)-C(16)-H(16) | 119.8 |
| C(2)-C(1)-P(1) | 121.02(13) | C(15)-C(16)-H(16) | 119.8 |
| C(6)-C(1)-P(1) | 122.01(13) | C(16)-C(17)-C(18) | 119.99(18) |
| F(1)-C(2)-C(3) | 118.40(17) | C(16)-C(17)-H(17) | 120.0 |
| F(1)-C(2)-C(1) | 117.63(16) | C(18)-C(17)-H(17) | 120.0 |
| C(3)-C(2)-C(1) | 123.97(17) | C(17)-C(18)-C(13) | 121.61(18) |
| C(2)-C(3)-C(4) | 117.97(18) | C(17)-C(18)-H(18) | 119.2 |
| C(2)-C(3)-H(3) | 121.0 | C(13)-C(18)-H(18) | 119.2 |
| C(4)-C(3)-H(3) | 121.0 | O(1)-C(19)-Cr(1) | 178.74(17) |
| C(5)-C(4)-C(3) | 120.24(18) | O(2)-C(20)-Cr(1) | 176.39(16) |
| C(5)-C(4)-H(4) | 119.9 | O(3)-C(21)-Cr(1) | 177.63(17) |
| C(3)-C(4)-H(4) | 119.9 | C(19)-Cr(1)-C(21) | 92.01(8) |
| C(4)-C(5)-C(6) | 120.35(18) | C(19)-Cr(1)-C(20) | 89.53(7) |
| C(4)-C(5)-H(5) | 119.8 | C(21)-Cr(1)-C(20) | 88.51(8) |
| C(6)-C(5)-H(5) | 119.8 | C(19)-Cr(1)-P(2) | 85.25(5) |
| C(5)-C(6)-C(1) | 120.71(17) | C(21)-Cr(1)-P(2) | 90.23(6) |
| C(5)-C(6)-H(6) | 119.6 | C(20)-Cr(1)-P(2) | 174.58(5) |
| C(1)-C(6)-H(6) | 119.6 | C(19)-Cr(1)-P(3) | 91.42(6) |
| C(8)-C(7)-C(12) | 117.08(15) | C(21)-Cr(1)-P(3) | 174.90(5) |
| C(8)-C(7)-P(2) | 121.29(13) | C(20)-Cr(1)-P(3) | 87.74(5) |
| C(12)-C(7)-P(2) | 121.61(13) | P(2)-Cr(1)-P(3) | 93.819(17) |
| F(2)-C(8)-C(7) | 117.06(16) | C(19)-Cr(1)-P(1) | 178.64(6) |
| F(2)-C(8)-C(9) | 120.04(17) | C(21)-Cr(1)-P(1) | 87.40(5) |
| C(7)-C(8)-C(9) | 122.80(17) | C(20)-Cr(1)-P(1) | 91.68(5) |
| C(10)-C(9)-C(8) | 118.61(17) | P(2)-Cr(1)-P(1) | 93.529(17) |
| C(10)-C(9)-H(9) | 120.7 | P(3)-Cr(1)-P(1) | 89.261(18) |
| C(8)-C(9)-H(9) | 120.7 | C(1)-P(1)-Cr(1) | 116.44(5) |
| C(9)-C(10)-C(11) | 120.46(16) | C(1)-P(1)-H(1A) | 108.2 |
| C(9)-C(10)-H(10) | 119.8 | Cr(1)-P(1)-H(1A) | 108.2 |
| C(11)-C(10)-H(10) | 119.8 | C(1)-P(1)-H(1B) | 108.2 |
| C(10)-C(11)-C(12) | 119.52(17) | Cr(1)-P(1)-H(1B) | 108.2 |
| C(10)-C(11)-H(11) | 120.2 | H(1A)-P(1)-H(1B) | 107.3 |
| C(12)-C(11)-H(11) | 120.2 | C(7)-P(2)-Cr(1) | 123.67(5) |
| C(11)-C(12)-C(7) | 121.53(18) | C(7)-P(2)-H(2A) | 106.4 |
| C(11)-C(12)-H(12) | 119.2 | Cr(1)-P(2)-H(2A) | 106.4 |
| C(7)-C(12)-H(12) | 119.2 | C(7)-P(2)-H(2B) | 106.4 |
| C(14)-C(13)-C(18) | 116.31(16) | Cr(1)-P(2)-H(2B) | 106.4 |
| C(14)-C(13)-P(3) | 121.45(14) | H(2A)-P(2)-H(2B) | 106.5 |

| | | | |
|---|---|---|---|
| C(18)-C(13)-P(3) | 122.13(14) | C(13)-P(3)-Cr(1) | 123.09(5) |
| F(3)-C(14)-C(15) | 119.09(17) | C(13)-P(3)-H(3A) | 106.6 |
| F(3)-C(14)-C(13) | 117.44(16) | Cr(1)-P(3)-H(3A) | 106.6 |
| C(15)-C(14)-C(13) | 123.47(17) | C(13)-P(3)-H(3B) | 106.6 |
| C(16)-C(15)-C(14) | 118.26(18) | Cr(1)-P(3)-H(3B) | 106.6 |
| C(16)-C(15)-H(15) | 120.9 | H(3A)-P(3)-H(3B) | 106.5 |
| C(14)-C(15)-H(15) | 120.9 | | |
| C(17)-C(16)-C(15) | 120.36(18) | | |

Symmetry transformations used to generate equivalent atoms: